ขอบเขตแม่นตรงของตัวประกอบวัตถุเทาสำหรับหลุมดำชนิดต่าง ๆ

นายไตรทศ งามปิติพันธ์

วิทยานิพนธ์นี้เป็นส่วนหนึ่งของการศึกษาตามหลักสูตรปริญญาวิทยาศาสตรดุษฎีบัณฑิต
สาขาวิชาฟิสิกส์ ภาควิชาฟิสิกส์
คณะวิทยาศาสตร์ จุฬาลงกรณ์มหาวิทยาลัย
ปีการศึกษา 2557

RIGOROUS BOUNDS ON GREYBODY FACTORS FOR VARIOUS TYPES OF
BLACK HOLES

Mr. Tritos Ngampitipan

A Dissertation Submitted in Partial Fulfillment of the Requirements
for the Degree of Doctor of Philosophy Program in Physics
Department of Physics
Faculty of Science
Chulalongkorn University
Academic Year 2014

Thesis Title   RIGOROUS BOUNDS ON GREYBODY FACTORS FOR VARIOUS TYPES OF BLACK HOLES

By   Mr. Tritos Ngampitipan

Field of Study   Physics

Thesis Advisor   Assistant Professor Auttakit Chatrabhuti, Ph.D.

Thesis Co-advisor   Assistant Professor Petarpa Boonserm, Ph.D.

Accepted by the Faculty of Science, Chulalongkorn University in Partial Fulfillment of the Requirements for the Doctoral Degree

.... Dean of the Faculty of Science

(Professor Supot Hannongbua, Dr. rer. nat.)

THESIS COMMITTEE

.... Chairman

(Assistant Professor Rattachat Mongkolnavin, Ph.D.)

.... Thesis Advisor

(Assistant Professor Auttakit Chatrabhuti, Ph.D.)

.... Thesis Co-advisor

(Assistant Professor Petarpa Boonserm, Ph.D.)

.... Examiner

(Assistant Professor Surachate Limkumnerd, Ph.D.)

.... Examiner

(Sathon Vijarnwannaluk, Ph.D.)

.... External Examiner

(Pitayuth Wongjun, Ph.D.)

ไตรทศ งามปิติพันธ์ : ขอบเขตแม่นตรงของตัวประกอบวัตถุเทาสำหรับหลุมดำชนิดต่าง ๆ. (RIGOROUS BOUNDS ON GREYBODY FACTORS FOR VARIOUS TYPES OF BLACK HOLES) อ.ที่ปรึกษาวิทยานิพนธ์หลัก : ผศ.ดร.อรรถกฤต ฉัตรภูติ, อ.ที่ปรึกษาวิทยานิพนธ์ร่วม : ผศ.ดร.เพชรอาภา บุญเสริม, 82 หน้า.

ผลลัพธ์ทางควอนตัมอย่างหนึ่งของหลุมดำคือรังสีฮอว์คิง การกระเจิงของรังสีฮอว์คิงจากกำแพงศักย์โน้มถ่วงซึ่งเกิดจากความโค้งงอของกาลอวกาศมีความคล้ายคลึงกับการกระเจิงของคลื่นสสารจากกำแพงศักย์ในกลศาสตร์ควอนตัม ในบริบทของหลุมดำ ความน่าจะเป็นของการส่งผ่านเป็นที่รู้จักกันในชื่อตัวประกอบวัตถุเทา ในวิทยานิพนธ์นี้จะคำนวณหาขอบเขตแม่นตรงของตัวประกอบวัตถุเทาสำหรับหลุมดำที่ไม่หมุน หลุมดำแบบเคอรร์-นิวแมน และหลุมดำสกปรก การคำนวณหาขอบเขตแม่นตรงของตัวประกอบวัตถุเทาสำหรับหลุมดำที่ไม่หมุนและหลุมดำสกปรกไม่ซับซ้อน อย่างไรก็ตาม ในกรณีของหลุมดำแบบเคอรร์-นิวแมนซึ่งเป็นหลุมดำแบบหมุนชนิดหนึ่ง พบว่า สถานการณ์ซับซ้อนขึ้นเพราะขอบเขตแม่นตรงของตัวประกอบวัตถุเทาขึ้นอยู่กับโหมดโมเมนตัมเชิงมุมของรังสีฮอว์คิง นอกจากนี้ยังมีปรากฏการณ์ใหม่เรียกว่าการแผ่รังสียิ่งยวดซึ่งเกิดขึ้นกับหลุมดำแบบหมุนเท่านั้นและไม่เคยเกิดขึ้นกับหลุมดำที่ไม่หมุน

ภาควิชา .... ฟิสิกส์ .... ลายมือชื่อนิสิต ....

สาขาวิชา .... ฟิสิกส์ .... ลายมือชื่อ อ.ที่ปรึกษาวิทยานิพนธ์หลัก ....

ปีการศึกษา .... 2557 .... ลายมือชื่อ อ.ที่ปรึกษาวิทยานิพนธ์ร่วม ....

5472821523 : MAJOR PHYSICS

KEYWORDS: BLACK HOLE/ GREYBODY FACTOR/ RIGOROUS BOUND

TRITOS NGAMPITIPAN : RIGOROUS BOUNDS ON GREYBODY FAC-
TORS FOR VARIOUS TYPES OF BLACK HOLES. ADVISOR : ASST.
PROF.   AUTTAKIT CHATRABHUTI, Ph.D., COADVISOR : ASST.
PROF.   PETARPA BOONSERM, Ph.D., 82 pp.

One of the quantum effects of black holes is Hawking radiation. Scatter-
ing of Hawking radiation from a gravitational potential barrier, resulting from
the curvature of spacetime, is analogous to the scattering of matter wave from a
potential barrier in quantum mechanics. In the context of black hole radiation,
the transmission probability is known as greybody factor. In this dissertation,
rigorous bounds on greybody factors for non-rotating black holes, Kerr-Newman
black holes, and dirty black holes are derived. For non-rotating black holes, in-
cluding dirty black holes, calculations of rigorous bounds on the greybody factors
are simple. However, for a Kerr-Newman black hole, which is a type of rotating
black holes, the situations are more complicated since the rigorous bounds on the
greybody factors depend on scalar angular momentum mode. Moreover, there is a
new phenomenon called super-radiance that arises in rotating black holes, which
is absent in the non-rotating black holes.

Department:.........Physics.........Student's Signature ....

Field of Study:........Physics........Advisor's Signature ....

Academic Year:.........2014.........Co-advisor's Signature ....

ACKNOWLEDGEMENTS

CONTENTS

LIST OF TABLES

LIST OF FIGURES

Chapter I

Introduction

Black holes are mysterious objects in the universe. The existence of black hole has been predicted by Einstein's general theory of relativity. From a classical point of view, it is believed that anything which enters a black hole cannot escape, not even light. As a result, they cannot directly be perceived by any observers, which consequently leads to their '**black hole**'. However, indirect observations are possible through its gravitational field. A black hole is a **singularity** surrounded by a surface known as the **event horizon** which acts as the boundary of the black hole. The singularity of a black hole is the spacetime region with infinite curvature, where all of the laws of physics break down. The event horizon separates the black hole from the universe. Anything can cross the event horizon within a finite time frame, while another observer simultaneously sees it approach the event horizon forever, albeit never really seeing it cross the event horizon. In nature, a black hole is the final fate of a dead star. When a star uses up all its fuel, the repulsive force from the pressure of the star cannot resist the gravitational attraction. It then starts to gravitationally collapse into a white dwarf, a neutron star or a black hole depending on its initial mass before collapsing. If the initial mass of a star is large enough, a black hole can be formed.

In the standard (four-dimensional) general relativity, classical black holes can be classified into four types. The first is the **Schwarzschild** black hole, which is the simplest black hole. It is an uncharged, non-rotating black hole. The second is the **Reissner-Nordström** black hole, which is a charged, non-rotating black hole. If we take the limit $Q \to 0$, where Q is the total charge of a black hole, from the Reissner-Nordström black hole, we will recover the Schwarzschild black hole. The third is the **Kerr** black hole, which is an uncharged, rotating black hole. If we take the limit $a \to 0$, where a is angular momentum per unit mass of a black hole, we will recover the Schwarzschild black hole. The last is the **Kerr-Newman** black hole, which is a charged, rotating black hole. The Kerr-Newman black hole is the most general black hole. If we take the limit $Q \to 0$ while keeping $a \neq 0$ on the Kerr-Newman black hole, we will recover the Kerr black hole. If we

take the limit $a \to 0$ while keeping $Q \neq 0$ on the Kerr-Newman black hole, we will recover the Reissner-Nordström black hole. If we take the limit $a \to 0$ and $Q \to 0$ on the Kerr-Newman black hole, we will recover the Schwarzschild black hole. In higher dimensions, the generalization of Schwarzschild black holes to d dimensions is called **Schwarzschild-Tangherlini** black holes. Moreover, there are black holes which are the solutions to the low-energy string theory. Each of these black holes is associated with a dilaton field. In this dissertation, we will study them in both $(2 + 1)$ and $(3 + 1)$ dimensions.

On the other hand, from a quantum point of view, Stephen Hawking showed, in 1974, that a black hole is not in actuality 'black' but rather can emit radiation, which became known as **Hawking radiation** [1]. By studying quantum field theory in a black hole background, he discovered that radiation. Hawking radiation is a thermal radiation with a **Hawking temperature** (in the unit $c = 1$, which will also be used throughout this dissertation)

$$T_H = \frac{\hbar \kappa}{2\pi k_B},$$ (1.1)

where $\hbar$ is the reduced Planck's constant, k_B is the Boltzmann constant, and κ is the surface gravity which is inversely proportional to the mass of a black hole. The emission of Hawking radiation leads to **black hole evaporation**. Eventually, a black hole will disappear. Due to its inverse proportion to mass, Hawking radiation has an increasing temperature while being emitted from a black hole. Hawking radiation propagates in a curved spacetime, which is the direct result of a black hole, according to general relativity. This nontrivial spacetime behaves as a gravitational potential barrier which scatters Hawking radiation. Therefore, part of it is reflected back into the black hole while the rest is transmitted out of the black hole. This phenomenon is analogous to a scattering phenomenon in one-dimensional potential problems in **quantum mechanics**. An observer away from the black hole can only observe the transmitted wave. This transmitted wave can be thought of as a greybody radiation because the incident wave, which is a blackbody radiation, is modified by the curvature of spacetime. In the black hole context, the transmission probability defines the so-called **greybody factor**, a quantity that tells us what fraction of initial Hawking radiation can reach infinity.

To obtain the greybody factor, we have to solve the Schrödinger-like equation. However, we cannot, in general, find the exact solutions. Consequently, various methods have been developed to derive the approximate solutions. Parikh [2], Fleming [3], and Lange [4] studied a shell of energy denoted as Hawking radiation emitted from the four-dimensional Schwarzschild and Reissner-Nordström

black holes. They used the WKB approximation to calculate the greybody factors. Fernando [5] studied a massless scalar field as Hawking radiation emitted from the charged and uncharged dilaton black holes in $(2 + 1)$ dimensions. She used the simple matching technique to obtain the greybody factors. She found that the greybody factors for the charged and uncharged dilaton black holes show similar behavior. Kim and Oh [6] studied a massless scalar field as Hawking radiation emitted from the charged dilaton black holes in $(3 + 1)$ dimensions. They also used the simple matching technique to obtain the greybody factors. Escobedo [7] also studied a massless scalar field as Hawking radiation. He used the simple matching technique and string theory computation to obtain the greybody factors at low frequencies for the five-dimensional black holes with three charges, and the monodromy matching technique to obtain the greybody factors at high frequencies for the four-dimensional Schwarzschild and Reissner-Nordström black holes. Besides the approximate solutions, Boonserm and Visser [8, 9, 10] have developed new methods to derive rigorous bounds on the greybody factors. They [11] studied a particle with arbitrary spin emitted from the four-dimensional Schwarzschild black holes. They then used the new methods to obtain the rigorous bounds on the greybody factors. Their methods can enhance the qualitatively understanding of black holes and give a new way of studying black hole greybody factors. Moreover, these new methods of deriving rigorous bounds on the greybody factors are valid in all frequency regimes while other approximations can only work in some limits.

In this dissertation, rigorous bounds on the greybody factors for various types of black holes are derived. A review of quantum mechanics and the basics of black holes are presented in Chapter II. Rigorous bounds on the greybody factors for non-rotating black holes, Kerr-Newman black holes, and dirty black holes are obtained in Chapter III-V, respectively. Finally, conclusions are drawn in Chapter VI.

Chapter II

Introduction to quantum mechanics and black holes

Quantum mechanics is a theory that successfully describes microscopic phenomena. There are several different formulations of quantum mechanics such as matrix mechanics founded by Werner Karl Heisenberg in 1925 and wave mechanics founded by Erwin Schrödinger in 1926. Wave mechanics is the primary focus of this dissertation. In this Chapter, the Schrödinger equation and some one-dimensional problems with various potentials such as a delta function potential, a rectangular barrier potential, an Eckart potential, and a Hulthen potential are studied.

2.1 Quantum mechanics

2.1.1 The Schrödinger equation

The dynamical equation that governs the motion of a particle is the time-dependent Schrödinger equation

$$i\hbar\frac{\partial\Psi(\vec{r},t)}{\partial t} = -\frac{\hbar^2}{2m}\nabla^2\Psi(\vec{r},t) + V(\vec{r},t)\Psi(\vec{r},t), \tag{2.1}$$

where $\Psi(\vec{r},t)$ is the wave function, $V(\vec{r},t)$ is the potential, and m is the particle's mass. The quantity $|\Psi(\vec{r},t)|^2$ is interpreted as the probability density. *In many cases*, the potential is time-independent, $V(\vec{r},t) = V(\vec{r})$, in which case the wave function is separable. Thus, we can write

$$\Psi(\vec{r},t) = \psi(\vec{r})f(t). \tag{2.2}$$

Substituting the above equation into equation (2.1), we obtain

$$i\hbar\psi(\vec{r})\frac{\mathrm{d}f(t)}{\mathrm{d}t} = -\frac{\hbar^2}{2m}f(t)\nabla^2\psi(\vec{r}) + V(\vec{r})\psi(\vec{r})f(t). \tag{2.3}$$

Multiplying by $1/\psi(\vec{r})f(t)$ on both sides gives

$$i\hbar\frac{1}{f(t)}\frac{\mathrm{d}f(t)}{\mathrm{d}t} = -\frac{\hbar^2}{2m}\frac{1}{\psi(\vec{r})}\nabla^2\psi(\vec{r}) + V(\vec{r}). \tag{2.4}$$

The left hand side contains functions that are only time variable t, while the right hand side contains functions that are only space variable $\vec{r}$. The equality of both sides requires that each side must be equal to a constant. This constant has the dimension of energy and is denoted by E. Therefore, we obtain two ordinary differential equations

$$\frac{1}{f(t)}\frac{\mathrm{d}f(t)}{\mathrm{d}t} = -\frac{iE}{\hbar} \tag{2.5}$$

and

$$-\frac{\hbar^2}{2m}\nabla^2\psi(\vec{r}) + V(\vec{r})\psi(\vec{r}) = E\psi(\vec{r}). \tag{2.6}$$

Equation (2.6) is called the time-independent Schrödinger equation. The solutions to equation (2.5) are given by

$$f(t) = e^{-iEt/\hbar} \tag{2.7}$$

while the solutions to equation (2.6) depend on the potential $V(\vec{r})$. Then the wave function (2.2) becomes

$$\Psi(\vec{r}, t) = \psi(\vec{r})e^{-iEt/\hbar}. \tag{2.8}$$

In one dimension, the time-independent Schrödinger equation reduces to

$$-\frac{\hbar^2}{2m}\frac{\mathrm{d}^2\psi(x)}{\mathrm{d}x^2} + V(x)\psi(x) = E\psi(x). \tag{2.9}$$

We can write it in another form by rearranging it

$$\frac{\mathrm{d}^2\psi(x)}{\mathrm{d}x^2} + \frac{2m}{\hbar^2}[E - V(x)]\psi(x) = 0. \tag{2.10}$$

2.1.2 The Conservation of Probability

We begin with the time-dependent Schrödinger equation

$$i\hbar\frac{\partial\Psi(\vec{r}, t)}{\partial t} = -\frac{\hbar^2}{2m}\nabla^2\Psi(\vec{r}, t) + V(\vec{r}, t)\Psi(\vec{r}, t). \tag{2.11}$$

Its complex conjugate is given by

$$-i\hbar\frac{\partial\Psi^*(\vec{r}, t)}{\partial t} = -\frac{\hbar^2}{2m}\nabla^2\Psi^*(\vec{r}, t) + V(\vec{r}, t)\Psi^*(\vec{r}, t). \tag{2.12}$$

Multiplying equation (2.11) by $\Psi^*(\vec{r}, t)$

$$i\hbar\Psi^*(\vec{r}, t)\frac{\partial\Psi(\vec{r}, t)}{\partial t} = -\frac{\hbar^2}{2m}\Psi^*(\vec{r}, t)\nabla^2\Psi(\vec{r}, t) + V(\vec{r}, t)\Psi^*(\vec{r}, t)\Psi(\vec{r}, t) \tag{2.13}$$

and equation (2.12) by $\Psi(\vec{r}, t)$

$$-i\hbar\Psi(\vec{r}, t)\frac{\partial\Psi^*(\vec{r}, t)}{\partial t} = -\frac{\hbar^2}{2m}\Psi(\vec{r}, t)\nabla^2\Psi^*(\vec{r}, t) + V(\vec{r}, t)\Psi(\vec{r}, t)\Psi^*(\vec{r}, t) \quad (2.14)$$

and by subtracting them, we obtain

$$i\hbar\frac{\partial}{\partial t}[\Psi^*(\vec{r}, t)\Psi(\vec{r}, t)] = -\frac{\hbar^2}{2m}[\Psi^*(\vec{r}, t)\nabla^2\Psi(\vec{r}, t) - \Psi(\vec{r}, t)\nabla^2\Psi^*(\vec{r}, t)]. \quad (2.15)$$

Using

$$\vec{\nabla}\cdot(a\vec{B}) = a\vec{\nabla}\cdot\vec{B} + \vec{\nabla}a\cdot\vec{B}, \quad (2.16)$$

we can recast equation (2.15) as

$$\frac{\partial\rho}{\partial t} + \vec{\nabla}\cdot\vec{J} = 0, \quad (2.17)$$

where $\rho = \Psi^*(\vec{r}, t)\Psi(\vec{r}, t)$ is the probability density and

$$\vec{J} = \frac{i\hbar}{2m}[\Psi(\vec{r}, t)\vec{\nabla}\Psi^*(\vec{r}, t) - \Psi^*(\vec{r}, t)\vec{\nabla}\Psi(\vec{r}, t)] \quad (2.18)$$

is the current density. Equation (2.17) is interpreted as **the conservation of probability**. In one dimension, these densities reduce to

$$\rho = \Psi^*(x, t)\Psi(x, t) \quad \text{and} \quad J = \frac{i\hbar}{2m}\left[\Psi(x, t)\frac{\partial\Psi^*(x, t)}{\partial x} - \Psi^*(x, t)\frac{\partial\Psi(x, t)}{\partial x}\right]. \quad (2.19)$$

For a system with a time-independent potential in which the wave function is given by equation (2.8), we obtain

$$\rho = \psi^*(x)\psi(x) \quad \text{and} \quad J = \frac{i\hbar}{2m}\left[\psi(x)\frac{d\psi^*(x)}{dx} - \psi^*(x)\frac{d\psi(x)}{dx}\right]. \quad (2.20)$$

In the next sections, we demonstrate how to apply the Schrödinger equation in various physical systems.

2.1.3 A delta function potential

A delta function potential takes the form [12]

$$V(x) = \alpha\delta(x), \quad (2.21)$$

where α is a positive constant and the delta function is defined by

$$\delta(x) = \begin{cases} 1 \text{ if } x = 0 \\ 0 \text{ if } x \neq 0 \end{cases}. \quad (2.22)$$

We are interested in a scattering state $E > 0$. We define

$$k^2 = \frac{2mE}{\hbar^2} \quad \text{and} \quad k_0 = \frac{m\alpha}{\hbar^2}. \tag{2.23}$$

The time-independent Schrödinger equation is

$$\frac{\mathrm{d}^2\psi(x)}{\mathrm{d}x^2} + \frac{2m}{\hbar^2}[E - \alpha\delta(x)]\psi(x) = 0. \tag{2.24}$$

For $x \neq 0$, the above equation reduces to

$$\frac{\mathrm{d}^2\psi(x)}{\mathrm{d}x^2} + k^2\psi(x) = 0. \tag{2.25}$$

Its most general solutions are given by

$$\psi(x) = \begin{cases} Ae^{ikx} + Be^{-ikx} & \text{if } x < 0 \\ Ce^{ikx} + De^{-ikx} & \text{if } x > 0 \end{cases}, \tag{2.26}$$

where Ae^{ikx} and Ce^{ikx} represent right-moving waves, while Be^{-ikx} and De^{-ikx} represent left-moving waves. Here, we are interested in a system in which waves are initially incident on the potential at $x = 0$, from the left. They can be reflected to the region $x < 0$ and be transmitted to the region $x > 0$. Thus, there are no left-moving waves in the region $x > 0$. That is $D = 0$ and equation (2.26) becomes

$$\psi(x) = \begin{cases} Ae^{ikx} + Be^{-ikx} & \text{if } x < 0 \\ Ce^{ikx} & \text{if } x > 0 \end{cases}, \tag{2.27}$$

The continuity of the wave functions at $x = 0$ leads to

$$A + B = C. \tag{2.28}$$

Since the potential is infinite at $x = 0$, the first derivatives of the wave functions are discontinuous. We can find the jump condition by rewriting the equation (2.24)

$$\frac{\mathrm{d}^2\psi(x)}{\mathrm{d}x^2} + k^2\psi(x) = 2k_0\delta(x)\psi(x) \tag{2.29}$$

and integrating over x both sides from $-\epsilon$ to ϵ

$$\int_{-\epsilon}^{\epsilon} \frac{\mathrm{d}^2\psi(x)}{\mathrm{d}x^2}\mathrm{d}x + \int_{-\epsilon}^{\epsilon} k^2\psi(x)\mathrm{d}x = \int_{-\epsilon}^{\epsilon} 2k_0\delta(x)\psi(x)\mathrm{d}x$$

$$\left.\frac{\mathrm{d}\psi(x)}{\mathrm{d}x}\right|_{-\epsilon}^{\epsilon} + \int_{-\epsilon}^{\epsilon} k^2\psi(x)\mathrm{d}x = 2k_0\psi(0). \tag{2.30}$$

Taking the limit $\epsilon \to 0$, we obtain

$$\left.\frac{\mathrm{d}\psi(x)}{\mathrm{d}x}\right|_{x=0^+} - \left.\frac{\mathrm{d}\psi(x)}{\mathrm{d}x}\right|_{x=0^-} = 2k_0\psi(0). \tag{2.31}$$

Substituting equation (2.27) into equation (2.31), we derive

$$ikC - ikA + ikB = 2k_0(A + B). \tag{2.32}$$

We can solve equation (2.28) and equation (2.32) to obtain B and C in terms of A

$$B = \frac{k_0 A}{ik - k_0} \quad \text{and} \quad C = \frac{ikA}{ik - k_0}. \tag{2.33}$$

Now, we calculate the transmission and reflection probabilities defined by

$$T = \left| \frac{J_{\text{transmitted}}}{J_{\text{incident}}} \right| \quad \text{and} \quad R = \left| \frac{J_{\text{reflected}}}{J_{\text{incident}}} \right|, \tag{2.34}$$

where J is given by the equation (2.20). Therefore, the incident current density is

$$J_{\text{incident}} = \frac{i\hbar}{2m} \left[\psi_{\text{incident}}(x) \frac{d\psi^*_{\text{incident}}(x)}{dx} - \psi^*_{\text{incident}}(x) \frac{d\psi_{\text{incident}}(x)}{dx} \right], \tag{2.35}$$

where from equation (2.27) $\psi_{\text{incident}}(x) = Ae^{ikx}$. Then,

$$J_{\text{incident}} = \frac{i\hbar}{2m} \left(-ik|A|^2 - ik|A|^2 \right) = \frac{\hbar k}{m} |A|^2. \tag{2.36}$$

Similarly, the transmitted current density is

$$J_{\text{transmitted}} = \frac{i\hbar}{2m} \left[\psi_{\text{trans}}(x) \frac{d\psi^*_{\text{trans}}(x)}{dx} - \psi^*_{\text{trans}}(x) \frac{d\psi_{\text{trans}}(x)}{dx} \right] \tag{2.37}$$

and the reflected current density is

$$J_{\text{reflected}} = \frac{i\hbar}{2m} \left[\psi_{\text{reflected}}(x) \frac{d\psi^*_{\text{reflected}}(x)}{dx} - \psi^*_{\text{reflected}}(x) \frac{d\psi_{\text{reflected}}(x)}{dx} \right], \tag{2.38}$$

where from equation (2.27) $\psi_{\text{trans}}(x) = Ce^{ikx}$ and $\psi_{\text{reflected}}(x) = Be^{-ikx}$. Then,

$$J_{\text{transmitted}} = \frac{i\hbar}{2m} \left(-ik|C|^2 - ik|C|^2 \right) = \frac{\hbar k}{m} |C|^2 \tag{2.39}$$

and

$$J_{\text{reflected}} = \frac{i\hbar}{2m} \left(ik|B|^2 + ik|B|^2 \right) = -\frac{\hbar k}{m} |B|^2. \tag{2.40}$$

From equation (2.34), we obtain

$$T = \left| \frac{C}{A} \right|^2 \quad \text{and} \quad R = \left| \frac{B}{A} \right|^2. \tag{2.41}$$

Using equation (2.33), the transmission and reflection probabilities are derived [13, 14]

$$T = \frac{k^2}{k^2 + k_0^2} \quad \text{and} \quad R = \frac{k_0^2}{k^2 + k_0^2}. \tag{2.42}$$

Note that

$$T + R = 1. \tag{2.43}$$

The transmission and reflection probabilities varying with k are plotted as shown in Figure 2.1 and Figure 2.2, respectively. We can see that the transmission probability tends to unify as k goes to infinity. We say, however, that this potential has no transmission resonances ($T = 1$). On the other hand, the reflection resonances ($R = 1$) occur at $k_0 \to \infty$. That is, when the potential is stronger than the threshold, penetration of a particle or wave through the potential becomes significantly more difficult.
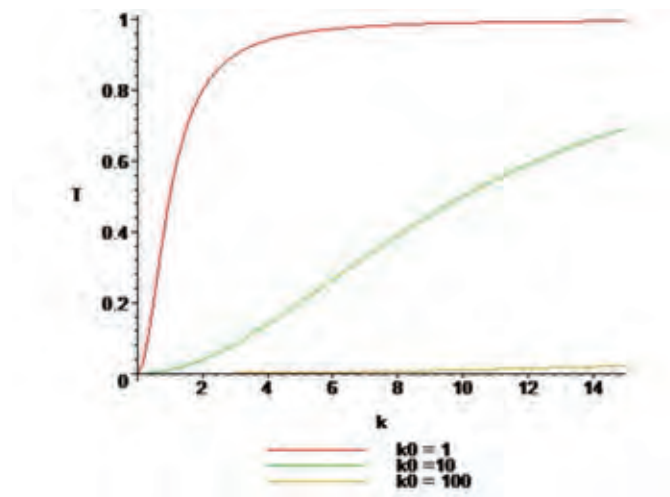
Figure 2.1: Plotting of transmission probabilities varying with k for the delta function potential with $k_0 = 1$, $k_0 = 10$, and $k_0 = 100$.
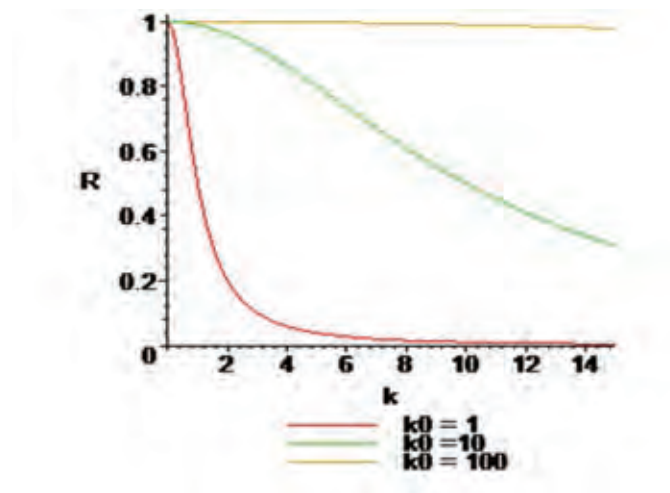
Figure 2.2: Plotting of reflection probabilities varying with k for the delta function potential with $k_0 = 1$, $k_0 = 10$, and $k_0 = 100$.

2.1.4   Rectangular barrier potential

The rectangular barrier potential has the form [15, 16]

$$V(x) = \begin{cases} V_0 \text{ if } |x| \leq a \\ 0 \ \text{ if otherwise} \end{cases}.$$

(2.44)

The shape of the rectangular barrier potential is shown in Figure 2.3. We are interested in two cases $E > V_0 > 0$ and $V_0 > E > 0$.
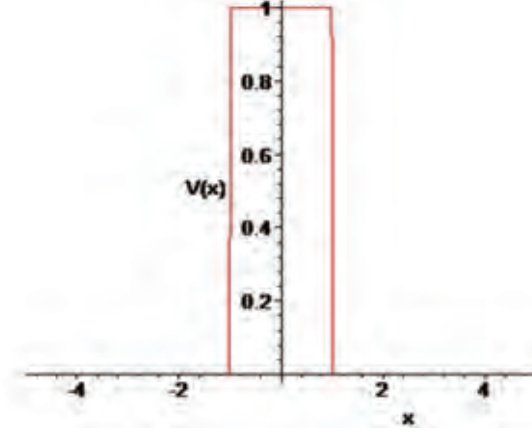
Figure 2.3: The rectangular barrier potential with $a = 1$ and $V_0 = 1$.

Case I: $E > V_0 > 0$

We define

$$k^2 = \frac{2mE}{\hbar^2}, \quad q^2 = \frac{2m(E - V_0)}{\hbar^2}, \quad \text{and} \ \ k_0^2 = \frac{2mV_0}{\hbar^2} = k^2 - q^2.$$

(2.45)

The time-independent Schrödinger equation is

$$\frac{\mathrm{d}^2 \psi(x)}{\mathrm{d}x^2} + \frac{2m}{\hbar^2}[E - V(x)]\psi(x) = 0.$$

(2.46)

When $|x| \leq a$, we obtain

$$\frac{\mathrm{d}^2 \psi(x)}{\mathrm{d}x^2} + q^2 \psi(x) = 0,$$

(2.47)

and when $|x| > a$, the Schrödinger equation becomes

$$\frac{\mathrm{d}^2 \psi(x)}{\mathrm{d}x^2} + k^2 \psi(x) = 0.$$

(2.48)

Their solutions are given by

$$\psi(x) = \begin{cases} Ae^{ikx} + Be^{-ikx} \text{ if } x < -a \\ Ce^{iqx} + De^{-iqx} \text{ if } -a < x < a \\ Ee^{ikx} \qquad\qquad \text{ if } x > a \end{cases}.$$

(2.49)

The continuity of the wave functions at $x = -a$ leads to

$$Ae^{-ika} + Be^{ika} = Ce^{-iqa} + De^{iqa} \tag{2.50}$$

and the continuity at $x = a$ leads to

$$Ee^{ika} = Ce^{iqa} + De^{-iqa}. \tag{2.51}$$

Since the potential is finite, derivatives of the wave functions are also continuous at $x = -a$ and $x = a$, leading to

$$Ae^{-ika} - Be^{ika} = \frac{q}{k}Ce^{-iqa} - \frac{q}{k}De^{iqa} \tag{2.52}$$

and

$$Ee^{ika} = \frac{q}{k}Ce^{iqa} - \frac{q}{k}De^{-iqa}. \tag{2.53}$$

Adding equation (2.50) to equation (2.52), we obtain

$$2Ae^{-ika} = \left(1 + \frac{q}{k}\right)Ce^{-iqa} + \left(1 - \frac{q}{k}\right)De^{iqa}, \tag{2.54}$$

leading to

$$(k + q)Ce^{-iqa} + (k - q)De^{iqa} = 2kAe^{-ika}. \tag{2.55}$$

The equality of equation (2.51) and equation (2.53) gives

$$C = -\frac{k + q}{k - q}De^{-2iqa}. \tag{2.56}$$

We can solve equation (2.55) and equation (2.56) to obtain C and D in terms of A

$$C = -\frac{2k(k + q)Ae^{-ika}}{(k - q)^2 e^{iqa} - (k + q)^2 e^{-3iqa}}e^{-2iqa} \tag{2.57}$$

and

$$D = \frac{2k(k - q)Ae^{-ika}}{(k - q)^2 e^{iqa} - (k + q)^2 e^{-3iqa}}. \tag{2.58}$$

Substituting C and D into equation (2.50) and equation (2.51), we obtain

$$B = \frac{(k^2 - q^2)\left(e^{2iqa} - e^{-2iqa}\right)A}{(k - q)^2 e^{2iqa} - (k + q)^2 e^{-2iqa}}e^{-2ika} \tag{2.59}$$

and

$$E = -\frac{4kqAe^{-2ika}}{(k - q)^2 e^{2iqa} - (k + q)^2 e^{-2iqa}}. \tag{2.60}$$

Therefore, the transmission probability and the reflection probability are [17, 18]

$$T = \left|\frac{E}{A}\right|^2 = \frac{4k^2 q^2}{4k^2 q^2 + k_0^4 \sin^2(2qa)} \quad \text{and} \quad R = \left|\frac{B}{A}\right|^2 = \frac{k_0^4 \sin^2(2qa)}{4k^2 q^2 + k_0^4 \sin^2(2qa)}. \tag{2.61}$$

Note that

$$T + R = 1. \tag{2.62}$$

The transmission and reflection probabilities varying with q are plotted as shown in Figure 2.4, Figure 2.5, and Figure 2.6. The effects of barrier heights V_0 of the potential on the probabilities when the width a of the potential is fixed are shown in Figure 2.4. It has been found that the higher the barrier of the potential is, the more the number of reflection resonances. This is similar to the case of the delta function potential: penetration of a particle or wave through the potential is harder to occur when the barrier height of the potential is large. The effects of the widths of the potential on the probabilities when the barrier height of the potential is fixed are shown in Figure 2.5 and 2.6. The results are that the reflection resonance can occur when the width increases. Analytically, the transmission resonances occur at

$$q = \frac{n\pi}{2a}, \tag{2.63}$$

where $n = 1, 2, 3, ...$, while the reflection resonance is at $k = 0$ for this potential.
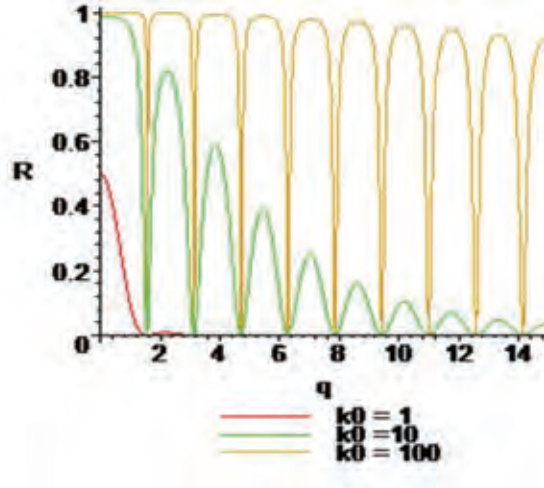
Figure 2.4: The effects of barrier heights V_0 of the potential on the probabilities for varying q in the rectangular barrier with $k_0 = 1$, $k_0 = 10$, and $k_0 = 100$ for $a = 1$.

Case II: $V_0 > E > 0$

We define

$$Q^2 = \frac{2m(V_0 - E)}{\hbar^2}. \tag{2.64}$$

The time-independent Schrödinger equation is

$$\frac{\mathrm{d}^2\psi(x)}{\mathrm{d}x^2} + \frac{2m}{\hbar^2}[E - V(x)]\psi(x) = 0. \tag{2.65}$$
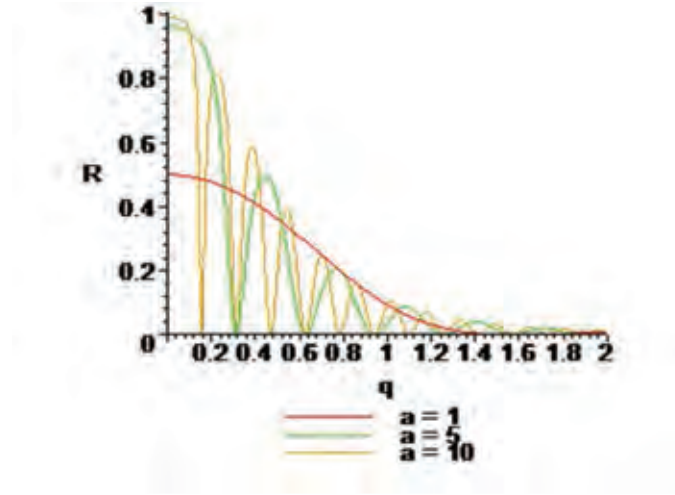
Figure 2.5: The effects of the widths a of the potential on the reflection probabilities varying with q in the rectangular barrier with $a = 1$, $a = 5$ and $a = 10$ for $k_0 = 1$.

When $|x| \leq a$, we obtain

$$\frac{\mathrm{d}^2\psi(x)}{\mathrm{d}x^2} - Q^2\psi(x) = 0, \tag{2.66}$$

and when $|x| > a$, the Schrödinger equation becomes

$$\frac{\mathrm{d}^2\psi(x)}{\mathrm{d}x^2} + k^2\psi(x) = 0. \tag{2.67}$$

Their solutions are given by

$$\psi(x) = \begin{cases} Ae^{ikx} + Be^{-ikx} & \text{if } x < -a \\ Ce^{Qx} + De^{-Qx} & \text{if } -a < x < a \\ Ee^{ikx} & \text{if } x > a \end{cases} \tag{2.68}$$

The continuity of the wave functions at $x = -a$ leads to

$$Ae^{-ika} + Be^{ika} = Ce^{-Qa} + De^{Qa} \tag{2.69}$$

and the continuity at $x = a$ leads to

$$Ee^{ika} = Ce^{Qa} + De^{-Qa}. \tag{2.70}$$

Since the potential is finite, derivatives of the wave functions are also continuous at $x = -a$ and $x = a$, leading to

$$Ae^{-ika} - Be^{ika} = -\frac{iQ}{k}Ce^{-Qa} + \frac{iQ}{k}De^{Qa} \tag{2.71}$$

and

$$Ee^{ika} = -\frac{iQ}{k}Ce^{Qa} + \frac{iQ}{k}De^{-Qa}. \tag{2.72}$$
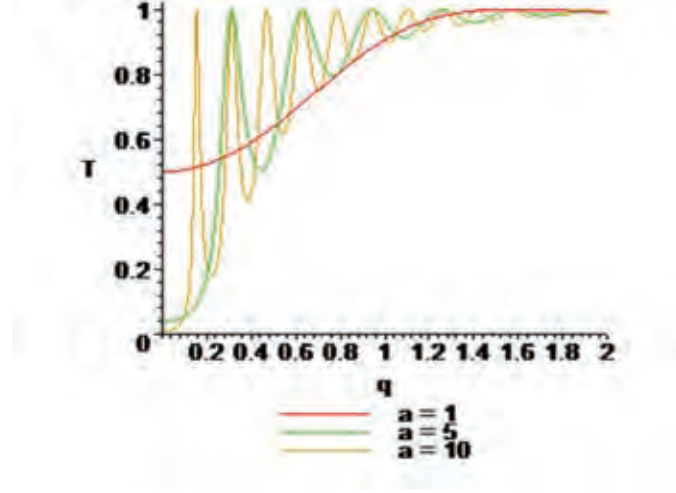
Figure 2.6: The effects of the widths a of the potential on the transmission probabilities varying with q in the rectangular barrier with $a = 1$, $a = 5$, and $a = 10$ for $k_0 = 1$.

Adding equation (2.69) to equation (2.71), we obtain

$$2Ae^{-ika} = \left(1 - \frac{iQ}{k}\right)Ce^{-Qa} + \left(1 + \frac{iQ}{k}\right)De^{Qa}, \tag{2.73}$$

leading to

$$(k - iQ)Ce^{-Qa} + (k + iQ)De^{Qa} = 2kAe^{-ika}. \tag{2.74}$$

The equality of equation (2.70) and equation (2.72) gives

$$C = -\frac{k - iQ}{k + iQ}De^{-2Qa}. \tag{2.75}$$

We can solve equation (2.74) and equation (2.75) to obtain C and D in terms of A

$$C = -\frac{(k - iQ)kAe^{-(Q+ik)a}}{(k^2 - Q^2)\sinh(2Qa) + 2ikQ\cosh(2Qa)} \tag{2.76}$$

and

$$D = \frac{(k + iQ)kAe^{(Q-ik)a}}{(k^2 - Q^2)\sinh(2Qa) + 2ikQ\cosh(2Qa)}. \tag{2.77}$$

Substituting C and D into equation (2.69) and equation (2.70), we obtain

$$B = \frac{(k^2 + Q^2)A\sinh(2Qa)e^{-2ika}}{(k^2 - Q^2)\sinh(2Qa) + 2ikQ\cosh(2Qa)}. \tag{2.78}$$

and

$$E = \frac{2iQkAe^{-2ika}}{(k^2 - Q^2)\sinh(2Qa) + 2ikQ\cosh(2Qa)}. \tag{2.79}$$

Therefore, the transmission probability is

$$T = \left|\frac{E}{A}\right|^2 = \frac{4k^2Q^2}{(k^2 - Q^2)^2\sinh^2(2Qa) + 4k^2Q^2\cosh^2(2Qa)} \tag{2.80}$$

and the reflection probability is

$$R = \left|\frac{B}{A}\right|^2 = \frac{k_0^4 \sinh^2(2Qa)}{(k^2 - Q^2)^2 \sinh^2(2Qa) + 4k^2Q^2 \cosh^2(2Qa)}.$$ (2.81)

We can see that in this case $T \neq 0$. It follows that a particle can penetrate the barrier from one side to the other, although the potential energy of the particle exceeds its total energy, which does not appear in classical physics. This is called tunneling.

2.1.5   An Eckart potential

An Eckart potential is an exponential-type potential and useful in physics and chemical physics. The Eckart potential takes the form [12]

$$V(x) = \frac{V_{-\infty} + V_{\infty}}{2} + \frac{V_{\infty} - V_{-\infty}}{2} \tanh\left(\frac{x}{a}\right) + \frac{V_0}{\cosh^2(x/a)}.$$ (2.82)

The shape of the Eckart potential is shown in Figure 2.7.
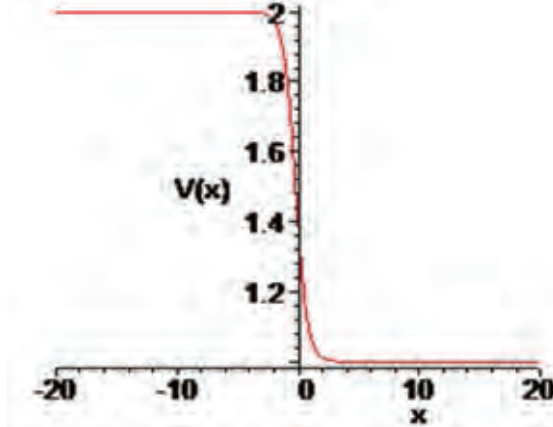
Figure 2.7: The Eckart potential with $V_{-\infty} = 2$, $V_{\infty} = 1$, $a = 3$, and $V_0 = -1/9$.

We define

$$k_{\pm\infty}^2 = \frac{2m(E - V_{\pm\infty})}{\hbar^2} \quad \text{and} \quad \bar{k} = \frac{k_{\infty} + k_{-\infty}}{2}.$$ (2.83)

The Eckart potential can be expressed in another form [19]

$$V(x) = -\frac{A\xi}{1 - \xi} - \frac{B\xi}{(1 - \xi)^2} + V_{-\infty},$$ (2.84)

where

$$\xi = -\exp\left(\frac{2x}{a}\right), \quad A = V_{\infty} - V_{-\infty}, \quad \text{and} \quad B = 4V_0.$$ (2.85)

The time-independent Schrödinger equation is

$$\frac{d^2\psi(x)}{dx^2} + \frac{2m}{\hbar^2}\left[E + \frac{A\xi}{1-\xi} + \frac{B\xi}{(1-\xi)^2} - V_{-\infty}\right]\psi(x) = 0. \tag{2.86}$$

Using the chain rule, we obtain

$$\frac{d\psi}{dx} = \frac{2\xi}{a}\frac{d\psi}{d\xi} \quad \text{and} \quad \frac{d^2\psi}{dx^2} = \frac{4\xi^2}{a^2}\frac{d^2\psi}{d\xi^2} + \frac{4\xi}{a^2}\frac{d\psi}{d\xi}. \tag{2.87}$$

The Schrödinger equation (2.86) becomes

$$\xi^2\frac{d^2\psi}{d\xi^2} + \xi\frac{d\psi}{d\xi} + \frac{ma^2}{2\hbar^2}\left[E + \frac{A\xi}{1-\xi} + \frac{B\xi}{(1-\xi)^2} - V_{-\infty}\right]\psi = 0. \tag{2.88}$$

Its solutions are given by [19]

$$\psi = (1-\xi)^{i\beta}\left(\frac{\xi}{\xi-1}\right)^{i\alpha} F\left[\frac{1}{2} + i(\alpha - \beta + \delta), -\frac{1}{2} + i(\alpha - \beta - \delta),\right.$$
$$\left.1 - 2i\beta, \frac{1}{1-\xi}\right], \tag{2.89}$$

where

$$\alpha = \frac{k_{-\infty}a}{2}, \ \beta = \frac{k_{\infty}a}{2}, \delta = \frac{i}{2}\sqrt{1 - \frac{8mV_0a^2}{\hbar^2}}, \tag{2.90}$$

and hypergeometric function $F(a, b, c, x)$ is defined by

$$F(a, b, c, z) = \sum_{n=0}^{\infty} \frac{(a)_n(b)_n}{(c)_n}\frac{z^n}{n!} \tag{2.91}$$

which diverges when $|z| \geq 1$. Here, $(q)_n$ is the Pochhammer symbol which is defined by

$$(q)_n = \begin{cases} 1 & \text{if } n = 0 \\ q(q+1)\dots(q+n-1) & \text{if } n > 0 \end{cases}. \tag{2.92}$$

However, this solution diverges when $\xi \to 0$. This problem can be solved using analytic extension, and we obtain

$$\psi = a_1\left(\frac{\xi}{\xi-1}\right)^{i\alpha}(1-\xi)^{i\beta}F\left[\frac{1}{2} + i(\alpha - \beta + \delta), -\frac{1}{2} + i(\alpha - \beta - \delta),\right.$$
$$\left.1 + 2i\alpha, \frac{\xi}{\xi-1}\right] + a_2\left(\frac{\xi}{\xi-1}\right)^{-i\alpha}(1-\xi)^{i\beta}F\left[\frac{1}{2} + i(-\alpha - \beta + \delta),\right.$$
$$\left.-\frac{1}{2} + i(-\alpha - \beta - \delta), 1 - 2i\alpha, \frac{\xi}{\xi-1}\right], \tag{2.93}$$

where

$$a_1 = \frac{\Gamma(1 - 2i\beta)\Gamma(-2i\alpha)}{\Gamma[(1/2) + i(-\alpha - \beta - \delta)]\Gamma[(1/2) + i(-\alpha - \beta + \delta)]} \tag{2.94}$$

and

$$a_2 = \frac{\Gamma(1 - 2i\beta)\Gamma(2i\alpha)}{\Gamma[(1/2) + i(\alpha - \beta - \delta)]\Gamma[(1/2) + i(\alpha - \beta + \delta)]}. \tag{2.95}$$

Note that this new solution converges when $\xi \to 0$. Here $\Gamma(t)$ is gamma function which is defined by

$$\Gamma(t) = \int_0^\infty x^{t-1}e^{-x}\mathrm{d}x. \tag{2.96}$$

Since $|\Gamma(2i\alpha)/\Gamma(-2i\alpha)| = 1$, we obtain [19]

$$R = \left|\frac{a_2}{a_1}\right|^2 = \left|\frac{\Gamma[(1/2) + i(\delta - \beta - \alpha)]\Gamma[(1/2) + i(-\delta - \beta - \alpha)]}{\Gamma[(1/2) + i(\delta - \beta + \alpha)]\Gamma[(1/2) + i(-\delta - \beta + \alpha)]}\right|^2. \tag{2.97}$$

From

$$|\Gamma(u + iv)\Gamma(1 - u + iv)| = \frac{\Gamma(u)\Gamma(1 - u)}{\sqrt{(\cosh 2\pi v - \cos 2\pi u)/2\sin^2 \pi u}}, \tag{2.98}$$

we obtain

$$R = \frac{\cosh[2\pi(\alpha - \beta)] + \cos(2\pi|\delta|)}{\cosh[2\pi(\alpha + \beta)] + \cos(2\pi|\delta|)}. \tag{2.99}$$

Using equation (2.90), we obtain

$$R = \frac{\cosh[\pi a(k_{-\infty} - k_\infty)] + \cos(\pi\sqrt{1 - 8mV_0a^2/\hbar^2})}{\cosh(2\pi\bar{k}a) + \cos(\pi\sqrt{1 - 8mV_0a^2/\hbar^2})}. \tag{2.100}$$

Therefore, the transmission probability is given by [20]

$$T = 1 - R = \frac{2\sinh(\pi k_{-\infty}a)\sinh(\pi k_\infty a)}{\cosh(2\pi\bar{k}a) + \cos(\pi\sqrt{1 - 8mV_0a^2/\hbar^2})}. \tag{2.101}$$

The transmission and reflection probabilities varying with V_0 are plotted as shown in Figure 2.8. The effects of a on the probabilities for $a = 1$ and $a = 2$ are shown in Figure 2.8 (a) and (b), respectively. When $a \to \infty$, the transmission probability approaches unity.

2.1.6 A Hulthen potential

A Hulthen potential is important and useful in nuclear and particle physics, atomic physics, condensed matter and chemical physics as well as the scattering problem for a relativistic particle. The Hulthen potential takes the form [21]

$$V(x) = \theta(-x)\frac{V_0}{e^{-ax} - q} + \theta(x)\frac{V_0}{e^{ax} - q}, \tag{2.102}$$

where V_0, a, and q all are real and positive with $q < 1$. $\theta(x)$ is the Heaviside step function defined by

$$\theta(x) = \begin{cases} 1, \text{ if } x > 0 \\ 0, \text{ if } x < 0 \end{cases}. \tag{2.103}$$
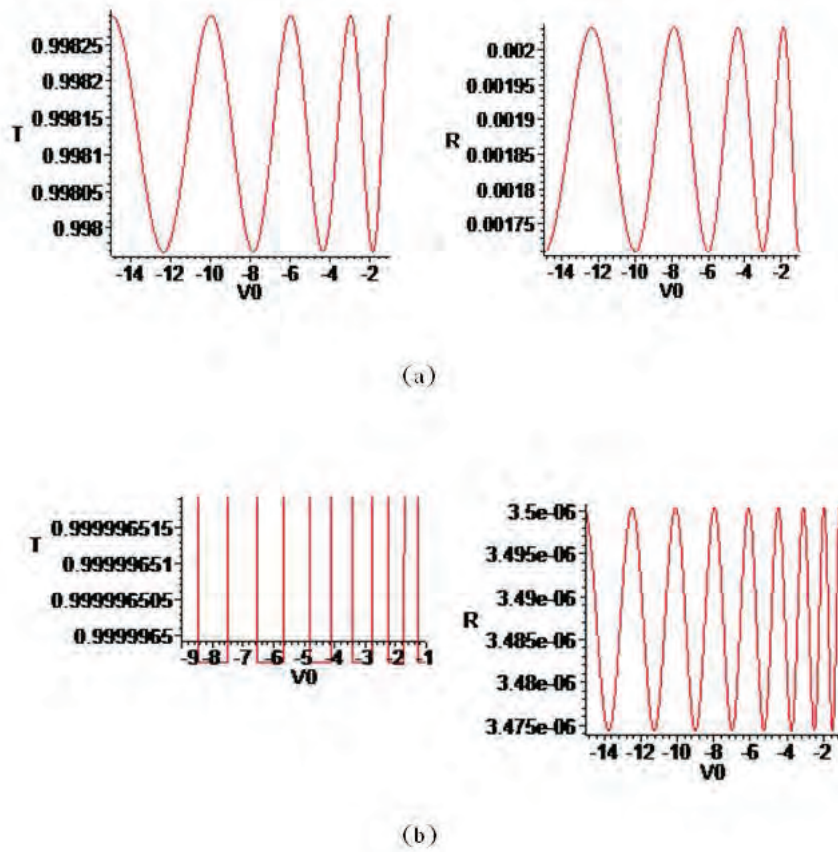
Figure 2.8: The effects of a on the probabilities varying with V_0 in the Eckart potential with (a) $a = 1$ and (b) $a = 2$ for $k_{-\infty} = 1$, $k_\infty = 2$, and $m = \hbar = 1$.
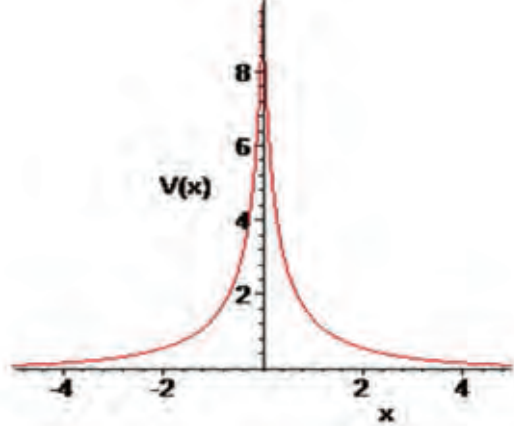
Figure 2.9: The Hulthen potential with $q = 0.9$, $a = 0.5$, and $V_0 = 1$.

The shape of the Hulthen potential is shown in Figure 2.9.

We are interested in the case $E > V(x) > 0$. The time-independent Schrödinger equation is

$$\frac{\mathrm{d}^2\psi(x)}{\mathrm{d}x^2} + \frac{2m}{\hbar^2}\left[E - \theta(-x)\frac{V_0}{e^{-ax} - q} - \theta(x)\frac{V_0}{e^{ax} - q}\right]\psi(x) = 0. \qquad (2.104)$$

From the matching condition, the transmission and reflection amplitudes for this potential are given, in terms of hypergeometric function $F(a, b, c, ; q)$, by (see [21])

$$t = \frac{(1-q)^{2\lambda}q^{2\mu}}{1+2\mu}[\{q(1+2\mu)(\lambda^2 - 2\lambda\mu + \mu^2 - \nu^2)F(1+\lambda-\mu-\nu, 1+\lambda-\mu+\nu, 2-2\mu; q)$$
$$F(\lambda+\mu-\nu, \lambda+\mu+\nu, 1+2\mu; q)\} - \{q(1-2\mu)(\lambda^2 + 2\lambda\mu + \mu^2 - \nu^2)$$
$$F(1+\lambda+\mu-\nu, 1+\lambda+\mu+\nu, 2+2\mu; q)F(\lambda-\mu-\nu, \lambda-\mu+\nu, 1-2\mu; q)\}$$
$$-\{(1-2\mu)(2\mu)(1+2\mu)F(\lambda+\mu-\nu, \lambda+\mu+\nu, 1+2\mu; q)$$
$$F(\lambda-\mu-\nu, \lambda-\mu+\nu, 1-2\mu; q)\}]$$
$$/[\{q(\lambda^2 + 2\lambda\mu + \mu^2 - \nu^2)F(1-\lambda-\mu-\nu, 1-\lambda-\mu+\nu, 2-2\mu; q)$$
$$F(\lambda-\mu-\nu, \lambda-\mu+\nu, 1-2\mu; q)\} + \{q(\lambda^2 - 2\lambda\mu + \mu^2 - \nu^2)$$
$$F(1+\lambda-\mu-\nu, 1+\lambda-\mu+\nu, 2-2\mu; q)F(-\lambda-\mu-\nu, -\lambda-\mu+\nu, 1-2\mu; q)\}$$
$$-\{(2\mu)(1-2\mu)F(\lambda-\mu-\nu, \lambda-\mu+\nu, 1-2\mu; q)$$
$$F(-\lambda-\mu-\nu, -\lambda-\mu+\nu, 1-2\mu; q)\}] \qquad (2.105)$$

and

$$r = -\frac{q^{1+2\mu}(\lambda^2 + 2\lambda\mu + \mu^2 - \nu^2)}{1+2\mu}\sqrt{\frac{E+k}{E-k}}[\{(1+2\mu)F(\lambda + \mu - \nu, \lambda + \mu + \nu, 1 + 2\mu; q)$$
$$F(1 - \lambda - \mu - \nu, 1 - \lambda - \mu + \nu, 2 - 2\mu; q)\} + \{(1 - 2\mu)$$
$$F(1 + \lambda + \mu - \nu, 1 + \lambda + \mu + \nu, 2 + 2\mu; q)F(-\lambda - \mu - \nu, -\lambda - \mu + \nu, 1 - 2\mu; q)\}]$$
$$/[\{q(\lambda^2 + 2\lambda\mu + \mu^2 - \nu^2)F(1 - \lambda - \mu - \nu, 1 - \lambda - \mu + \nu, 2 - 2\mu; q)$$
$$F(\lambda - \mu - \nu, \lambda - \mu + \nu, 1 - 2\mu; q)\} + \{q(\lambda^2 - 2\lambda\mu + \mu^2 - \nu^2)$$
$$F(1 + \lambda - \mu - \nu, 1 + \lambda - \mu + \nu, 2 - 2\mu; q)F(-\lambda - \mu - \nu, -\lambda - \mu + \nu, 1 - 2\mu; q)\}$$
$$-\{(2\mu)(1 - 2\mu)F(\lambda - \mu - \nu, \lambda - \mu + \nu, 1 - 2\mu; q)$$
$$F(-\lambda - \mu - \nu, -\lambda - \mu + \nu, 1 - 2\mu; q)\}], \tag{2.106}$$

where $\mu = ik/a$, $\nu = ip/a$, $\lambda = iV_0/aq$, $p^2 = (E + V_0/q)^2 - m^2$, and $k^2 = E^2 - m^2$. The transmission and reflection probabilities are derived from

$$T = |t|^2 \quad \text{and} \quad R = |r|^2. \tag{2.107}$$

We can check that

$$T + R = 1. \tag{2.108}$$

The transmission and reflection probabilities for varying E are shown in Figure 2.10. There are both transmission and reflection resonances. In Figure 2.10 (a) and 2.10 (b), we describe how the diffuseness a has an effect on the probabilities with the other parameters where m, V_0, and q are fixed.
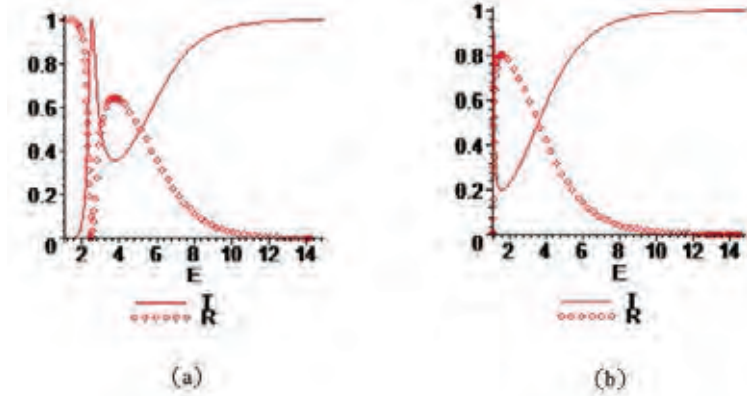
Figure 2.10: Plotting of transmission and reflection probabilities for varying E for a Hulthen potential with (a) $a = 0.5$ and (b) $a = 1$ when $m = 1$, $V_0 = 1$, and $q = 0.9$.

2.1.7 Rigorous bounds on transmission probabilities

In this subsection, we introduce rigorous bounds on transmission probabilities developed by Boonserm and Visser [8, 9, 10]. We start with the time-independent Schrödinger equation

$$\frac{\mathrm{d}^2\psi(x)}{\mathrm{d}x^2} + k^2(x)\psi(x) = 0, \tag{2.109}$$

where

$$k^2(x) = \frac{2m}{\hbar^2}[E - V(x)] \tag{2.110}$$

and $V(x)$ is the potential which asymptotes to a constant

$$V(x \to \pm\infty) \to V_{\pm\infty}. \tag{2.111}$$

Therefore, the solutions in the asymptotic regions are given by

$$\psi(x \to \pm\infty) \approx \begin{cases} \alpha\dfrac{e^{ik_{-\infty}x}}{\sqrt{k_{-\infty}}} + \beta\dfrac{e^{-ik_{-\infty}x}}{\sqrt{k_{-\infty}}} & \text{for } x \to -\infty \\ \dfrac{e^{ik_\infty x}}{\sqrt{k_\infty}} & \text{for } x \to \infty \end{cases}, \tag{2.112}$$

where

$$k_{\pm\infty} = \frac{\sqrt{2m(E - V_{\pm\infty})}}{\hbar}. \tag{2.113}$$

The reflection and transmission probabilities are defined by

$$R = \left|\frac{\beta}{\alpha}\right|^2 \quad \text{and} \quad T = \left|\frac{1}{\alpha}\right|^2. \tag{2.114}$$

From $T + R = 1$, we have the relation

$$|\alpha|^2 - |\beta|^2 = 1. \tag{2.115}$$

For any region, we assume the solutions

$$\psi(x) = a(x)\frac{e^{i\varphi(x)}}{\sqrt{\varphi'(x)}} + b(x)\frac{e^{-i\varphi(x)}}{\sqrt{\varphi'(x)}}, \tag{2.116}$$

where $\varphi'(x) \neq 0$. Here $\varphi(x)$ is real and $a(x)$ and $b(x)$ are complex. In the asymptotic regions, these solutions should reduce to equation (2.112). Thus, we have the conditions

$$\begin{aligned} \varphi'(x \to \pm\infty) &\to k_{\pm\infty} \\ a(x \to -\infty) &\to \alpha \\ a(x \to \infty) &\to 1 \\ b(x \to -\infty) &\to \beta \\ b(x \to \infty) &\to 0. \end{aligned} \tag{2.117}$$

We choose a gauge condition

$$\frac{d}{dx}\left[\frac{a(x)}{\sqrt{\varphi'(x)}}\right]e^{i\varphi(x)} + \frac{d}{dx}\left[\frac{b(x)}{\sqrt{\varphi'(x)}}\right]e^{-i\varphi(x)} = 0 \tag{2.118}$$

so that

$$\frac{d\psi(x)}{dx} = i\sqrt{\varphi'(x)}\left[a(x)e^{i\varphi(x)} - b(x)e^{-i\varphi(x)}\right]. \tag{2.119}$$

Thus, the second derivative is given by

$$\begin{aligned}\frac{d^2\psi(x)}{dx^2} &= -\frac{[\varphi'(x)]^2}{\sqrt{\varphi'(x)}}\left[a(x)e^{i\varphi(x)} + b(x)e^{-i\varphi(x)}\right] + \frac{2i\varphi'(x)}{\sqrt{\varphi'(x)}}\frac{da(x)}{dx}e^{i\varphi(x)} \\ &\quad -i\frac{\varphi''(x)}{\sqrt{\varphi'(x)}}b(x)e^{-i\varphi(x)} \end{aligned} \tag{2.120}$$

$$\begin{aligned} &= -\frac{[\varphi'(x)]^2}{\sqrt{\varphi'(x)}}\left[a(x)e^{i\varphi(x)} + b(x)e^{-i\varphi(x)}\right] - \frac{2i\varphi'(x)}{\sqrt{\varphi'(x)}}\frac{db(x)}{dx}e^{-i\varphi(x)} \\ &\quad +i\frac{\varphi''(x)}{\sqrt{\varphi'(x)}}a(x)e^{i\varphi(x)}. \end{aligned} \tag{2.121}$$

Comparing the above equation with equation (2.109), we obtain

$$\begin{aligned}\frac{da(x)}{dx} &= \frac{1}{2\varphi'(x)}\left[\varphi''(x)b(x)e^{-2i\varphi(x)}\right. \\ &\quad \left. +i\left\{k^2(x) - \varphi'(x)^2\right\}\left\{a(x) + b(x)e^{-2i\varphi(x)}\right\}\right] \end{aligned} \tag{2.122}$$

$$\begin{aligned}\frac{db(x)}{dx} &= \frac{1}{2\varphi'(x)}\left[\varphi''(x)a(x)e^{2i\varphi(x)}\right. \\ &\quad \left. -i\left\{k^2(x) - \varphi'(x)^2\right\}\left\{b(x) + a(x)e^{2i\varphi(x)}\right\}\right]. \end{aligned} \tag{2.123}$$

For any complex number, we have

$$\frac{d|a(x)|}{dx} = \frac{1}{2|a(x)|}\left[a^*(x)\frac{da(x)}{dx} + a(x)\frac{da^*(x)}{dx}\right]. \tag{2.124}$$

Using equation (2.122), we obtain

$$\begin{aligned}\frac{d|a(x)|}{dx} &= \frac{1}{2|a(x)|}\frac{1}{2\varphi'(x)}\left[\varphi''(x)\left\{a^*(x)b(x)e^{-2i\varphi(x)} + a(x)b^*(x)e^{2i\varphi(x)}\right\}\right. \\ &\quad \left. +i\left\{k^2(x) - \varphi'(x)^2\right\}\left\{a^*(x)b(x)e^{-2i\varphi(x)} + a(x)b^*(x)e^{2i\varphi(x)}\right\}\right] \end{aligned} \tag{2.125}$$

Then,

$$\frac{d|a(x)|}{dx} = \frac{1}{2|a(x)|}\frac{1}{2\varphi'(x)}\text{Re}\left(\left[\varphi''(x) + i\left\{k^2(x) - \varphi'(x)^2\right\}\right]a^*(x)b(x)e^{-2i\varphi(x)}\right). \tag{2.126}$$

Using an inequality

$$\text{Re}(AB) \leq |A||B|, \tag{2.127}$$

we obtain

$$\frac{\mathrm{d}|a(x)|}{\mathrm{d}x} \leq \vartheta(x)|b(x)|, \tag{2.128}$$

where

$$\vartheta(x) = \frac{\sqrt{[\varphi''(x)]^2 + [k^2(x) - \{\varphi'(x)\}^2]^2}}{2|\varphi'(x)|}. \tag{2.129}$$

We introduce a new positive function $h(x)$ defined by $h(x) \equiv |\varphi'(x)|$. Then,

$$\vartheta(x) = \frac{\sqrt{[h'(x)]^2 + [k^2(x) - h^2(x)]^2}}{2h(x)}. \tag{2.130}$$

Using equation (2.115), we have

$$|a(x)|^2 - |b(x)|^2 = 1. \tag{2.131}$$

Thus, we obtain

$$\frac{\mathrm{d}|a(x)|}{\mathrm{d}x} \leq \vartheta(x)\sqrt{a^2(x) - 1}. \tag{2.132}$$

Integrating the above inequality gives

$$\left[\cosh^{-1}|a(x)|\right]_{x_i}^{x_f} \leq \int_{x_i}^{x_f} \vartheta(x)\mathrm{d}x. \tag{2.133}$$

Using the conditions in equation (2.117), when $x_i \to -\infty$ and $x_f \to \infty$, we obtain

$$\cosh^{-1}|\alpha| \leq \int_{-\infty}^{\infty} \vartheta(x)\mathrm{d}x. \tag{2.134}$$

Therefore, we obtain

$$|\alpha| \leq \cosh\left[\int_{-\infty}^{\infty} \vartheta(x)\mathrm{d}x\right]. \tag{2.135}$$

From equation (2.114), this leads to

$$T \geq \operatorname{sech}^2\left[\int_{-\infty}^{\infty} \vartheta(x)\mathrm{d}x\right]. \tag{2.136}$$

This is the rigorous bound on the transmission probability which will be applied to black hole systems in the next chapter.

2.1.8   Summary in quantum mechanics

So far, we have reviewed the Schrödinger equation and some one-dimensional problems with various potentials such as a delta function potential, a rectangular barrier potential, an Eckart potential, and a Hulthen potential. All the potentials can be summarized in table II.1.

Name	Scattering	Tunneling
A delta function potential	able to occur	no occurrence
Rectangular barrier potential	able to occur	able to occur
An Eckart potential	able to occur	no occurrence
A Hulthen potential	able to occur	able to occur

Table II.1: All the potentials

The transmission probabilities for each potential are summarized in table II.2. These potentials are useful for studying Hawking radiation since one-dimensional problems in quantum mechanics and Hawking radiation are quite similar in terms of their mathematical structures. In particular, equations of motion concerning Hawking radiation in the black hole backgrounds take the form of the Schrödinger-like equations with various potentials. Moreover, the rigorous bounds on the transmission probabilities have been derived. These bounds are the heart of this dissertation. After this, the derivation and general aspects of black holes and their classification will be introduced.

Name	Transmission probability (T)
A delta function potential	$T = \frac{k^2}{k^2 + k_0^2}$
Rectangular barrier potential	$T = \frac{4k^2 q^2}{4k^2 q^2 + k_0^4 \sin^2(2qa)}$
An Eckart potential	$T = \frac{\sinh(\pi k_{-\infty} a)\sinh(\pi k_{\infty} a)}{\sinh^2(\pi \bar{k} a) + \cos^2(\pi\sqrt{1/4 - 2mV_0 a^2/\hbar^2})}$
A Hulthen potential	$T = |t|^2$, where t is from equation (2.105)

Table II.2: The summary of the transmission probabilities for each potential.

2.2   Black holes

2.2.1   The Schwarzschild solution

General relativity describes gravity in terms of an elegant mathematical structure. There is no concept of gravitational force in this theory. Instead, gravitation is manifested by the curvature of spacetime. One of the consequences of general relativity is the existence of black holes. For most of these matters, we follow [22].

The geometry of spacetime representing gravitation is described by **Ein-**

stein's field equation

$$R_{\mu\nu} - \frac{1}{2}Rg_{\mu\nu} = 8\pi GT_{\mu\nu}, \tag{2.137}$$

where $R_{\mu\nu}$ is the Ricci tensor, R is the Ricci scalar, $g_{\mu\nu}$ is the metric tensor, G is Newton's gravitational constant, and $T_{\mu\nu}$ is the energy-momentum tensor. This equation explains how spacetime is curved by mass and energy. The first exact solution to Einstein's field equation was obtained by Karl Schwarzschild in 1916. To solve the equation, he considered the empty spacetime outside a massive spherical object, such as a star, and assumed the spacetime to be static, spherically symmetric, and asymptotically flat. Under these assumptions, he obtained the solution

$$ds^2 = -\left(1 - \frac{2GM}{r}\right)dt^2 + \left(1 - \frac{2GM}{r}\right)^{-1}dr^2 + r^2d\Omega^2, \tag{2.138}$$

where M is the mass of the massive spherical object and $d\Omega^2 = d\theta^2 + \sin^2\theta d\phi^2$ is the metric on a unit two-sphere. This solution is known as the **Schwarzschild metric**. Moreover, according to **Birkhoff's theorem**, the Schwarzschild solution presents a unique solution in a vacuum with a spherical symmetry. There are two singularities in this solution, at $r = 0$ and $r = 2GM$. The point $r = 0$ is a true singularity while the surface $r = 2GM$ is not; it is just a coordinate singularity. To see this, consider a coordinate-independent quantity such as the scalar $R^{\mu\nu\rho\sigma}R_{\mu\nu\rho\sigma}$. The calculation yields [22]

$$R^{\mu\nu\rho\sigma}R_{\mu\nu\rho\sigma} = \frac{48G^2M^2}{r^6}, \tag{2.139}$$

where $R_{\mu\nu\rho\sigma}$ is the Riemann tensor. This shows that $r = 0$ is a true singularity while the surface $r = 2GM$ is not.

2.2.2 Schwarzschild black holes

In this section, we will explore the curvature of a spherically symmetric spacetime generated by a massive spherical body of mass M whose radius is smaller than $2GM$. We start by considering radial null geodesics, given by [22]

$$ds^2 = 0 = -\left(1 - \frac{2GM}{r}\right)dt^2 + \left(1 - \frac{2GM}{r}\right)^{-1}dr^2. \tag{2.140}$$

That is

$$\frac{dt}{dr} = \pm\left(1 - \frac{2GM}{r}\right)^{-1}. \tag{2.141}$$

This describes light paths on the spacetime. When a ray of light approaches $r = 2GM$, we obtain $\mathrm{d}t/\mathrm{d}r \to \pm\infty$. It follows that from an observer's point of view, he sees that light never seems to cross $r = 2GM$. From the light's point of view, however, the proper time light takes to travel from outside $r = 2GM$ to the region $r < 2GM$ is given by [23]

$$\tau = \frac{r_{\mathrm{out}}^{3/2}}{\sqrt{2GM}} \left[\frac{\pi}{2} - \arcsin \sqrt{\frac{r_{\mathrm{in}}}{r_{\mathrm{out}}}} + \sqrt{\left(\frac{r_{\mathrm{in}}}{r_{\mathrm{out}}} \right) \left(1 - \frac{r_{\mathrm{in}}}{r_{\mathrm{out}}} \right)} \right], \qquad (2.142)$$

where $r_{\mathrm{out}} > 2GM$ and $r_{\mathrm{in}} < 2GM$. We have determined that τ is finite. This indicates that it is not problematic for light or even for anything to pass $r = 2GM$. To determine the behavior of light when crossing $r = 2GM$ boundary, let us transform the coordinate t into the new coordinate v defined by [22]

$$v = t + r_*, \qquad (2.143)$$

where r_* is the **tortoise coordinate** given by

$$r_* = r + 2GM \ln \left(\frac{r}{2GM} - 1 \right). \qquad (2.144)$$

These new coordinates (v, r, θ, ϕ) are known as **Eddington-Finkelstein coordinates**. According to these terms, the Schwarzschild solution in equation (2.138) becomes

$$\mathrm{d}s^2 = - \left(1 - \frac{2GM}{r} \right) \mathrm{d}v^2 + 2\mathrm{d}v\mathrm{d}r + r^2 \mathrm{d}\Omega^2. \qquad (2.145)$$

In this new form of the solution, $r = 2GM$ is no longer a singularity. It only presents as a coordinate singularity when the original coordinates are used (t, r, θ, ϕ), as we have mentioned above. Consider radial null geodesics, as we have done in equation (2.140), in the new coordinates given by

$$\mathrm{d}s^2 = 0 = - \left(1 - \frac{2GM}{r} \right) \mathrm{d}v^2 + 2\mathrm{d}v\mathrm{d}r. \qquad (2.146)$$

That is

$$\frac{\mathrm{d}v}{\mathrm{d}r} = 0 \quad \text{or} \quad \frac{\mathrm{d}v}{\mathrm{d}r} = 2 \left(1 - \frac{2GM}{r} \right)^{-1}. \qquad (2.147)$$

Using equation (2.143), $\mathrm{d}v/\mathrm{d}r = 0$ or $v = \text{constant}$ corresponds to $\mathrm{d}t/\mathrm{d}r = -(1 - 2GM/r)^{-1}$, which is negative for $r > 2GM$. This is the ingoing null geodesics. On the other hand, $\mathrm{d}v/\mathrm{d}r = 2(1 - 2GM/r)^{-1}$ corresponds to $\mathrm{d}t/\mathrm{d}r = (1 - 2GM/r)^{-1}$, which is positive for $r > 2GM$. This is the outgoing null geodesics. This means that if light starts from $r > 2GM$ and travels in the direction of decreasing r, it can cross $r = 2GM$ into $r < 2GM$ and continue to travel in the same direction towards the massive spherical object of mass M whose radius is smaller than $2GM$.

If light starts from $r < 2GM$, it still travels in the direction of decreasing r. So, it cannot cross $r = 2GM$ into $r > 2GM$; it is confined to the region $r < 2GM$. That is, light passing $r = 2GM$ from outside cannot come back. As a result, we can never see that object. Therefore, it obtains the name **black hole**. The surface $r = 2GM$ is called an **event horizon** because we can never see any event occurring inside the sphere $r = 2GM$. Despite not being able to observe it, we can indirectly detect a black hole through its gravitational field. The Schwarzschild spacetime is shown in Figure 2.11.
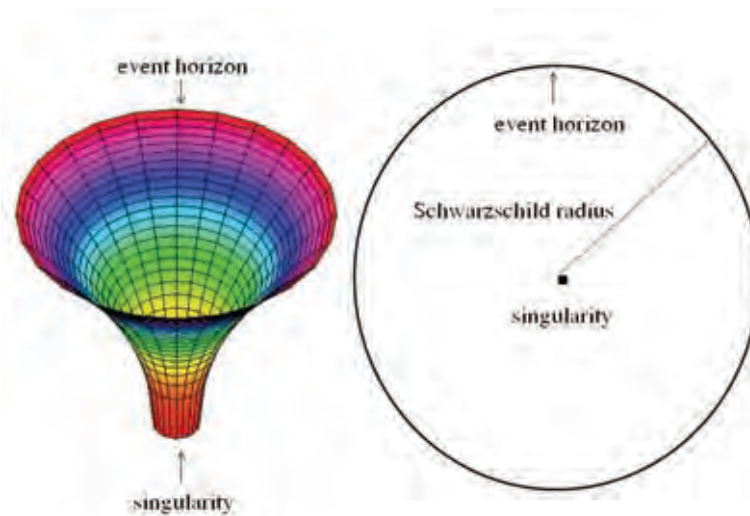
Figure 2.11: The Schwarzschild spacetime.

Nowadays, we believe that black holes exist in nature from astrophysical observations. They are possibly formed by the gravitational collapse of very massive stars. A star is generally supported by internal pressure resulting from nuclear fusion. When all the nuclear fuel has been consumed, a star starts to collapse as its gravitational attraction starts overcoming the pressure. If this collapse is not stopped, a star continuously decreases in size until it becomes smaller than $2GM$ and the process ultimately results in the formation of a black hole.

2.2.3 Reissner-Nordström black holes

In this section, we consider a more general situation where a black hole is charged. In this case, we still assume the static, spherically symmetric, and asymptotically flat spacetime. However, outside a massive spherical object, a vacuum no longer persists because of the presence of charges. Under these assumptions, the solution

to Einstein's field equation (2.137) is given by [22]

$$ds^2 = -\Delta dt^2 + \Delta^{-1} dr^2 + r^2 d\Omega^2, \tag{2.148}$$

where

$$\Delta = 1 - \frac{2GM}{r} + \frac{G\left(Q^2 + P^2\right)}{r^2}. \tag{2.149}$$

This solution is known as the **Reissner-Nordström metric**. In this expression, M is the mass of the massive spherical object, Q is the total electric charge, and P is the total magnetic charge. There are three singularities in this solution, at $r = 0$ and $r = r_\pm$, where

$$r_\pm = GM \pm \sqrt{G^2 M^2 - G\left(Q^2 + P^2\right)}. \tag{2.150}$$

Like the Schwarzschild case, the point $r = 0$ is a true singularity while the surfaces $r = r_\pm$ are not; they are just coordinate singularities. We can check this by computing the scalar $R^{\mu\nu\rho\sigma} R_{\mu\nu\rho\sigma}$. The calculation yields

$$R^{\mu\nu\rho\sigma} R_{\mu\nu\rho\sigma} = \frac{48\left[GMr - G\left(Q^2 + P^2\right)\right]^2}{r^8} + \frac{2G^2\left(Q^2 + P^2\right)}{r^8}. \tag{2.151}$$

This shows that $r = 0$ is a true singularity while the surfaces $r = r_\pm$ are not. The event horizons are located at $r = r_\pm$. There are possibly zero, one, or two event horizons depending on the values of GM^2 and $Q^2 + P^2$.

Case I: $GM^2 < Q^2 + P^2$ **[22]**

In this case, there are no coordinate singularities and hence no event horizons. However, there is still a true singularity at $r = 0$. Since there is no event horizon surrounding the singularity, it is called a **naked singularity**. Anything could travel to the singularity and could come back. A massive spherical object in this case is not a black hole since it could be seen by an observer. The **cosmic censorship conjecture**, however, states that all singularities must be surrounded by event horizons. Consequently, the situation in this case is considered to be unphysical.

Case II: $GM^2 = Q^2 + P^2$ **[22]**

In this case, there is only a coordinate singularity and hence only one event horizon located at $r = GM$. A black hole, in this case, is thus known as an **extremal**

Reissner-Nordström black hole. The total energy is equal to the energy contribution from the electromagnetic fields. An observer can cross the event horizon into the black hole and come back to the outside, but another asymptotically flat spacetime. This is shown in Figure 2.12
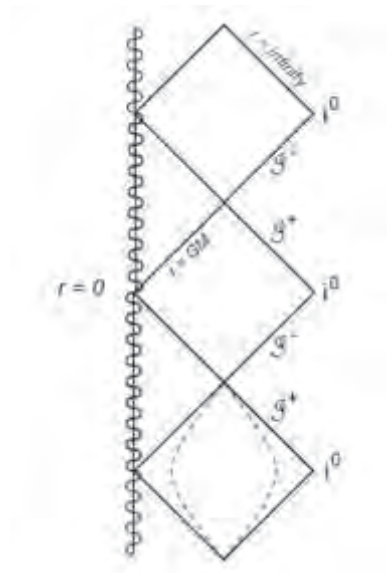
Figure 2.12: The Penrose diagram for an extremal black hole [7].

An extremal black hole plays a role in supersymmetric theories. However, it is unstable because adding even a small amount of mass to it can cause it to become a black hole, akin to the next case.

Case III: $GM^2 > Q^2 + P^2$ **[22]**

As for this case, there are two coordinate singularities and hence two event horizons located at $r = r_\pm$, the inner one being at $r = r_-$ and the outer one at $r = r_+$, as shown in Figure 2.13. This is a **realistic black hole**. The energy from the electromagnetic fields is less than the total energy. The surface $r = r_+$ has the same role as the surface $r = 2GM$ of the Schwarzschild black hole. When an observer passes the surface $r = r_+$, he necessarily moves in the direction of decreasing r. Another observer outside this charged black hole sees the same phenomena as he is outside the Schwarzschild black hole; he sees that the infalling observer approaches the surface $r = r_+$ and never seems to cross it. For the infalling observer, after passing the surface $r = r_+$, he continues to move in the direction of decreasing r until he arrives at the surface $r = r_-$. After crossing the surface $r = r_-$, he can choose to move to the singularity at $r = 0$ or to go back to the surface $r = r_-$ and cross it again. This time, he is forced to move in the direction of increasing r

until he arrives at the surface $r = r_+$ and cross it to the outside of the black hole which is not the same place as the original location of entrance. He can choose to go back into the black hole again, which is a different black hole from the first black hole he entered, and can choose to repeat the journey as many times as he desires. This is shown in Figure 2.14
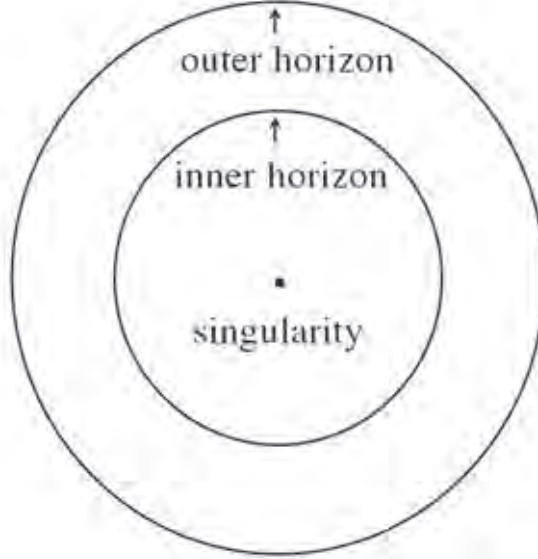
Figure 2.13: The realistic Reissner-Nordström black hole.

2.2.4 Kerr black holes

So far, we have considered Schwarzschild black holes and Reissner-Nordström black holes, both of which are non-rotating black holes. In this section, we consider rotating black holes. Unlike non-rotating black holes, the assumptions based on a static and spherically symmetric spacetime can no longer be made for rotating black holes. They can, however, possess axial symmetry around the axis of rotation. Under this assumption, the solution to Einstein's field equation (2.137) in the **Boyer-Lindquist coordinates** is given by [24, 25]

$$\mathrm{d}s^2 = -\frac{\Delta}{\Sigma}\left(\mathrm{d}t - a\sin^2\theta \mathrm{d}\phi\right)^2 + \frac{\sin^2\theta}{\Sigma}\left[a\mathrm{d}t - \left(r^2 + a^2\right)\mathrm{d}\phi\right]^2 + \frac{\Sigma}{\Delta}\mathrm{d}r^2 + \Sigma\mathrm{d}\theta^2,$$
(2.152)

where

$$\Delta(r) = r^2 - 2GMr + a^2 \quad\text{and}\quad \Sigma(r,\theta) = r^2 + a^2\cos^2\theta.$$
(2.153)

This solution is known as the **Kerr metric**. In this expression, M is the mass of the black hole and $a = J/M$ is the angular momentum per unit mass, where J is

Figure 2.14: The Penrose diagram for a realistic black hole [7].

the angular momentum. There are three singularities in this solution, at $\Sigma = 0$ and $r = r_\pm$, where

$$r_\pm = GM \pm \sqrt{G^2 M^2 - a^2}. \tag{2.154}$$

Like the previous cases, $\Sigma = 0$ is a true singularity while the surfaces $r = r_\pm$ are not; they are just coordinate singularities. We can check that the scalar $R^{\mu\nu\rho\sigma} R_{\mu\nu\rho\sigma}$ diverges at $\Sigma = 0$. As in the Reissner-Nordström black hole, the event horizons are located at $r = r_\pm$. There are possibly zero, one, or two event horizons depending on the values of GM and a. The $GM < a$ case represents a naked singularity and hence is not a black hole. The $GM = a$ case is an extremal black hole, which is unstable. The $GM > a$ case signifies a usual black hole.

Now, we turn to a true singularity at $\Sigma = 0$. Since $\Sigma = r^2 + a^2 \cos^2 \theta$ results from the sum of two nonnegative quantities, it can vanish if both of the quantities vanish. That is

$$r = 0 \quad \text{and} \quad \theta = \frac{\pi}{2}. \tag{2.155}$$

The result will be interpreted here. Consider the Kerr metric in equation (2.152). If we take the limit $M \to 0$, we will obtain [22]

$$ds^2 = -dt^2 + \frac{r^2 + a^2 \cos^2 \theta}{r^2 + a^2} dr^2 + \left(r^2 + a^2 \cos^2 \theta\right)^2 d\theta^2 + \left(r^2 + a^2\right) \sin^2 \theta d\phi^2. \tag{2.156}$$

This is the metric of a flat spacetime in ellipsoidal coordinates, which are related to Cartesian coordinates by

$$x = \sqrt{r^2 + a^2}\sin\theta\cos\phi$$
$$y = \sqrt{r^2 + a^2}\sin\theta\sin\phi. \tag{2.157}$$
$$z = r\cos\theta$$

Thus, the singularity $r = 0$ and $\theta = \pi/2$ corresponds to

$$x^2 + y^2 = a^2. \tag{2.158}$$

This is a ring singularity. The rotation of the black hole spreads the Schwarzschild point singularity out over a ring. An observer can go inside the ring and exit to another spacetime, a different spacetime from the first. The Kerr black hole is shown in Figure 2.15.
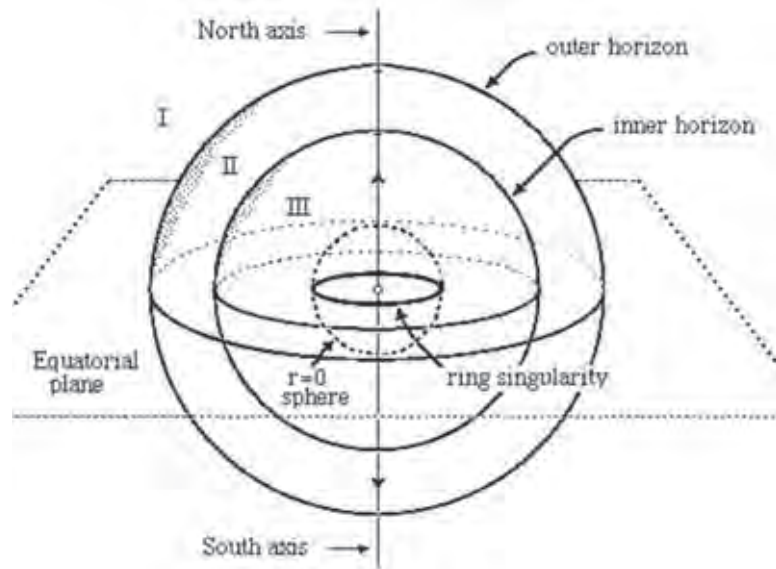
Figure 2.15: The Kerr black hole [26].

2.2.5 Kerr-Newman black holes

In this section, we consider a more general situation where a rotating black hole is charged. We still assume an axial symmetry around the axis of rotation. Under this assumption, the solution to Einstein's field equation (2.137) in the Boyer-Lindquist coordinates is given by [27, 28]

$$ds^2 = -\frac{\Delta}{\Sigma}\left(dt - a\sin^2\theta d\phi\right)^2 + \frac{\sin^2\theta}{\Sigma}\left[a dt - \left(r^2 + a^2\right)d\phi\right]^2 + \frac{\Sigma}{\Delta}dr^2 + \Sigma d\theta^2, \tag{2.159}$$

where

$$\Delta(r) = r^2 - 2GMr + a^2 + Q^2 \quad \text{and} \quad \Sigma(r,\theta) = r^2 + a^2 \cos^2\theta. \tag{2.160}$$

This solution is known as the **Kerr-Newman metric**. In this expression, M is the mass of the black hole, $a = J/M$ is the angular momentum per unit mass, where J is the angular momentum, and Q is the charge of the black hole. There are three singularities in this solution, at $\Sigma = 0$ and $r = r_{\pm}$, where

$$r_{\pm} = GM \pm \sqrt{G^2 M^2 - a^2 - Q^2}. \tag{2.161}$$

Like the previous cases, $\Sigma = 0$ is a true singularity while the surfaces $r = r_{\pm}$ are not; they are just coordinate singularities.

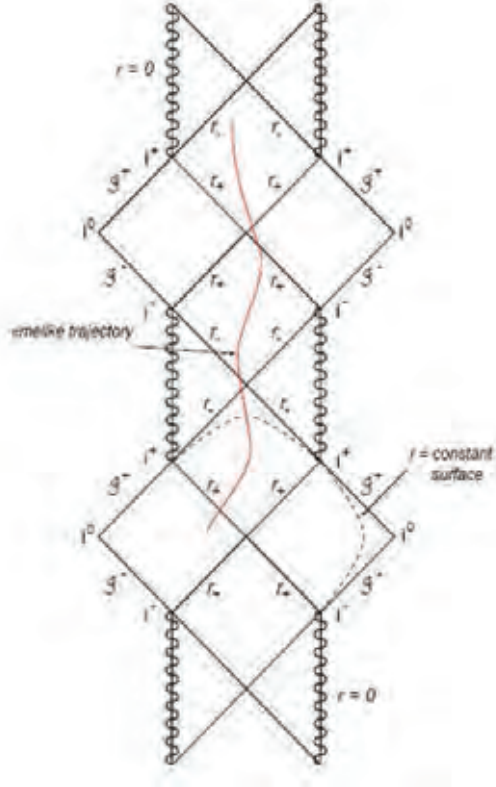As in the Kerr black hole, the event horizons are located at $r = r_{\pm}$. There are possibly zero, one, or two event horizons depending on the values of GM and $\sqrt{a^2 + Q^2}$. The $GM < \sqrt{a^2 + Q^2}$ case represents a naked singularity and hence is not a black hole. The $GM = \sqrt{a^2 + Q^2}$ case is an extremal black hole, which is unstable. The $GM > \sqrt{a^2 + Q^2}$ case signifies a usual black hole.

2.2.6   Summary in black holes

In the black hole section, we have reviewed the derivation and classification of classical black holes. A classical black hole signifies the belief that anything that enters a black hole cannot escape, not even light. As a result, it cannot directly be seen by an observer. A black hole is a singularity surrounded by a surface known as an event horizon, which acts as a boundary of the black hole. The singularity of a black hole is the spacetime region with infinite curvature, where all of the laws of physics break down. The event horizon separates the black hole from the rest of the universe. Anything can cross the event horizon within a finite time frame, while another observer simultaneously sees it approach the event horizon forever; meaning that the observer will never see it actually cross the event horizon.

In this chapter, we have introduced Schwarzschild black holes, Reissner-Nordström black holes, Kerr black holes and Kerr-Newman black holes. For non-rotating black holes such as Schwarzschild black holes and Reissner-Nordström black holes, their singularities are point singularities, whereas for rotating black holes such as Kerr black holes and Kerr-Newman black holes, their singularities become ring singularities as a result of rotation. The Schwarzschild black holes have only one event horizon while the others have two event horizons (in the

usual case). Here is the summary of different types of black holes in the standard (four-dimensional) general relativity as shown in Figure 2.16.
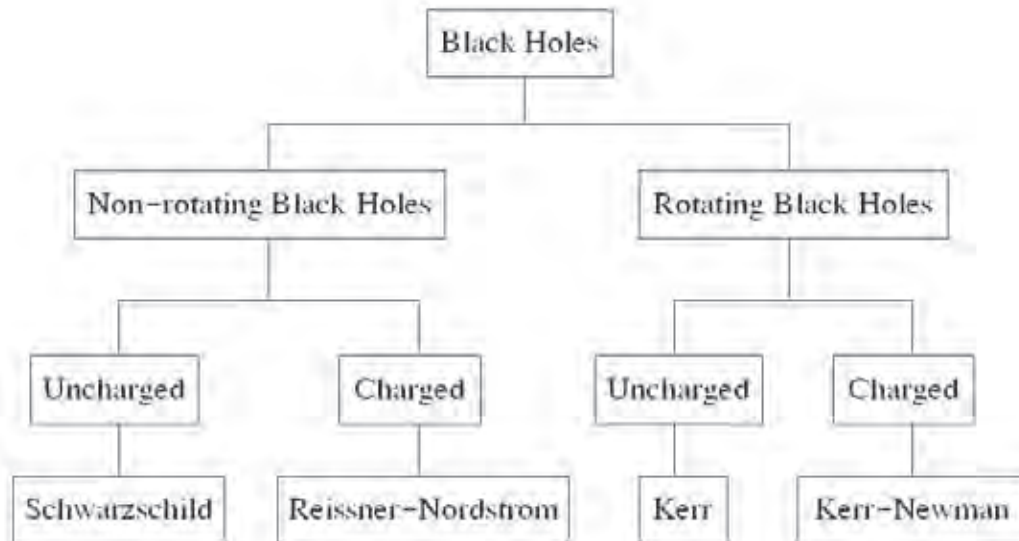
Figure 2.16: Classification of black holes.

In the next chapters, we will study quantum of black holes. In particular, we will study Hawking radiation emitted from various types of black holes.

Chapter III

Greybody factors for non-rotating black holes

In this chapter, the concept of greybody factors is introduced and greybody factor computation is performed for non-rotating black holes by placing some rigorous bounds developed by Boonserm and Visser [8, 9, 10]. We start by deriving the Regge-Wheeler equations for static and spherically symmetric black holes. After that, we will study the rigorous bounds on the greybody factors for massless scalar fields emitted from Reissner-Nordström black holes, Schwarzschild-Tangherlini black holes, charged dilatonic black holes in (2 + 1) dimensions, and charged dilatonic black holes in (3 + 1) dimensions. As for most of the contents in this chapter, we obtained the information from [29].

3.1 The Regge-Wheeler equations for static and spherically symmetric black holes

As outlined in chapter II, Stephen Hawking showed that a black hole can emit **Hawking radiation** [1] when the quantum effects are taken into account. We will start this section by studying Hawking radiation emitted from a static and spherically symmetric black hole in d dimensions.

A static and spherically symmetric black hole in d dimensions can be described by

$$\mathrm{d}s^2 = -A(r)\mathrm{d}t^2 + \frac{1}{B(r)}\mathrm{d}r^2 + r^2\mathrm{d}\Omega_{d-2}^2, \tag{3.1}$$

where $\mathrm{d}\Omega_{d-2}^2$ is the metric on $(d-2)$-sphere and is given by

$$\mathrm{d}\Omega_{d-2}^2 = \mathrm{d}\theta_1^2 + \sin^2\theta_1\mathrm{d}\theta_2^2 + \sin^2\theta_1\sin^2\theta_2\mathrm{d}\theta_3^2 + \ldots + \sin^2\theta_1\cdots\sin^2\theta_{d-3}\mathrm{d}\theta_{d-2}^2. \tag{3.2}$$

We are interested in a massless uncharged scalar field emitted from this black hole. The equation of motion of this scalar field on the black hole background is

$$\frac{1}{\sqrt{-g}}\partial_\mu\left(\sqrt{-g}g^{\mu\nu}\partial_\nu\Phi\right) = 0. \tag{3.3}$$

This equation is known as the **Klein-Gordon equation**. To calculate g, we explicitly write the metric tensor

$$
[g_{\mu\nu}] = \begin{bmatrix}
-A(r) & 0 & 0 & 0 & \cdots & 0 \\
0 & B^{-1}(r) & 0 & 0 & \cdots & 0 \\
0 & 0 & r^2 & 0 & \cdots & 0 \\
0 & 0 & 0 & r^2\sin^2\theta_1 & \cdots & 0 \\
\vdots & \vdots & \vdots & \vdots & \ddots & 0 \\
0 & 0 & 0 & 0 & \cdots & r^2\sin^2\theta_1\cdots\sin^2\theta_{d-3}
\end{bmatrix} \tag{3.4}
$$

and the inverse metric

$$
[g^{\mu\nu}] = \begin{bmatrix}
-A^{-1}(r) & 0 & 0 & 0 & \cdots & 0 \\
0 & B(r) & 0 & 0 & \cdots & 0 \\
0 & 0 & r^{-2} & 0 & \cdots & 0 \\
0 & 0 & 0 & r^{-2}\sin^{-2}\theta_1 & \cdots & 0 \\
\vdots & \vdots & \vdots & \vdots & \ddots & 0 \\
0 & 0 & 0 & 0 & \cdots & r^{-2}\sin^{-2}\theta_1\cdots\sin^{-2}\theta_{d-3}
\end{bmatrix}. \tag{3.5}
$$

Then, we obtain

$$
g = -\frac{A(r)}{B(r)} r^{2(d-2)} \sin^{2(d-3)}\theta_1 \sin^{2(d-4)}\theta_2 \cdots \sin^2\theta_{d-3}. \tag{3.6}
$$

Therefore, we have

$$
\sqrt{-g} = \sqrt{\frac{A(r)}{B(r)}} r^{d-2} \sin^{d-3}\theta_1 \sin^{d-4}\theta_2 \cdots \sin\theta_{d-3}. \tag{3.7}
$$

Expanding equation (3.3) gives

$$
\frac{1}{\sqrt{-g}}\frac{\partial}{\partial t}\left(\sqrt{-g}\,g^{tt}\frac{\partial\Phi}{\partial t}\right) + \frac{1}{\sqrt{-g}}\frac{\partial}{\partial r}\left(\sqrt{-g}\,g^{rr}\frac{\partial\Phi}{\partial r}\right)
$$
$$
+ \left[\frac{1}{\sqrt{-g}}\frac{\partial}{\partial\theta_1}\left(\sqrt{-g}\,g^{\theta_1\theta_1}\frac{\partial\Phi}{\partial\theta_1}\right) + \ldots + \frac{1}{\sqrt{-g}}\frac{\partial}{\partial\theta_{d-3}}\left(\sqrt{-g}\,g^{\theta_{d-3}\theta_{d-3}}\frac{\partial\Phi}{\partial\theta_{d-3}}\right)\right]
$$
$$
+ \frac{1}{\sqrt{-g}}\frac{\partial}{\partial\theta_{d-2}}\left(\sqrt{-g}\,g^{\theta_{d-2}\theta_{d-2}}\frac{\partial\Phi}{\partial\theta_{d-2}}\right) = 0.
$$

We observe that $\sqrt{-g}$ is independent of t and θ_{d-2}. Then, we obtain

$$
\frac{\partial}{\partial t}\left(g^{tt}\frac{\partial\Phi}{\partial t}\right) + \frac{1}{\sqrt{-g}}\frac{\partial}{\partial r}\left(\sqrt{-g}\,g^{rr}\frac{\partial\Phi}{\partial r}\right) + \left[\frac{1}{\sqrt{-g}}\frac{\partial}{\partial\theta_1}\left(\sqrt{-g}\,g^{\theta_1\theta_1}\frac{\partial\Phi}{\partial\theta_1}\right)\right.
$$
$$
\left. + \ldots + \frac{1}{\sqrt{-g}}\frac{\partial}{\partial\theta_{d-3}}\left(\sqrt{-g}\,g^{\theta_{d-3}\theta_{d-3}}\frac{\partial\Phi}{\partial\theta_{d-3}}\right)\right] + \frac{\partial}{\partial\theta_{d-2}}\left(g^{\theta_{d-2}\theta_{d-2}}\frac{\partial\Phi}{\partial\theta_{d-2}}\right) = 0.
$$

Substituting $g^{\mu\nu}$ into the above equation gives

$$-\frac{1}{A(r)}\frac{\partial^2\Phi}{\partial t^2} + \sqrt{\frac{B(r)}{A(r)}}r^{2-d}\frac{\partial}{\partial r}\left[\sqrt{\frac{A(r)}{B(r)}}r^{d-2}B(r)\frac{\partial\Phi}{\partial r}\right]$$

$$+\left[\frac{1}{r^2\sin^{d-3}\theta_1}\frac{\partial}{\partial\theta_1}\left(\sin^{d-3}\theta_1\frac{\partial\Phi}{\partial\theta_1}\right) + \cdots\right.$$

$$+\frac{1}{r^2\sin^2\theta_1\cdots\sin^2\theta_{d-4}\sin\theta_{d-3}}\frac{\partial}{\partial\theta_{d-3}}\left(\sin\theta_{d-3}\frac{\partial\Phi}{\partial\theta_{d-3}}\right)\right]$$

$$+\frac{1}{r^2\sin^2\theta_1\cdots\sin^2\theta_{d-3}}\frac{\partial^2\Phi}{\partial\theta_{d-2}^2} = 0. \qquad (3.8)$$

We assume the solution to be

$$\Phi(t,r,\Omega) = e^{i\omega t}\varphi_\ell(r)Y_{\ell m}(\Omega), \qquad (3.9)$$

where ω is the frequency of the wave and $Y_{\ell m}(\Omega)$ are the spherical harmonics on the $(d-2)$-dimensional sphere. Then,

$$\frac{\varphi_\ell(r)Y_{\ell m}(\Omega)}{A(r)}\omega^2 e^{i\omega t} + \frac{e^{i\omega t}Y_{\ell m}(\Omega)}{r^{d-2}}\sqrt{\frac{B(r)}{A(r)}}\frac{\mathrm{d}}{\mathrm{d}r}\left[\sqrt{\frac{A(r)}{B(r)}}r^{d-2}B(r)\frac{\mathrm{d}\varphi_\ell(r)}{\mathrm{d}r}\right]$$

$$+ e^{i\omega t}\varphi_\ell(r)\left[\frac{1}{r^2\sin^{d-3}\theta_1}\frac{\partial}{\partial\theta_1}\left(\sin^{d-3}\theta_1\frac{\partial Y_{\ell m}(\Omega)}{\partial\theta_1}\right) + \cdots\right.$$

$$+\frac{1}{r^2\sin^2\theta_1\cdots\sin^2\theta_{d-4}\sin\theta_{d-3}}\frac{\partial}{\partial\theta_{d-3}}\left(\sin\theta_{d-3}\frac{\partial Y_{\ell m}(\Omega)}{\partial\theta_{d-3}}\right)\right]$$

$$+\frac{e^{i\omega t}\varphi_\ell(r)}{r^2\sin^2\theta_1\cdots\sin^2\theta_{d-3}}\frac{\partial^2 Y_{\ell m}(\Omega)}{\partial\theta_{d-2}^2} = 0.$$

Multiplying the above equation by $r^2/\left[e^{i\omega t}\varphi_\ell(r)Y_{\ell m}(\Omega)\right]$ gives

$$\frac{\omega^2 r^2}{A(r)} + \frac{1}{r^{d-4}\varphi_\ell(r)}\sqrt{\frac{B(r)}{A(r)}}\frac{\mathrm{d}}{\mathrm{d}r}\left[\sqrt{\frac{A(r)}{B(r)}}r^{d-2}B(r)\frac{\mathrm{d}\varphi_\ell(r)}{\mathrm{d}r}\right]$$

$$+\frac{1}{Y_{\ell m}(\Omega)}\left[\frac{1}{\sin^{d-3}\theta_1}\frac{\partial}{\partial\theta_1}\left(\sin^{d-3}\theta_1\frac{\partial Y_{\ell m}(\Omega)}{\partial\theta_1}\right) + \cdots\right.$$

$$+\frac{1}{\sin^2\theta_1\cdots\sin^2\theta_{d-4}\sin\theta_{d-3}}\frac{\partial}{\partial\theta_{d-3}}\left(\sin\theta_{d-3}\frac{\partial Y_{\ell m}(\Omega)}{\partial\theta_{d-3}}\right)\right]$$

$$+\frac{1}{\sin^2\theta_1\cdots\sin^2\theta_{d-3}}\frac{1}{Y_{\ell m}(\Omega)}\frac{\partial^2 Y_{\ell m}(\Omega)}{\partial\theta_{d-2}^2} = 0. \qquad (3.10)$$

We see that the r-dependent part and the angular part in equation (3.10) are separated. Since the angular part satisfies

$$\frac{1}{\sin^{d-3}\theta_1}\frac{\partial}{\partial\theta_1}\left[\sin^{d-3}\theta_1\frac{\partial Y_{\ell m}(\Omega)}{\partial\theta_1}\right] + \cdots$$

$$+\frac{1}{\sin^2\theta_1\cdots\sin^2\theta_{d-4}\sin\theta_{d-3}}\frac{\partial}{\partial\theta_{d-3}}\left[\sin\theta_{d-3}\frac{\partial Y_{\ell m}(\Omega)}{\partial\theta_{d-3}}\right]$$

$$+\frac{1}{\sin^2\theta_1\cdots\sin^2\theta_{d-3}}\frac{\partial^2 Y_{\ell m}(\Omega)}{\partial\theta_{d-2}^2} = -\ell(\ell+d-3)Y_{\ell m}(\Omega),$$

equation (3.10) becomes

$$\frac{\omega^2 r^2}{A(r)} + \frac{1}{r^{d-4}\varphi_\ell(r)} \sqrt{\frac{B(r)}{A(r)}} \frac{\mathrm{d}}{\mathrm{d}r} \left[\sqrt{\frac{A(r)}{B(r)}} r^{d-2} B(r) \frac{\mathrm{d}\varphi_\ell(r)}{\mathrm{d}r} \right] - \ell(\ell + d - 3) = 0. \quad (3.11)$$

By multiplying the above equation with $A(r)\varphi_\ell(r)/r^2$, we obtain

$$\omega^2 \varphi_\ell(r) + \frac{1}{r^{d-2}} \sqrt{A(r)B(r)} \frac{\mathrm{d}}{\mathrm{d}r} \left[r^{d-2} \sqrt{A(r)B(r)} \frac{\mathrm{d}\varphi_\ell(r)}{\mathrm{d}r} \right]$$
$$- \ell(\ell + d - 3) \frac{A(r)\varphi_\ell(r)}{r^2} = 0. \quad (3.12)$$

To simplify this equation, let us introduce a new coordinate r_* related to r by

$$r_* = z(r), \quad (3.13)$$

where $z(r)$ is expected to simplify the equation (3.12). The use of the chain rule gives

$$\frac{\mathrm{d}}{\mathrm{d}r} = \frac{\mathrm{d}r_*}{\mathrm{d}r} \frac{\mathrm{d}}{\mathrm{d}r_*} = z'(r) \frac{\mathrm{d}}{\mathrm{d}r_*}. \quad (3.14)$$

Then, equation (3.12) becomes

$$\omega^2 \varphi_\ell(r) + \frac{1}{r^{d-2}} \sqrt{A(r)B(r)} z'(r) \frac{\mathrm{d}}{\mathrm{d}r_*} \left[r^{d-2} \sqrt{A(r)B(r)} z'(r) \frac{\mathrm{d}\varphi_\ell(r)}{\mathrm{d}r_*} \right]$$
$$- \ell(\ell + d - 3) \frac{A(r)\varphi_\ell(r)}{r^2} = 0.$$

If we choose

$$\frac{\mathrm{d}r_*}{\mathrm{d}r} = z'(r) = \frac{1}{\sqrt{A(r)B(r)}}, \quad (3.15)$$

we obtain

$$\omega^2 \varphi_\ell(r) + \frac{1}{r^{d-2}} \frac{\mathrm{d}}{\mathrm{d}r_*} \left[r^{d-2} \frac{\mathrm{d}\varphi_\ell(r)}{\mathrm{d}r_*} \right] - \ell(\ell + d - 3) \frac{A(r)\varphi_\ell(r)}{r^2} = 0. \quad (3.16)$$

The new coordinate r_* is known as the **tortoise coordinate** which has already been introduced in chapter II. Moreover, equation (3.16) can be made simpler by letting

$$\varphi_\ell(r) = r^{(2-d)/2} \psi_\ell(r). \quad (3.17)$$

Then,

$$\frac{\mathrm{d}\varphi_\ell(r)}{\mathrm{d}r_*} = r^{(2-d)/2} \frac{\mathrm{d}\psi_\ell(r)}{\mathrm{d}r_*} + \frac{2-d}{2} r^{-d/2} \sqrt{A(r)B(r)} \psi_\ell(r). \quad (3.18)$$

By multiplying the above equation with r^{d-2}, we obtain

$$r^{d-2} \frac{\mathrm{d}\varphi_\ell(r)}{\mathrm{d}r_*} = r^{(d-2)/2} \frac{\mathrm{d}\psi_\ell(r)}{\mathrm{d}r_*} + \frac{2-d}{2} r^{(d-4)/2} \sqrt{A(r)B(r)} \psi_\ell(r). \quad (3.19)$$

Differentiation with respect to r_* gives

$$\frac{\mathrm{d}}{\mathrm{d}r_*}\left[r^{d-2}\frac{\mathrm{d}\varphi_\ell(r)}{\mathrm{d}r_*}\right] = r^{(d-2)/2}\frac{\mathrm{d}^2\psi_\ell(r)}{\mathrm{d}r_*^2} + \frac{d-2}{2}r^{(d-4)/2}\sqrt{A(r)B(r)}\frac{\mathrm{d}\psi_\ell(r)}{\mathrm{d}r_*}$$

$$+\frac{2-d}{2}r^{(d-4)/2}\sqrt{A(r)B(r)}\frac{\mathrm{d}\psi_\ell(r)}{\mathrm{d}r_*}$$

$$+\frac{\mathrm{d}}{\mathrm{d}r_*}\left[\frac{2-d}{2}r^{(d-4)/2}\sqrt{A(r)B(r)}\right]\psi_\ell(r). \qquad (3.20)$$

The second term and the third term cancel and we are left with

$$\frac{\mathrm{d}}{\mathrm{d}r_*}\left[r^{d-2}\frac{\mathrm{d}\varphi_\ell(r)}{\mathrm{d}r_*}\right] = r^{(d-2)/2}\frac{\mathrm{d}^2\psi_\ell(r)}{\mathrm{d}r_*^2} - \frac{d-2}{2}\frac{\mathrm{d}}{\mathrm{d}r_*}\left[r^{(d-4)/2}\sqrt{A(r)B(r)}\right]\psi_\ell(r).$$
$$(3.21)$$

By substituting equation (3.17) and equation (3.21) into equation (3.16), we obtain

$$\omega^2 r^{(2-d)/2}\psi_\ell(r) + \frac{1}{r^{(d-2)/2}}\frac{\mathrm{d}^2\psi_\ell(r)}{\mathrm{d}r_*^2} - \frac{d-2}{2r^{d-2}}\frac{\mathrm{d}}{\mathrm{d}r_*}\left[r^{(d-4)/2}\sqrt{A(r)B(r)}\right]\psi_\ell(r)$$

$$- \ell(\ell+d-3)\frac{A(r)\psi_\ell(r)}{r^{(d+2)/2}} \qquad\qquad = 0.$$

Multiplying the above equation by $r^{(d-2)/2}$ gives

$$\omega^2\psi_\ell(r) + \frac{\mathrm{d}^2\psi_\ell(r)}{\mathrm{d}r_*^2} - \frac{d-2}{2r^{(d-2)/2}}\frac{\mathrm{d}}{\mathrm{d}r_*}\left[r^{(d-4)/2}\sqrt{A(r)B(r)}\right]\psi_\ell(r)$$

$$- \ell(\ell+d-3)\frac{A(r)\psi_\ell(r)}{r^2} \qquad\qquad = 0. \qquad (3.22)$$

We can write

$$\frac{\mathrm{d}^2\psi_\ell(r)}{\mathrm{d}r_*^2} + \left[\omega^2 - V_\ell(r)\right]\psi_\ell(r) = 0, \qquad (3.23)$$

where the effective potential $V_\ell(r)$ is given by

$$V_\ell(r) = \frac{\ell(\ell+d-3)A(r)}{r^2} + \frac{(d-2)\sqrt{A(r)B(r)}}{2r^{(d-2)/2}}\frac{\mathrm{d}}{\mathrm{d}r}\left[r^{(d-4)/2}\sqrt{A(r)B(r)}\right]. \quad (3.24)$$

The equation (3.23) is known as the **Regge-Wheeler equation**. It appears to be like the Schrödinger equation mentioned in chapter II. Figure 3.1 shows the potential, representing the curvature of spacetime. When the scalar field is scattered by this potential, part of it will be reflected back into the black hole and the rest will be transmitted out of the black hole. What is observed by an observer away from the black hole is the transmitted scalar field. This transmitted wave can be thought of as a greybody radiation because the incident wave, which is a blackbody radiation, is modified by the curvature of spacetime. Therefore, the transmission probability is called a **greybody factor**.

For one-dimensional scattering problems, there are a number of very general and robust bounds that can be placed on the greybody factors [8]. Further developments in generic contexts can be found in [9, 30, 31, 32]. For the developments
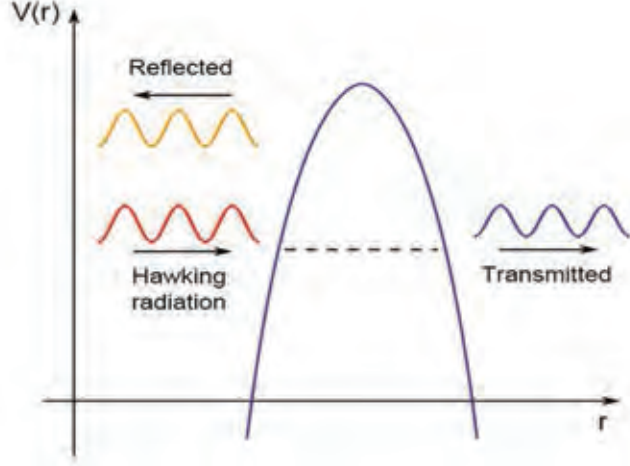
Figure 3.1: The scattering of Hawking radiation from the potential representing the curvature of spacetime [7].

concerning the applications to black hole greybody factors, see [11, 29, 33]. Using equation (2.136), the rigorous bound on the greybody factor is given by Boonserm and Visser [8, 9, 10]

$$T \geq \operatorname{sech}^2 \left[\int_{-\infty}^{\infty} \vartheta(r) \mathrm{d}r_* \right], \tag{3.25}$$

where

$$\vartheta(r) = \frac{\sqrt{[h'(r)]^2 + [\omega^2 - V_\ell(r) - h^2(r)]^2}}{2h(r)}, \tag{3.26}$$

for any positive function $h(r)$. If we choose $h(r) = \omega$, then

$$T \geq \operatorname{sech}^2 \left[\frac{1}{2\omega} \int_{-\infty}^{\infty} V_\ell(r) \mathrm{d}r_* \right]. \tag{3.27}$$

These methods of deriving rigorous bounds on the greybody factors are valid in all frequency regimes no matter ω is very low or very high.

3.2 Greybody factors for Reissner-Nordström black holes

The Reissner-Nordström metric is given by

$$\mathrm{d}s^2 = -\Delta(r)\mathrm{d}t^2 + \Delta^{-1}(r)\mathrm{d}r^2 + r^2\mathrm{d}\Omega^2, \tag{3.28}$$

where

$$\Delta(r) = 1 - \frac{2GM}{r} + \frac{G\left(Q^2 + P^2\right)}{r^2} \tag{3.29}$$

or

$$\Delta(r) = \left(1 - \frac{r_+}{r}\right)\left(1 - \frac{r_-}{r}\right), \tag{3.30}$$

with

$$r_+ = GM + \sqrt{G^2M^2 - G\left(Q^2 + P^2\right)} \tag{3.31}$$

is the outer event horizon and

$$r_- = GM - \sqrt{G^2M^2 - G\left(Q^2 + P^2\right)} \tag{3.32}$$

is the inner event horizon. Comparing equation (3.28) with equation (3.1), we find

$$A(r) = B(r) = \Delta(r) \quad \text{and} \quad d = 4. \tag{3.33}$$

We are interested in a massless uncharged scalar field emitted from this black hole. From equation (3.23), the Regge-Wheeler equation is

$$\frac{\mathrm{d}^2\psi_\ell(r)}{\mathrm{d}r_*^2} + \left[\omega^2 - V_\ell(r)\right]\psi_\ell(r) = 0. \tag{3.34}$$

In this case, from equation (3.15), the tortoise coordinate r_* is given by

$$\frac{\mathrm{d}r_*}{\mathrm{d}r} = \frac{1}{\Delta(r)} \tag{3.35}$$

and from equation (3.24), we have the effective potential

$$V_\ell(r) = \frac{\ell(\ell+1)\Delta(r)}{r^2} + \frac{\Delta(r)}{r}\frac{\mathrm{d}\Delta(r)}{\mathrm{d}r}. \tag{3.36}$$

The shape of the Reissner-Nordström potential with $\ell = 1$, $Q = 1$, and $M = 2$ is shown in Figure 3.2.
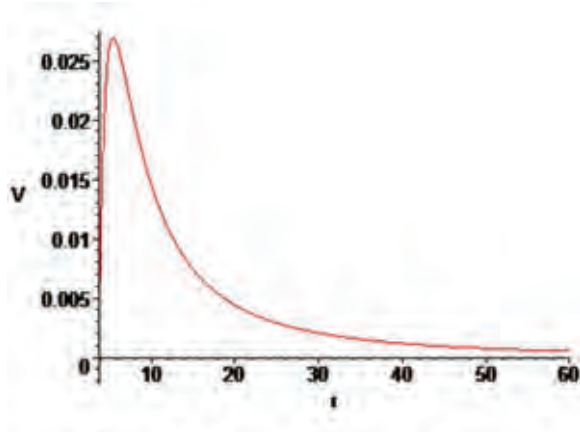
Figure 3.2: The Reissner-Nordström potential.

For a black hole with $GM^2 > Q^2 + P^2$, the rigorous bound on the greybody factor for $h(r) = \omega$ is given by

$$T \geq \mathrm{sech}^2\left[\frac{1}{2\omega}\int_{-\infty}^{\infty} V_\ell(r)\mathrm{d}r_*\right]. \tag{3.37}$$

Substituting the effective potential $V_\ell(r)$ from equation (3.36) gives

$$T \geq \text{sech}^2 \left[\frac{1}{2\omega} \int_{-\infty}^{\infty} \left\{ \frac{\ell(\ell+1)\Delta(r)}{r^2} + \frac{\Delta(r)}{r} \frac{d\Delta(r)}{dr} \right\} dr_* \right].$$ (3.38)

Using the tortoise coordinate in equation (3.35), we obtain

$$T \geq \text{sech}^2 \left[\frac{1}{2\omega} \int_{r_+}^{\infty} \left\{ \frac{\ell(\ell+1)}{r^2} + \frac{1}{r} \frac{d\Delta(r)}{dr} \right\} dr \right].$$ (3.39)

Substituting $\Delta(r)$ from equation (3.29) gives

$$T \geq \text{sech}^2 \left[\frac{1}{2\omega} \int_{r_+}^{\infty} \left\{ \frac{\ell(\ell+1)}{r^2} + \frac{2GM}{r^3} - \frac{2G(Q^2+P^2)}{r^4} \right\} dr \right].$$ (3.40)

Performing the integral gives

$$T \geq \text{sech}^2 \left[\frac{1}{2\omega} \left\{ \frac{\ell(\ell+1)}{r_+} + \frac{GM}{r_+^2} - \frac{2G(Q^2+P^2)}{3r_+^3} \right\} \right].$$ (3.41)

If the black holes have no electric charges or magnetic charges, then $r_+ = 2GM$ and the above bound reduces to

$$T \geq \text{sech}^2 \left[\frac{2\ell(\ell+1)+1}{8GM\omega} \right],$$ (3.42)

which is exactly the bound for the Schwarzschild black holes emitting spinless particles [11]. From Figure 3.3, the graph is plotted by setting $\ell = 1$, $G = 1$ $M = 20$, and $\omega = 2$ as a function of $q_{\text{total}} = \sqrt{Q^2 + P^2}$. The graph shows that when the magnitude of charges increase, the bound on the greybody factor decreases. That is, the charges resist the tunneling of the uncharged scalar particles.
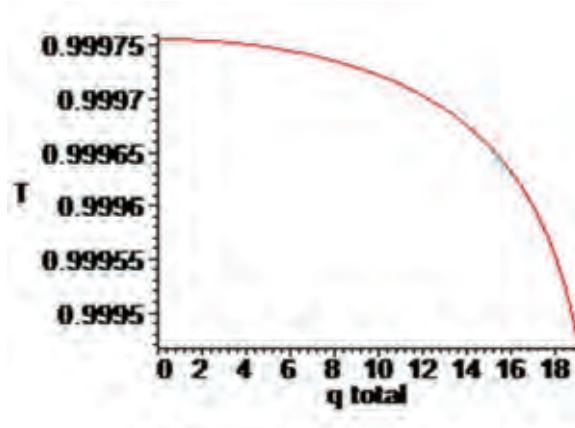
Figure 3.3: Dependence of the bound on the greybody factor on the Reissner-Nordström black hole charges.

3.3 Greybody factors for Schwarzschild-Tangherlini black holes

The Schwarzschild-Tangherlini metric in d dimensions is given by [7, 34]

$$\mathrm{d}s^2 = -f(r)\mathrm{d}t^2 + \frac{1}{f(r)}\mathrm{d}r^2 + r^2\mathrm{d}\Omega_{d-2}^2, \tag{3.43}$$

where

$$f(r) = 1 - \left(\frac{r_0}{r}\right)^{d-3} \tag{3.44}$$

and the Schwarzschild radius r_0 in d dimensions, which is the event horizon radius, is given by

$$r_0 = \frac{16\pi GM}{(d-2)\Omega_{d-2}}, \tag{3.45}$$

with

$$\Omega_{d-2} = \frac{2\pi^{(d-1)/2}}{\Gamma\left(\dfrac{d-1}{2}\right)}. \tag{3.46}$$

Comparing equation (3.43) with equation (3.1), we find

$$A(r) = B(r) = f(r). \tag{3.47}$$

We are interested in a massless uncharged scalar field emitted from this black hole. From equation (3.23), the derived Regge-Wheeler equation is

$$\frac{\mathrm{d}^2\psi_\ell(r)}{\mathrm{d}r_*^2} + \left[\omega^2 - V_\ell(r)\right]\psi_\ell(r) = 0. \tag{3.48}$$

In this case, from equation (3.15), the tortoise coordinate r_* is given by

$$\frac{\mathrm{d}r_*}{\mathrm{d}r} = \frac{1}{f(r)} \tag{3.49}$$

and from equation (3.24), we have the effective potential

$$V_\ell(r) = \frac{\ell(\ell+d-3)f(r)}{r^2} + \frac{(d-2)(d-4)}{4}\frac{f^2(r)}{r^2} + \frac{d-2}{2}\frac{f(r)}{r}\frac{\mathrm{d}f(r)}{\mathrm{d}r}. \tag{3.50}$$

The shape of the Schwarzschild-Tangherlini potential with $\ell = 1$ and $GM = 1$ for various d's is shown in Figure 3.4.

The rigorous bound on the greybody factor for $h(r) = \omega$ is given by

$$T \geq \mathrm{sech}^2\left[\frac{1}{2\omega}\int_{-\infty}^{\infty}V_\ell(r)\mathrm{d}r_*\right]. \tag{3.51}$$
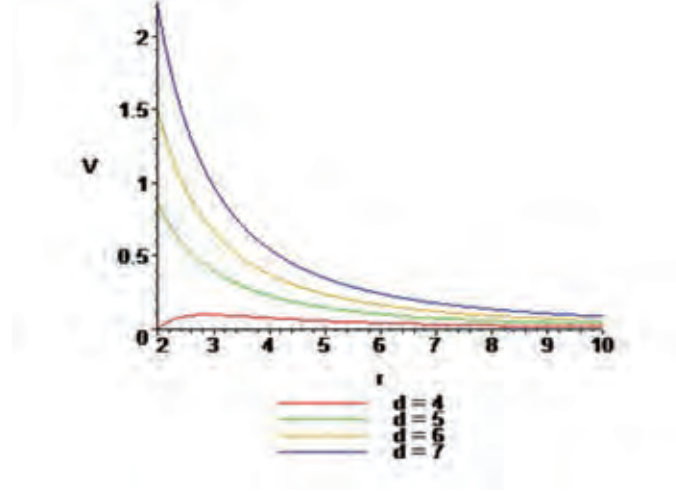
Figure 3.4: The Schwarzschild-Tangherlini potential.

Substituting the effective potential $V_\ell(r)$ from equation (3.50) gives

$$T \geq \mathrm{sech}^2 \left[\frac{1}{2\omega} \int_{-\infty}^{\infty} \left\{ \frac{\ell(\ell + d - 3)f(r)}{r^2} + \frac{(d-2)(d-4)}{4} \frac{f^2(r)}{r^2} \right. \right.$$
$$\left. \left. + \frac{d-2}{2} \frac{f(r)}{r} \frac{\mathrm{d}f(r)}{\mathrm{d}r} \right\} \mathrm{d}r_* \right]. \tag{3.52}$$

Using the tortoise coordinate in equation (3.49), we obtain

$$T \geq \mathrm{sech}^2 \left[\frac{1}{2\omega} \int_{r_0}^{\infty} \left\{ \frac{\ell(\ell + d - 3)}{r^2} + \frac{(d-2)(d-4)}{4} \frac{f(r)}{r^2} \right. \right.$$
$$\left. \left. + \frac{d-2}{2r} \frac{\mathrm{d}f(r)}{\mathrm{d}r} \right\} \mathrm{d}r \right]. \tag{3.53}$$

Substituting $f(r)$ from equation (3.44) gives

$$T \geq \mathrm{sech}^2 \left[\frac{1}{2\omega} \int_{r_0}^{\infty} \left\{ \frac{\ell(\ell + d - 3)}{r^2} + \frac{(d-2)(d-4)}{4r^2} \right. \right.$$
$$\left. \left. - \frac{(d-2)(d-4)}{4} \frac{r_0^{d-3}}{r^{d-1}} + \frac{(d-2)(d-3)r_0^{d-3}}{2r^{d-1}} \right\} \mathrm{d}r \right]. \tag{3.54}$$

Simplifying the above equation, we obtain

$$T \geq \mathrm{sech}^2 \left[\frac{1}{2\omega} \int_{r_0}^{\infty} \left\{ \frac{\ell(\ell + d - 3)}{r^2} + \frac{(d-2)(d-4)}{4r^2} \right. \right.$$
$$\left. \left. + \frac{(d-2)^2 r_0^{d-3}}{4r^{d-1}} \right\} \mathrm{d}r \right]. \tag{3.55}$$

Performing the integral gives

$$T \geq \mathrm{sech}^2 \left[\frac{1}{2\omega} \left\{ \frac{\ell(\ell + d - 3)}{r_0} + \frac{(d-2)(d-4)}{4r_0} + \frac{d-2}{4r_0} \right\} \right]. \tag{3.56}$$

Finally, we obtain

$$T \geq \text{sech}^2 \left[\frac{4\ell(\ell + d - 3) + (d-2)(d-3)}{8\omega r_0} \right].$$ (3.57)

If $d = 4$, then $r_0 = 2GM$, and this bound reduces to

$$T \geq \text{sech}^2 \left[\frac{2\ell(\ell + 1) + 1}{8GM\omega} \right],$$ (3.58)

which is exactly the bound for the four-dimensional Schwarzschild black holes emitting spinless particles [11]. From Figure 3.5, the graph is plotted by setting $\ell = 1$, $GM = 2$, and $\omega = 2$. The point $d = 4$ corresponds to the four-dimensional Schwarzschild black hole. The graph shows that when the dimension increases, the bound on the greybody factor decreases. Note that for $d \geq 7$, the Schwarzschild-Tangherlini black hole hardly emits radiation.
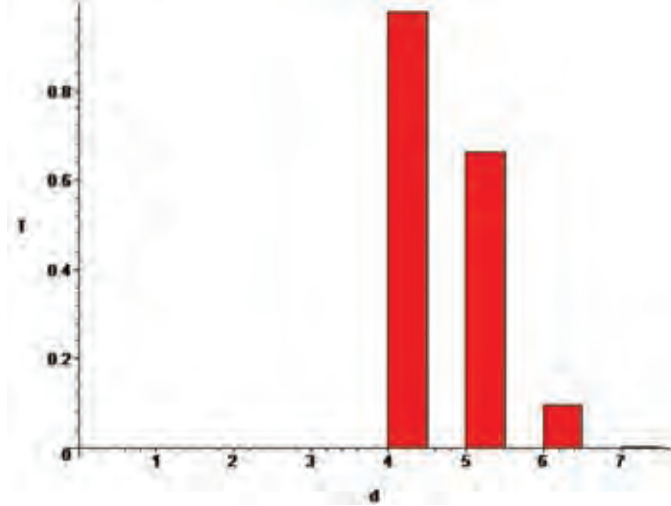
Figure 3.5: Dependence of the bound on the greybody factor on the dimension.

3.4 Greybody factors for charged dilatonic black holes in (2 + 1) dimensions

The charged dilatonic black holes in (2 + 1) dimensions is a solution to the low-energy string theory in (2 + 1) dimensions which is described by the Einstein-Maxwell-dilaton action [5]

$$S = \int \mathrm{d}^3 x \sqrt{-g} \left[R - 4(\nabla\phi)^2 - e^{-4\phi} F_{\mu\nu} F^{\mu\nu} + 2e^{4\phi\Lambda} \right],$$ (3.59)

where Λ is the cosmological constant, ϕ is a dilaton field, and $F_{\mu\nu}$ is the Maxwell's field strength. This action gives the solution

$$ds^2 = -f(r)dt^2 + \frac{4r^2}{f(r)}dr^2 + r^2d\theta^2,$$ (3.60)

where

$$f(r) = -2Mr + 8\Lambda r^2 + 8Q^2.$$ (3.61)

This is the metric of charged dilatonic black holes in $(2 + 1)$ dimensions. For $M > 8Q\sqrt{\Lambda}$, this spacetime describes a black hole with two event horizons

$$r_\pm = \frac{M \pm \sqrt{M^2 - 64Q^2\Lambda}}{8\Lambda}.$$ (3.62)

Comparing equation (3.60) with equation (3.1), we find

$$A(r) = f(r), \quad B(r) = \frac{f(r)}{4r^2}, \quad \text{and} \quad d = 3.$$ (3.63)

We are interested in a massless uncharged scalar field emitted from this black hole. From equation (3.23), the derived Regge-Wheeler equation is

$$\frac{d^2\psi_m(r)}{dr_*^2} + \left[\omega^2 - V_m(r)\right]\psi_m(r) = 0.$$ (3.64)

In this case, from equation (3.15), the tortoise coordinate r_* is given by

$$\frac{dr_*}{dr} = \frac{2r}{f(r)}$$ (3.65)

and from equation (3.24), we have the effective potential

$$V_m(r) = -(8m^2\Lambda + 6m\Lambda) + 14\Lambda^2 r + \left(\frac{5M^2}{8} + 2m^2M\right)\frac{1}{r}$$
$$-(4MQ^2 + 8m^2Q^2)\frac{1}{r^2} + \frac{6Q^4}{r^3}.$$ (3.66)

The shape of the potential of $(2 + 1)$-dimensional charged dilatonic black holes with $m = 1$, $\Lambda = 0.1$, $Q = 1$, and $M = 10$ is shown in Figure 3.6.

The tortoise coordinate r_* can explicitly be written as

$$r_* = \frac{1}{4\Lambda(r_+ - r_-)}\left[r_+ \ln(r - r_+) - r_- \ln(r - r_-)\right].$$ (3.67)

In case of an uncharged black hole, the tortoise coordinate r_* can be written as

$$r_* = \frac{1}{4\Lambda}\ln|r - r_h|.$$ (3.68)
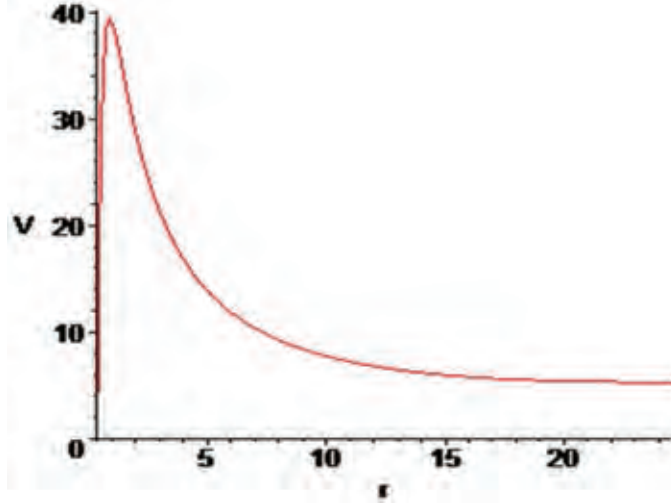
Figure 3.6: The potential of $(2 + 1)$-dimensional charged dilatonic black holes.

The rigorous bound on the greybody factor for $h(r) = \omega$ is [29]

$$T \geq \mathrm{sech}^2 \left[\frac{-368\Lambda m(4m + 3) + 644M\Lambda - 2576Q^2\Lambda + 115M^2 + 368m^2M}{60\omega\sqrt{M^2 - 64Q^2\Lambda}} \right.$$
$$- \frac{5\sqrt{M^2 - 64Q^2\Lambda}}{8\omega} - \frac{5M + 16m^2}{16\omega} \ln \left| \frac{r_-}{r_+} \right|$$
$$\left. - \frac{23Q^2(3Q^2 - 2M - 4m^2)}{15\omega\Lambda} \right]. \tag{3.69}$$

The effect of charges on the bound, on the greybody factor, is shown in Figure 3.7. The graph is plotted by setting $m = 0$, $M = 10$, $\omega = 2$, and $\Lambda = 0.1$. The graph shows that when the charges increase, the bound on the greybody factor decreases. This result is similar to the Reissner-Nordström black hole's result. That is, the charges resist the tunneling of the uncharged scalar particles.

The effect of the cosmological constant on the greybody factor bound is shown in Figure 3.8. The graph is plotted by setting $m = 0$, $M = 10$, $\omega = 2$, and $Q = 1$. The graph shows that when the value of the cosmological constant increases, the bound also increases. That is, the cosmological constant makes the gravitational potential produced by the black hole transparent.

3.5 Greybody factors for charged dilatonic black holes in $(3 + 1)$ dimensions

The charged dilatonic black holes in $(3 + 1)$ dimensions is a solution to the low-energy string theory in $(3 + 1)$ dimensions which is described by the dilaton gravity
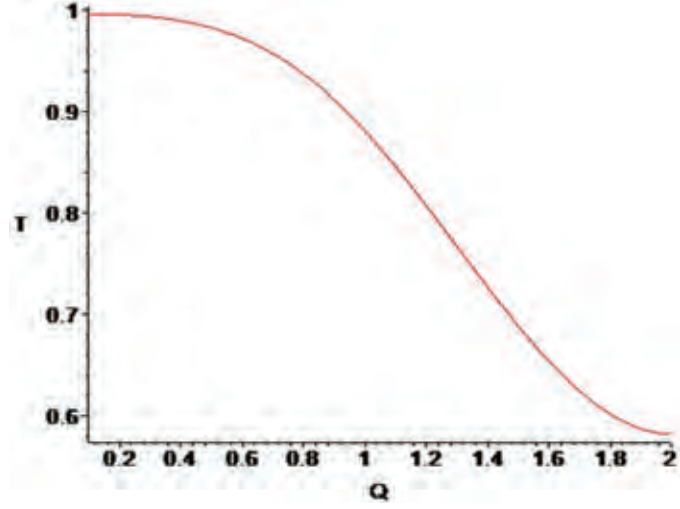
Figure 3.7: Dependence of the bound on the greybody factor on the charges.
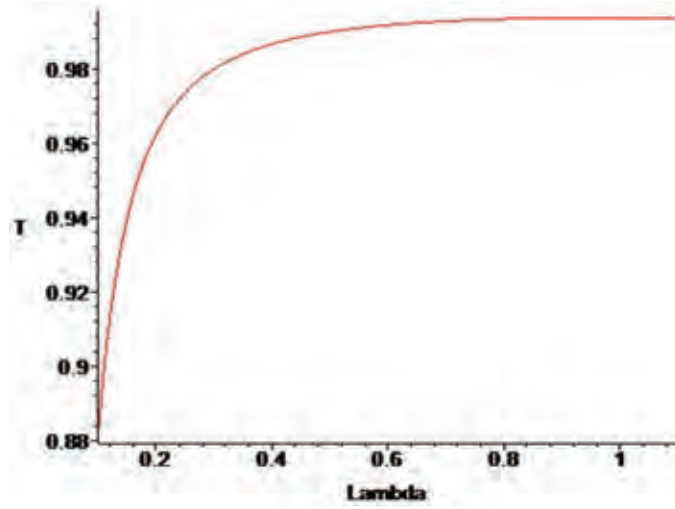
Figure 3.8: Dependence of the bound on the greybody factor on the cosmological constant.

action [6]

$$S = \int d^4x \sqrt{-g} \left[R - 2(\nabla\phi)^2 - e^{-2\phi} F_{\mu\nu} F^{\mu\nu} \right], \tag{3.70}$$

where ϕ is a dilaton field and $F_{\mu\nu}$ is the Maxwell's field strength. This action gives the metric of charged dilatonic black holes in $(3 + 1)$ dimensions

$$ds^2 = -f(r)dt^2 + \frac{1}{f(r)}dr^2 + R^2(r)d\Omega^2, \tag{3.71}$$

where

$$f(r) = 1 - \frac{r_+}{r} \quad \text{and} \quad R^2(r) = r^2 \left(1 - \frac{r_-}{r} \right), \tag{3.72}$$

with

$$r_+ = 2M \quad \text{and} \quad r_- = \frac{Q^2}{M}. \tag{3.73}$$

The event horizon radius is given by $r = r_+$ corresponding to $R(r_+) = \sqrt{r_+^2 - r_+ r_-}$. If $r_- = 0$ which corresponds to $Q = 0$, the metric (3.71) reduces to the Schwarzschild metric. By the coordinate transformation

$$r = \frac{r_- + \sqrt{4R^2 + r_-^2}}{2},$$
(3.74)

the metric (3.71) can be rewritten as

$$ds^2 = -\mathcal{F}(R)dt^2 + \frac{1}{\mathcal{F}(R)H^2(R)}dR^2 + R^2 d\Omega^2,$$
(3.75)

where

$$\mathcal{F}(R) = 1 + \frac{r_+ r_-}{2R^2} - \frac{r_+ \sqrt{4R^2 + r_-^2}}{2R^2} \quad \text{and} \quad H^2(R) = \frac{4R^2}{4R^2 + r_-^2}.$$
(3.76)

Comparing equation (3.75) with equation (3.1), we find

$$A(r) = \mathcal{F}(R), \quad B(r) = \mathcal{F}(R)H^2(R), \quad \text{and} \quad d = 4.$$
(3.77)

We are interested in a massless uncharged scalar field emitted from this black hole. From equation (3.23), the derived Regge-Wheeler equation is

$$\frac{d^2\psi_\ell(R)}{dR_*^2} + \left[\omega^2 - V_\ell(R)\right]\psi_\ell(R) = 0.$$
(3.78)

In this case, from equation (3.15), the tortoise coordinate R_* is given by

$$\frac{dR_*}{dR} = \frac{1}{\mathcal{F}(R)H(R)}$$
(3.79)

and from equation (3.24), we have the effective potential

$$V_\ell(R) = \frac{\ell(\ell+1)\mathcal{F}(R)}{R^2} + \frac{\mathcal{F}(R)H(R)}{R}\frac{d}{dR}[\mathcal{F}(R)H(R)].$$
(3.80)

The shape of the potential of $(3 + 1)$-dimensional charged dilatonic black holes with $\ell = 0$, $r_+ = 4$, and $r_- = 0.5$ is shown in Figure 3.9.

Choosing $h(r) = \omega$, the rigorous bound on the greybody factor for $\ell = 0$ is given by

$$T \geq \text{sech}^2\left[\frac{1}{2\omega}\int_{-\infty}^{\infty} V_{\ell=0}(R)dR_*\right].$$
(3.81)

Substituting the effective potential $V_{\ell=0}(R)$ from equation (3.80) gives

$$T \geq \text{sech}^2\left[\frac{1}{2\omega}\int_{-\infty}^{\infty} \frac{\mathcal{F}(R)H(R)}{R}\frac{d}{dR}[\mathcal{F}(R)H(R)]dR_*\right].$$
(3.82)

Using the tortoise coordinate in equation (3.79), we obtain

$$T \geq \text{sech}^2\left[\frac{1}{2\omega}\int_{R(r_+)}^{\infty} \frac{1}{R}\frac{d}{dR}[\mathcal{F}(R)H(R)]dR\right].$$
(3.83)
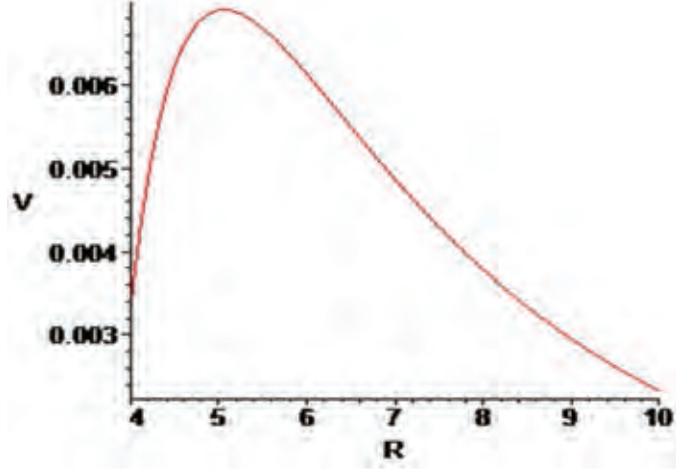
Figure 3.9: The potential of $(3+1)$-dimensional charged dilatonic black holes.

Integrating by parts gives

$$\int_{R(r_+)}^{\infty} \frac{1}{R} \frac{d}{dR}[\mathcal{F}(R)H(R)]dR = \frac{\mathcal{F}(R)H(R)}{R}\bigg|_{R(r_+)}^{\infty} + \int_{R(r_+)}^{\infty} \frac{\mathcal{F}(R)H(R)}{R^2}dR$$
$$= \int_{R(r_+)}^{\infty} \frac{\mathcal{F}(R)H(R)}{R^2}dR, \qquad (3.84)$$

where $\mathcal{F}(R(r_+)) = 0$. Substituting $\mathcal{F}(R)$ and $H(R)$ from equation (3.76) gives

$$T \geq \operatorname{sech}^2 \left[\frac{1}{2\omega} \int_{R(r_+)}^{\infty} \left(\frac{2}{R\sqrt{4R^2 + r_-^2}} + \frac{r_+ r_-}{R^3\sqrt{4R^2 + r_-^2}} - \frac{r_+}{R^3} \right) dR \right]. \qquad (3.85)$$

Let $u = \sqrt{4R^2 + r_-^2}$, so $du = 4R/\sqrt{4R^2 + r_-^2}dR$. Then,

$$\int_{R(r_+)}^{\infty} \frac{2}{R\sqrt{4R^2 + r_-^2}}dR = \int_{2r_+ - r_-}^{\infty} \frac{1}{2R^2}du = \int_{2r_+ - r_-}^{\infty} \frac{2}{u^2 - r_-^2}du \qquad (3.86)$$

and

$$\int_{R(r_+)}^{\infty} \frac{r_+ r_-}{R^3\sqrt{4R^2 + r_-^2}}dR = \int_{2r_+ - r_-}^{\infty} \frac{r_+ r_-}{4R^4}du = \int_{2r_+ - r_-}^{\infty} \frac{4r_+ r_-}{(u^2 - r_-^2)^2}du. \qquad (3.87)$$

By partial fractions,

$$\frac{2r_-}{u^2 - r_-^2} = \frac{1}{u - r_-} - \frac{1}{u + r_-} \qquad (3.88)$$

and

$$\frac{4r_+ r_-}{(u^2 - r_-^2)^2} = \frac{r_+}{r_-^2}\left(\frac{1}{u + r_-} - \frac{1}{u - r_-} \right) + \frac{r_+}{r_-}\left[\frac{1}{(u - r_-)^2} + \frac{1}{(u + r_-)^2} \right], \qquad (3.89)$$

then

$$\int_{2r_+ - r_-}^{\infty} \frac{2}{u^2 - r_-^2}du = \frac{1}{r_-}\ln\left(\frac{u - r_-}{u + r_-} \right)\bigg|_{2r_+ - r_-}^{\infty} = \frac{1}{r_-}\ln\left(\frac{r_+}{r_+ - r_-} \right) \qquad (3.90)$$

and

$$\int_{2r_+-r_-}^{\infty} \frac{4r_+r_-}{(u^2-r_-^2)^2}du = \frac{r_+}{r_-^2}\ln\left(\frac{u+r_-}{u-r_-}\right)\bigg|_{2r_+-r_-}^{\infty} - \frac{r_+}{r_-}\left(\frac{1}{u-r_-}+\frac{1}{u+r_-}\right)\bigg|_{2r_+-r_-}^{\infty}$$

$$= -\frac{r_+}{r_-^2}\ln\left(\frac{r_+}{r_+-r_-}\right) + \frac{r_+}{2r_-}\left(\frac{1}{r_+-r_-}+\frac{1}{r_+}\right). \tag{3.91}$$

Therefore,

$$T \geq \text{sech}^2\left[\frac{1}{2\omega}\left\{\frac{1}{r_-}\ln\left(\frac{r_+}{r_+-r_-}\right) - \frac{r_+}{r_-^2}\ln\left(\frac{r_+}{r_+-r_-}\right) + \frac{r_+}{2r_-(r_+-r_-)}\right.\right.$$
$$\left.\left. +\frac{1}{2r_-} - \frac{1}{2(r_+-r_-)}\right\}\right]. \tag{3.92}$$

Finally, we obtain

$$T \geq \text{sech}^2\left[\frac{1}{2\omega r_-}\left\{1 - \frac{r_+-r_-}{r_-}\ln\left(\frac{r_+}{r_+-r_-}\right)\right\}\right]. \tag{3.93}$$

If $r_- = 0$, the rigorous bound on the greybody factor for $\ell = 0$ becomes

$$T \geq \text{sech}^2\left(\frac{1}{4\omega r_+}\right), \tag{3.94}$$

which is the rigorous bound on the greybody factor for the Schwarzschild black hole [11]. The effect of charges on the greybody factor bound is shown in Figure 3.10. The graph is plotted by setting $r_+ = 4$ and $r_- = 3.125, 2, 0$. The graph shows that when the charges increase, the bound on the greybody factor decreases. This result is also similar to the Reissner-Nordström black hole's and the $(2+1)$ dimensional charged dilatonic black hole's results. That is, the charges resist the tunneling of the uncharged scalar particles.
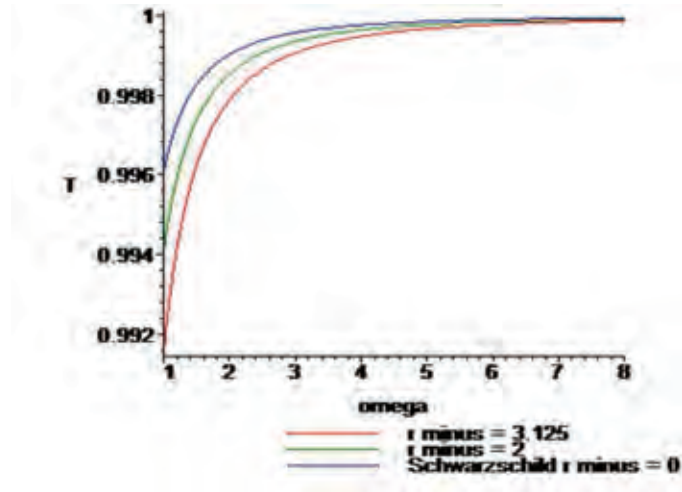
Figure 3.10: Dependence of the bound on the greybody factor on the charges.

3.6   Discussion

In this Chapter, we started by obtaining the Regge-Wheeler equations for the static and spherically symmetric black holes. Then, we calculated the rigorous bounds on the greybody factors for massless scalar fields emitted from non-rotating black holes. In particular, we studied the Reissner-Nordström black holes, Schwarzschild-Tangherlini black holes, charged dilatonic black holes in $(2+1)$ dimensions, and charged dilatonic black holes in $(3+1)$ dimensions. In calculating the rigorous bounds on the greybody factors, we started with the Klein-Gordon equation in curved spacetime which governs the motion of a scalar field in a black hole background. By separating the variables and introducing the tortoise coordinate, we obtained the radial equation of the Klein-Gordon equation in the form of the Schrödinger-like equation. Then, we used the methods developed by Boonserm and Visser [8, 9, 10] to derive rigorous bounds on the greybody factors. We assumed spherical symmetry so that the problems could become one dimensional.

It is straightforward to derive rigorous bounds on the greybody factors for non-rotating black holes. In particular, we have chosen $h(r) = \omega$ for all non-rotating black holes, which have been studied in this chapter.

Chapter IV

Greybody factors for Kerr-Newman black holes

In this chapter, we calculate the rigorous bounds on the greybody factors for Kerr-Newman black holes, the rotating black holes with charges. The occurrence of rotation of black holes considerably increases the level of difficulty of calculations. In particular, the Kerr or Kerr-Newman black holes are generally much more difficult to work with than the Schwarzschild or Reissner-Nordström black holes. We also introduce the concept of superradiance, a new phenomenon for rotating black holes which does not occur for non-rotating black holes. For the contents in this chapter, we follow from [35].

4.1 Radial Teukolsky equation

The Kerr-Newman metric is given by [27, 28]

$$\mathrm{d}s^2 = -\frac{\Delta}{\Sigma}\left(\mathrm{d}t - a\sin^2\theta\mathrm{d}\phi\right)^2 + \frac{\sin^2\theta}{\Sigma}\left[a\mathrm{d}t - \left(r^2 + a^2\right)\mathrm{d}\phi\right]^2 + \frac{\Sigma}{\Delta}\mathrm{d}r^2 + \Sigma\mathrm{d}\theta^2, \quad (4.1)$$

where

$$\Delta(r) = r^2 - 2GMr + a^2 + Q^2 = \left(r - r_+\right)\left(r - r_-\right)$$
$$\Sigma(r,\theta) = r^2 + a^2\cos^2\theta. \quad (4.2)$$

Here M is the mass of the black hole, and $a = J/M$ is the angular momentum per unit mass, where J is the angular momentum, and Q is its charge. The quantities $r_\pm$ are given by

$$r_\pm = GM \pm \sqrt{G^2M^2 - a^2 - Q^2}. \quad (4.3)$$

They denote the locations of the inner and outer horizons. When $Q \to 0$, we recover the Kerr spacetime [24, 25]. We are interested in a massless uncharged scalar field emitted from this black hole. The equation of motion of this scalar field on the black hole background is

$$\frac{1}{\sqrt{-g}}\partial_\mu\left(\sqrt{-g}g^{\mu\nu}\partial_\nu\Phi\right) = 0. \quad (4.4)$$

4.1.1   Spheroidal harmonics

We assume the solution to be [36]

$$\Phi(t, r, \theta, \phi) = e^{-i\omega t} \frac{\psi_{\ell m}(r)}{\sqrt{r^2 + a^2}} S_{\ell m}(\theta) e^{im\phi}, \tag{4.5}$$

where $S_{\ell m}(\theta) e^{im\phi}$ are the **spheroidal harmonics**, which generalize the usual spherical harmonics $Y_{\ell m}(\theta, \phi)$, and satisfy the differential equation [37]

$$\left[\frac{1}{\sin\theta} \frac{\mathrm{d}}{\mathrm{d}\theta} \left(\sin\theta \frac{\mathrm{d}}{\mathrm{d}\theta} \right) - a^2\omega^2 \sin^2\theta - \frac{m^2}{\sin^2\theta} + 2ma\omega + \lambda_{\ell m}(a\omega) \right] S_{\ell m}(\theta) = 0, \tag{4.6}$$

where $\lambda_{\ell m}(a\omega)$ is the separation constant which generalizes the usual quantity $\ell(\ell + 1)$ occurring for spherical harmonics. In the slow-rotation limit, we have [38, 39, 40, 41]

$$\lambda_{\ell m}(a\omega) = \ell(\ell + 1) - 2ma\omega + (H_{\ell+1,m} - H_{\ell m})(a\omega)^2 + O[(a\omega)^3], \tag{4.7}$$

where

$$H_{\ell m} = \frac{2\ell\left(\ell^2 - m^2\right)}{4\ell^2 - 1} \tag{4.8}$$

is related to the confluent Heun functions [42, 43, 44, 45]. Let $\mathrm{d}u = \sin\theta \mathrm{d}\theta$, then

$$\frac{\mathrm{d}}{\mathrm{d}\theta} = \frac{\mathrm{d}u}{\mathrm{d}\theta} \frac{\mathrm{d}}{\mathrm{d}u} = \sin\theta \frac{\mathrm{d}}{\mathrm{d}u}. \tag{4.9}$$

Therefore,

$$\frac{1}{\sin\theta} \frac{\mathrm{d}}{\mathrm{d}\theta} \left[\sin\theta \frac{\mathrm{d}S_{\ell m}(\theta)}{\mathrm{d}\theta} \right] = \frac{\mathrm{d}}{\mathrm{d}u} \left[\sin^2\theta \frac{\mathrm{d}S_{\ell m}(\theta)}{\mathrm{d}u} \right]. \tag{4.10}$$

Equation (4.6) becomes

$$\frac{\mathrm{d}}{\mathrm{d}u} \left[\sin^2\theta \frac{\mathrm{d}S_{\ell m}(\theta)}{\mathrm{d}u} \right] = \left[a^2\omega^2 \sin^2\theta + \frac{m^2}{\sin^2\theta} - 2ma\omega - \lambda_{\ell m}(a\omega) \right] S_{\ell m}(\theta). \tag{4.11}$$

If we multiply the above equation by $S_{\ell m}(\theta)$ and perform an integration by parts, we can see that the differential operator is negatively definite in the sense that

$$\int S_{\ell m}(\theta) \frac{\mathrm{d}}{\mathrm{d}u} \left[\sin^2\theta \frac{\mathrm{d}S_{\ell m}(\theta)}{\mathrm{d}u} \right] \mathrm{d}u = -\int \sin^2\theta \left[\frac{\mathrm{d}S_{\ell m}(\theta)}{\mathrm{d}u} \right]^2 \mathrm{d}u \leq 0. \tag{4.12}$$

Consequently,

$$\lambda_{\ell m}(a\omega) + 2ma\omega \geq a^2\omega^2 \sin^2\theta + \frac{m^2}{\sin^2\theta} \geq 0. \tag{4.13}$$

Moreover,

$$\lambda_{\ell m}(a\omega) \geq a^2\omega^2 \sin^2\theta - 2ma\omega + \frac{m^2}{\sin^2\theta} = \left(a\omega \sin\theta - \frac{m}{\sin\theta} \right)^2 \geq 0. \tag{4.14}$$

4.1.2   Effective potential

From equation (4.4), the radial equation for the solution (4.5) is given by [46]

$$\left[\frac{d^2}{dr_*^2} - U_{\ell m}(r)\right] \psi_{\ell m}(r) = 0. \tag{4.15}$$

This equation is known as the **radial Teukolsky equation**. Here, the tortoise coordinate r_* is defined by

$$\frac{dr_*}{dr} = \frac{r^2 + a^2}{\Delta} = \frac{r^2 + a^2}{(r - r_+)(r - r_-)}. \tag{4.16}$$

It can explicitly be written as

$$r_* = r + \frac{r_+^2 + a^2}{r_+ - r_-} \ln(r - r_+) - \frac{r_-^2 + a^2}{r_+ - r_-} \ln(r - r_-). \tag{4.17}$$

Thus, we see that

$$\lim_{r \to r_+} r_* \to -\infty \quad \text{and} \quad \lim_{r \to \infty} r_* \to \infty. \tag{4.18}$$

Now, we define the quantities

$$\varpi = \frac{a}{r^2 + a^2} \quad \text{and} \quad \Omega_+ = \frac{a}{r_+^2 + a^2}, \tag{4.19}$$

where $\varpi(r)$ is related to frame dragging and Ω_+ is the angular velocity of the event horizon. The effective potential $U_{\ell m}(r)$ is

$$U_{\ell m}(r) = V_{\ell m}(r) - (\omega - m\varpi)^2, \tag{4.20}$$

where

$$V_{\ell m}(r) = \frac{\Delta}{(r^2 + a^2)^2} \left[\lambda_{\ell m}(a\omega) + W_{MQJ}(r)\right]. \tag{4.21}$$

Here,

$$W_{MQJ}(r) = \frac{(r\Delta)'}{r^2 + a^2} - \frac{3r^2\Delta}{(r^2 + a^2)^2}, \tag{4.22}$$

which depends only on the spacetime geometry, not on the multipole (ℓm) under consideration. This definition of $V_{\ell m}(r)$ is now as close as possible to the one in chapter III and in references [11, 29, 33], and to the general (non-relativistic quantum mechanical) analyses with references [8, 9, 30, 31, 32]. In the absence of rotation, $a \to 0$, this radial Teukolsky equation reduces to the Regge-Wheeler equation [47, 48, 49].

4.1.3 Positivity properties

We have already seen that the separation constant $\lambda_{\ell m}(a\omega)$ is positive. We can show that the quantity $W_{MQJ}(r)$ is also positive. To see this, we write

$$\Delta = (r - r_+)(r - r_-), \quad r_+ + r_- = 2GM, \quad r_+ r_- = a^2 + Q^2. \tag{4.23}$$

Then, we have

$$0 \le \frac{a^2}{r_+} \le r_- \le r_+, \quad \text{and} \quad 0 \le \frac{Q^2}{r_+} \le r_- \le r_+. \tag{4.24}$$

Furthermore, from equation (4.3) we observe that

$$a \le GM \quad \text{and} \quad |Q| \le GM. \tag{4.25}$$

Now, consider

$$\begin{aligned}
(r\Delta)' &= [r(r - r_+)(r - r_-)]' \\
&= (r - r_+)(r - r_-) + r(r - r_+) + r(r - r_-) \\
&= 3r^2 - 2r(r_+ + r_-) + r_+ r_-.
\end{aligned} \tag{4.26}$$

Then,

$$\begin{aligned}
W_{MQJ}(r) &\propto (r\Delta)'\left(r^2 + a^2\right) - 3r^2\Delta \\
&= \left[3r^2 - 2r(r_+ + r_-) + r_+ r_-\right]\left(r^2 + a^2\right) - 3r^2(r - r_+)(r - r_-) \\
&= [0]r^4 + [-2(r_+ + r_-) + 3(r_+ + r_-)]r^3 + \left(3a^2 + r_+ r_- - 3r_+ r_-\right)r^2 \\
&\quad + \left[-2a^2(r_+ + r_-)\right]r + \left(a^2 r_+ r_-\right)r^0 \\
&= (r_+ + r_-)r^3 + \left(3a^2 - 2r_+ r_-\right)r^2 - 2a^2(r_+ + r_-)r + a^2 r_+ r_- \\
&= r^2\left(rr_+ + rr_- - 2r_+ r_-\right) + a^2 r(2r - r_+ - r_-) + a^2\Delta \\
&\ge 0
\end{aligned} \tag{4.27}$$

in the region outside the outer horizon ($r \ge r_+$). Moreover,

$$\lim_{r \to \infty} W_{MQJ} = 0 \quad \text{and} \quad W_{MQJ}(r_+) = \frac{r_+(r_+ - r_-)}{r_+^2 + a^2}. \tag{4.28}$$

Thus, we see that $V_{\ell m} \to 0$ occurs both at the outer horizon r_+ and at spatial infinity.

4.1.4 Superradiance

In general, when an incident wave is scattered from an object, some of its energy will be absorbed by that object. As a result, the reflected wave propagates with

energy lower than that of the incident wave. However, in some special systems, an object loses its energy to a wave when the scattering occurs. Consequently, the energy of the reflected wave is higher than that of the incident wave. This phenomenon is known as **superradiance** [50]. Mathematically, superradiance is a phenomenon where the reflection coefficients are greater than unity. For example, superradiance can occur when a scalar wave is scattered from a rotating black hole [51, 52]. Moreover, superradiance can also occur in a system where electromagnetic waves are scattered from a rotating and electrically conductive cylinder [53, 54].

There are no superradiance phenomena occurring in non-relativistic quantum mechanics since the Schrödinger equation has first order time derivative. This leads to a potential which is linear in the total energy term [55]

$$U(r) = V(r) - \omega. \tag{4.29}$$

On the other hand, the Klein-Gordon equation is second order in time derivative so a potential is quadratic in the total energy term

$$U(r) = V(r) - (\omega - m\varpi)^2. \tag{4.30}$$

This potential leads to [56]

$$R = 1 - \frac{\omega - m\Omega_+}{\omega} T. \tag{4.31}$$

Superradiance occurs when $R > 1$. This corresponds to

$$\omega < m\Omega_+. \tag{4.32}$$

Equation (4.31) is flux conservation rather than probability conservation and can be rewritten as [55]

$$F_{\text{reflected}} + F_{\text{transmitted}} = 1, \tag{4.33}$$

where $F_{\text{reflected}} = R$ and $F_{\text{transmitted}} = [(\omega - m\Omega_+)/\omega]T$. If $F_{\text{transmitted}} \geq 0$, equation (4.31) can reduce to probability conservation. If $F_{\text{transmitted}} < 0$, we have to interpret all quantities in terms of fluxes.

In case of a Kerr-Newman black hole, superradiance occurs if the condition

$$0 < \omega < m\Omega_+ \tag{4.34}$$

is satisfied, where ω is the frequency of a scalar wave. We define the quantity

$$m_* = \frac{\omega}{\Omega_+}. \tag{4.35}$$

Then,

- the modes $m < m_*$ are not superradiant;

- the modes $m \geq m_*$ are superradiant.

We shall soon see further details regarding the superradiance phenomenon in the subsequent discussion.

4.2 Non-superradiant modes ($m < m_*$)

We divide the discussion of the non-superradiant modes into three cases,

- $m = 0$, zero-angular-momentum modes;

- $m < 0$, negative-angular-momentum modes;

- $m \in (0, m_*)$, low-lying positive-angular-momentum modes.

4.2.1 Zero-angular-momentum modes ($m = 0$)

This case is simple and is a guiding template for all the other cases. Some preliminary work on these zero-angular-momentum modes in the Kerr-Newman spacetime can be found in reference [57]. Using equation (2.136), the rigorous bound on the greybody factor is given by

$$T_{\ell m} \geq \operatorname{sech}^2 \left[\int_{-\infty}^{\infty} \frac{\sqrt{[\tilde{h}'(r_*)]^2 + [U_{\ell m}(r) + \tilde{h}^2(r_*)]^2}}{2\tilde{h}(r_*)} \mathrm{d}r_* \right], \qquad (4.36)$$

for any positive function $\tilde{h}(r_*)$. In this case, we set $m = 0$. Then,

$$U_{\ell,m=0}(r) = -\omega^2 + \frac{\Delta}{(r^2 + a^2)^2} \left[\lambda_{\ell,m=0} + W_{MQJ}(r) \right]. \qquad (4.37)$$

We choose an appropriate function $\tilde{h}(r_*)$ in order that the bounds can be calculated. In this dissertation, we let $\tilde{h}(r_*) = \omega > 0$. Therefore,

$$T_{\ell,m=0} \geq \operatorname{sech}^2 \left[\frac{1}{2\omega} \int_{-\infty}^{\infty} \left| \frac{\Delta}{(r^2 + a^2)^2} \left[\lambda_{\ell,m=0} + W_{MQJ}(r) \right] \right| \mathrm{d}r_* \right]. \qquad (4.38)$$

Changing the integration variable from $\mathrm{d}r_*$ to $\mathrm{d}r$ using equation (4.16), we obtain

$$T_{\ell,m=0} \geq \operatorname{sech}^2 \left[\frac{1}{2\omega} \int_{r_+}^{\infty} \left| \frac{1}{r^2 + a^2} \left[\lambda_{\ell,m=0} + W_{MQJ}(r) \right] \right| \mathrm{d}r \right]. \qquad (4.39)$$

This corresponds to the Case I bound of reference [8]. Since $\lambda_{\ell m}$ and $W_{MQJ}(r)$ are always positive, which have already been checked above, we can write

$$T_{\ell,m=0} \geq \mathrm{sech}^2 \left[\frac{1}{2\omega} \int_{r_+}^{\infty} \frac{1}{r^2 + a^2} \left[\lambda_{\ell,m=0} + W_{MQJ}(r) \right] \mathrm{d}r \right]. \tag{4.40}$$

We can separate this integral into two integrals, each of which can be explicitly evaluated in closed form. The first integral can be calculated, yielding

$$\int_{r_+}^{\infty} \frac{\lambda_{\ell,m=0}}{r^2 + a^2} \mathrm{d}r = \lambda_{\ell,m=0}(a\omega) \frac{\arctan(a/r_+)}{a}. \tag{4.41}$$

For evaluating the second integral, we define the dimensionless quantity

$$K_{MQJ} = r_+ \int_{r_+}^{\infty} \frac{W_{MQJ}}{r^2 + a^2} \mathrm{d}r = r_+ \int_{r_+}^{\infty} \frac{1}{r^2 + a^2} \left[\frac{(r\Delta)'}{r^2 + a^2} - \frac{3r^2 \Delta}{(r^2 + a^2)^2} \right] \mathrm{d}r. \tag{4.42}$$

Integrating by parts, we obtain

$$K_{MQJ} = r_+ \int_{r_+}^{\infty} \left[-(r\Delta) \left[(r^2 + a^2)^{-2} \right]' - \frac{3r^2 \Delta}{(r^2 + a^2)^3} \right] \mathrm{d}r, \tag{4.43}$$

where the boundary terms vanish. Then,

$$K_{MQJ} = r_+ \int_{r_+}^{\infty} \frac{(4-3)r^2 \Delta}{(r^2 + a^2)^3} \mathrm{d}r = r_+ \int_{r_+}^{\infty} \frac{r^2 \Delta}{(r^2 + a^2)^3} \mathrm{d}r. \tag{4.44}$$

Finally, we obtain

$$K_{MQJ} = \frac{3}{8} \frac{\arctan(a/r_+)}{a/r_+} + \frac{r_+ r_-}{8a^2} \left[\frac{\arctan(a/r_+)}{a/r_+} - \frac{r_+^2}{r_+^2 + a^2} \right]$$
$$+ \frac{1}{8} \frac{r_+ (3a + r_+ - 2r_-)}{r_+^2 + a^2}. \tag{4.45}$$

In the limit $a \to 0$, we obtain

$$\lim_{a \to 0} \frac{\arctan(a/r_+)}{a/r_+} = 1 \tag{4.46}$$

$$\lim_{a \to 0} \frac{1}{a^2} \left[\frac{\arctan(a/r_+)}{a/r_+} - \frac{r_+^2}{r_+^2 + a^2} \right] = \frac{2}{3r_+^2}. \tag{4.47}$$

Therefore,

$$\lim_{a \to 0} K_{MQJ} = \frac{3}{8} + \frac{1}{12} \frac{r_-}{r_+} + \frac{1}{8} \frac{r_+ - 2r_-}{r_+} = \frac{3r_+ - r_-}{6r_+}. \tag{4.48}$$

Substituting equation (4.41) and equation (4.45) into equation (4.40), we obtain

$$T_{\ell,m=0} \geq \mathrm{sech}^2 \left(\frac{I_{\ell,m=0}}{2\omega r_+} \right), \tag{4.49}$$

where

$$I_{\ell,m=0} = \lambda_{\ell,m=0}(a\omega) \frac{\arctan(a/r_+)}{a/r_+} + K_{MQJ}. \tag{4.50}$$

It can explicitly be written as

$$I_{\ell,m=0} = \left[\lambda_{\ell,m=0}(a\omega) + \frac{3}{8} \right] \frac{\arctan(a/r_+)}{a/r_+} + \frac{r_+ r_-}{8a^2} \left[\frac{\arctan(a/r_+)}{a/r_+} - \frac{r_+^2}{r_+^2 + a^2} \right]$$
$$+ \frac{1}{8} \frac{r_+ (3a + r_+ - 2r_-)}{r_+^2 + a^2}. \tag{4.51}$$

4.2.2 Negative-angular-momentum modes ($m < 0$)

In this subsection, we consider the $m < 0$ case. Recall the rigorous bound on the greybody factor

$$T_{\ell m} \geq \text{sech}^2 \left[\int_{-\infty}^{\infty} \frac{\sqrt{[\tilde{h}'(r_*)]^2 + \left[U_{\ell m}(r) + \tilde{h}^2(r_*) \right]^2}}{2\tilde{h}(r_*)} \mathrm{d}r_* \right] \tag{4.52}$$

for any positive function $\tilde{h}(r_*)$. Using the triangle inequality,

$$\sqrt{a^2 + b^2} \leq |a| + |b| \tag{4.53}$$

for all real numbers a and b, we obtain

$$T_{\ell,m<0} \geq \text{sech}^2 \left[\frac{1}{2} \int_{-\infty}^{\infty} \left| \frac{\tilde{h}'(r_*)}{\tilde{h}(r_*)} \right| \mathrm{d}r_* + \int_{-\infty}^{\infty} \frac{\left| U_{\ell,m<0}(r) + \tilde{h}^2(r_*) \right|}{2\tilde{h}(r_*)} \mathrm{d}r_* \right]. \tag{4.54}$$

We need $\tilde{h}(r_*)$ to be monotone, $\tilde{h}'(r_*) > 0$ or $\tilde{h}'(r_*) < 0$. Then,

$$T_{\ell,m<0} \geq \text{sech}^2 \left[\frac{1}{2} \left| \ln \left[\frac{\tilde{h}(\infty)}{\tilde{h}(-\infty)} \right] \right| + \int_{-\infty}^{\infty} \frac{\left| U_{\ell,m<0}(r) + \tilde{h}^2(r_*) \right|}{2\tilde{h}(r_*)} \mathrm{d}r_* \right]. \tag{4.55}$$

We choose

$$h(r) = \omega - m\varpi, \tag{4.56}$$

where $h(r) = \tilde{h}(r_*)$. We see that

$$\tilde{h}'(r_*) = \frac{\mathrm{d}\tilde{h}(r_*)}{\mathrm{d}r_*} = \frac{\mathrm{d}r}{\mathrm{d}r_*} \frac{\mathrm{d}h(r)}{\mathrm{d}r} = \frac{\Delta}{r^2 + a^2} \frac{2mar}{(r^2 + a^2)^2} < 0 \tag{4.57}$$

for $m < 0$. Then, $\tilde{h}(r_*)$ is monotonic. Moreover, we see that this $\tilde{h}(r_*)$ is always positive for $m < 0$. Then, we have

$$\frac{\tilde{h}(\infty)}{\tilde{h}(-\infty)} = \frac{h(\infty)}{h(r_+)} = \frac{\omega}{\omega - m\Omega_+} = \frac{1}{1 - m\Omega_+/\omega} < 1. \tag{4.58}$$

Thus,

$$\frac{1}{2} \left| \ln \left[\frac{\tilde{h}(\infty)}{\tilde{h}(-\infty)} \right] \right| = \frac{1}{2} \ln(1 - m\Omega_+/\omega). \tag{4.59}$$

Furthermore, in this case, we have $\omega - m\Omega_+ > \tilde{h}(r_*) > \omega$. Then,

$$\int_{-\infty}^{\infty} \frac{\left| U_{\ell,m<0}(r) + \tilde{h}^2(r_*) \right|}{2\tilde{h}(r_*)} \mathrm{d}r_* = \int_{-\infty}^{\infty} \frac{|V_{\ell,m<0}(r)|}{2\tilde{h}(r_*)} \mathrm{d}r_* < \int_{-\infty}^{\infty} \frac{V_{\ell,m<0}(r)}{2\omega} \mathrm{d}r_*. \tag{4.60}$$

Therefore,

$$T_{\ell,m<0} \geq \operatorname{sech}^2 \left[\frac{1}{2} \ln(1 - m\Omega_+/\omega) + \int_{-\infty}^{\infty} \frac{V_{\ell,m<0}(r)}{2\omega} \mathrm{d}r_* \right]. \qquad (4.61)$$

The second term is almost identical to what we performed for $m = 0$. Therefore,

$$T_{\ell,m<0} \geq \operatorname{sech}^2 \left[\frac{1}{2} \ln(1 - m\Omega_+/\omega) + \frac{I_{\ell,m<0}}{2\omega r_+} \right], \qquad (4.62)$$

where

$$I_{\ell,m<0} = \left[\lambda_{\ell,m<0}(a\omega) + \frac{3}{8} \right] \frac{\arctan(a/r_+)}{a/r_+} + \frac{r_+ r_-}{8a^2} \left[\frac{\arctan(a/r_+)}{a/r_+} - \frac{r_+^2}{r_+^2 + a^2} \right]$$
$$+ \frac{1}{8} \frac{r_+ \left(3a + r_+ - 2r_-\right)}{r_+^2 + a^2}. \qquad (4.63)$$

For $m < 0$, we have $-m \leq \ell$. Therefore, we obtain the weaker bound

$$T_{\ell,m<0} \geq \operatorname{sech}^2 \left[\frac{1}{2} \ln(1 + \ell\Omega_+/\omega) + \frac{I_{\ell,m<0}}{2\omega r_+} \right]. \qquad (4.64)$$

4.2.3 Low-lying positive-angular-momentum modes $[m \in (0, m_*)]$

In this subsection, we consider the $m \in (0, m_*)$ case. Similar to the previous case, we obtain

$$T_{\ell,m\in(0,m_*)} \geq \operatorname{sech}^2 \left[\frac{1}{2} \left| \ln \left[\frac{\tilde{h}(\infty)}{\tilde{h}(-\infty)} \right] \right| + \int_{-\infty}^{\infty} \frac{\left| U_{\ell,m\in(0,m_*)}(r) + \tilde{h}^2(r_*) \right|}{2\tilde{h}(r_*)} \mathrm{d}r_* \right]. \qquad (4.65)$$

We choose

$$h(r) = \omega - m\varpi, \qquad (4.66)$$

where $h(r) = \tilde{h}(r_*)$. We see that

$$\tilde{h}'(r_*) = \frac{\mathrm{d}\tilde{h}(r_*)}{\mathrm{d}r_*} = \frac{\mathrm{d}r}{\mathrm{d}r_*} \frac{\mathrm{d}h(r)}{\mathrm{d}r} = \frac{\Delta}{r^2 + a^2} \frac{2mar}{(r^2 + a^2)^2} > 0 \qquad (4.67)$$

for $m \in (0, m_*)$. Then, $\tilde{h}(r_*)$ is monotonic. Moreover, we see that this $\tilde{h}(r_*)$ is always positive for $m \in (0, m_*)$. Then, we have

$$\frac{\tilde{h}(\infty)}{\tilde{h}(-\infty)} = \frac{h(\infty)}{h(r_+)} = \frac{\omega}{\omega - m\Omega_+} = \frac{1}{1 - m\Omega_+/\omega} > 1. \qquad (4.68)$$

Thus,

$$\frac{1}{2} \left| \ln \left[\frac{\tilde{h}(\infty)}{\tilde{h}(-\infty)} \right] \right| = -\frac{1}{2} \ln(1 - m\Omega_+/\omega). \qquad (4.69)$$

Furthermore, in this case, we have $\omega - m\Omega_+ < \tilde{h}(r_*) < \omega$. Then,

$$\int_{-\infty}^{\infty} \frac{\left| U_{\ell,m\in(0,m_*)}(r) + \tilde{h}^2(r_*) \right|}{2\tilde{h}(r_*)} \mathrm{d}r_* = \int_{-\infty}^{\infty} \frac{|V_{\ell,m\in(0,m_*)}|}{2\tilde{h}(r_*)} \mathrm{d}r_* < \int_{-\infty}^{\infty} \frac{V_{\ell,m\in(0,m_*)}}{2(\omega - m\Omega_+)} \mathrm{d}r_*.$$
(4.70)

Therefore,

$$T_{\ell,m\in(0,m_*)} \geq \mathrm{sech}^2 \left[-\frac{1}{2} \ln(1 - m\Omega_+/\omega) + \frac{1}{2} \int_{-\infty}^{\infty} \frac{V_{\ell,m\in(0,m_*)}}{\omega - m\Omega_+} \mathrm{d}r_* \right].$$
(4.71)

The second term is almost identical to what we performed for $m = 0$. Therefore,

$$T_{\ell,m\in(0,m_*)} \geq \mathrm{sech}^2 \left[-\frac{1}{2} \ln(1 - m\Omega_+/\omega) + \frac{I_{\ell,m\in(0,m_*)}}{2(\omega - m\Omega_+)r_+} \right],$$
(4.72)

where

$$I_{\ell,m\in(0,m_*)} = \left[\lambda_{\ell,m\in(0,m_*)}(a\omega) + \frac{3}{8} \right] \frac{\arctan(a/r_+)}{a/r_+} + \frac{r_+ r_-}{8a^2} \left[\frac{\arctan(a/r_+)}{a/r_+} - \frac{r_+^2}{r_+^2 + a^2} \right]$$
$$+ \frac{1}{8} \frac{r_+ (3a + r_+ - 2r_-)}{r_+^2 + a^2}.$$
(4.73)

For $m > 0$, we have $m \leq \ell$. Therefore, we obtain the weaker bound

$$T_{\ell,m\in(0,m_*)} \geq \mathrm{sech}^2 \left[-\frac{1}{2} \ln(1 - \ell\Omega_+/\omega) + \frac{I_{\ell,m\in(0,m_*)}}{2(\omega - \ell\Omega_+)r_+} \right].$$
(4.74)

4.2.4 Summary (non-superradiant modes)

We have defined

$$I_{\ell m} = \lambda_{\ell m}(a\omega) \frac{\arctan(a/r_+)}{a/r_+} + K_{MQJ},$$
(4.75)

where

$$K_{MQJ} = \frac{3}{8} \frac{\arctan(a/r_+)}{a/r_+} + \frac{r_+ r_-}{8a^2} \left[\frac{\arctan(a/r_+)}{a/r_+} - \frac{r_+^2}{r_+^2 + a^2} \right]$$
$$+ \frac{1}{8} \frac{r_+ (3a + r_+ - 2r_-)}{r_+^2 + a^2}.$$
(4.76)

Then, for the non-superradiant modes

$$T_{\ell,m\leq 0} \geq \mathrm{sech}^2 \left[\frac{1}{2} \ln(1 - m\Omega_+/\omega) + \frac{I_{\ell,m\leq 0}}{2\omega r_+} \right],$$
(4.77)

and

$$T_{\ell,m\in(0,m_*)} \geq \mathrm{sech}^2 \left[-\frac{1}{2} \ln(1 - m\Omega_+/\omega) + \frac{I_{\ell,m\in(0,m_*)}}{2(\omega - m\Omega_+)r_+} \right].$$
(4.78)

These bounds can also be written as

$$T_{\ell,m\leq0} \geq \text{sech}^2\left[\frac{1}{2}\ln(1 - m/m_*) + \frac{I_{\ell,m\leq0}}{2\omega r_+}\right],$$ (4.79)

and

$$T_{\ell,m\in(0,m_*)} \geq \text{sech}^2\left[-\frac{1}{2}\ln(1 - m/m_*) + \frac{I_{\ell,m\in(0,m_*)}}{2\omega(1 - m/m_*)r_+}\right].$$ (4.80)

These are the best general bounds we have been able to establish for the non-superradiant modes.

4.3 Superradiant modes $(m \geq m_*)$

In this section, we consider the superradiant modes. The rigorous bound on the greybody factor is given by

$$T_{\ell m} \geq \text{sech}^2\left[\int_{-\infty}^{\infty} \frac{\sqrt{[\tilde{h}'(r_*)]^2 + [U_{\ell m}(r) + \tilde{h}^2(r_*)]^2}}{2\tilde{h}(r_*)}dr_*\right],$$ (4.81)

for any positive function $\tilde{h}(r_*)$. It can more explicitly be written as

$$T_{\ell m} \geq \text{sech}^2\left[\int_{-\infty}^{\infty} \frac{\sqrt{[\tilde{h}'(r_*)]^2 + \left[V_{\ell m}(r) - [\omega - m\varpi(r)]^2 + \tilde{h}^2(r_*)\right]^2}}{2\tilde{h}(r_*)}dr_*\right].$$ (4.82)

Using the triangle inequality in equation (4.53), we obtain

$$T_{\ell m} \geq \text{sech}^2\left[\frac{1}{2}\int_{-\infty}^{\infty}\left|\frac{\tilde{h}'(r_*)}{\tilde{h}(r_*)}\right|dr_* + \int_{-\infty}^{\infty}\frac{\left|V_{\ell m}(r) - [\omega - m\varpi(r)]^2 + \tilde{h}^2(r_*)\right|}{2\tilde{h}(r_*)}dr_*\right].$$ (4.83)

Using the triangle inequality,

$$|a + b| \leq |a| + |b|$$ (4.84)

for all real numbers a and b, we obtain

$$T_{\ell m} \geq \text{sech}^2\left[\frac{1}{2}\int_{-\infty}^{\infty}\left|\frac{\tilde{h}'(r_*)}{\tilde{h}(r_*)}\right|dr_* + \int_{-\infty}^{\infty}\frac{V_{\ell m}(r)}{2\tilde{h}(r_*)}dr_*\right.$$
$$\left. + \int_{-\infty}^{\infty}\frac{\left|\tilde{h}^2(r_*) - [\omega - m\varpi(r)]^2\right|}{2\tilde{h}(r_*)}dr_*\right].$$ (4.85)

The third integral is finite if $h^2(\infty) = \omega^2$ and $h^2(r_+) = (\omega - m\Omega_+)^2$. We observe that when $m = 2\omega/\Omega_+ = 2m_*$, we obtain $\omega^2 = (\omega - m\Omega_+)^2$. Therefore, we divide the superradiant mode into two cases

- $m \in [m_*, 2m_*)$.

- $m \in [2m_*, \infty)$.

4.3.1   Low-lying superradiant modes $[m \in [m_*, 2m_*)]$

In this case, we have $\omega^2 > (\omega - m\Omega_+)^2$. We choose

$$
h(r) = \begin{cases} m\Omega_+ - \omega & \text{if } r_+ < r < r_0 \\ \omega - \dfrac{ma}{r^2 + a^2} & \text{if } r \geq r_0 \end{cases}, \tag{4.86}
$$

where $h(r) = \tilde{h}(r_*)$ and r_0 is the point at which $\omega - ma/(r^2 + a^2) = m\Omega_+ - \omega$. That is

$$
r_0 = \sqrt{r_+^2 + \frac{2(m - m_*)}{2m_* - m}(r_+^2 + a^2)}. \tag{4.87}
$$

The derivative of $\tilde{h}(r_*)$ is

$$
\tilde{h}'(r_*) = \frac{\mathrm{d}\tilde{h}(r_*)}{\mathrm{d}r_*} = \frac{\mathrm{d}r}{\mathrm{d}r_*}\frac{\mathrm{d}h(r)}{\mathrm{d}r} = \begin{cases} 0 & \text{if } r_+ < r < r_0 \\ \dfrac{\Delta}{r^2 + a^2}\dfrac{2mar}{(r^2 + a^2)^2} & \text{if } r \geq r_0 \end{cases}. \tag{4.88}
$$

We see that $\tilde{h}'(r_*) \geq 0$. Then, $\tilde{h}(r_*)$ is positive and monotone. Moreover, $\tilde{h}(r_*) \geq m\Omega_+ - \omega$ occurs everywhere. Therefore,

$$
\int_{-\infty}^{\infty} \frac{|\tilde{h}'(r_*)|}{\tilde{h}(r_*)}\mathrm{d}r_* = |\ln h(r)|_{r_+}^{\infty} = \ln\left(\frac{\omega}{m\Omega_+ - \omega}\right) = -\ln(m/m_* - 1). \tag{4.89}
$$

The $V_{\ell m}(r)$ integral is evaluated, yielding

$$
\int_{-\infty}^{\infty} \frac{V_{\ell m}(r)}{2\tilde{h}(r_*)}\mathrm{d}r_* \leq \int_{-\infty}^{\infty} \frac{V_{\ell m}(r)}{2(m\Omega_+ - \omega)} = \frac{I_{\ell m}}{2(m\Omega_+ - \omega)r_+} = \frac{I_{\ell m}}{2\omega(m/m_* - 1)r_+}, \tag{4.90}
$$

where $I_{\ell m}$ is the same quantity as before. Finally, the remaining integral to be performed is

$$
J_m^{\text{low}} = \int_{-\infty}^{\infty} \frac{\tilde{h}^2(r_*) - [\omega - m\varpi(r)]^2}{2\tilde{h}(r_*)}\mathrm{d}r_*. \tag{4.91}
$$

Substituting $\tilde{h}(r_*)$, we obtain

$$
J_m^{\text{low}} = \int_{r_+}^{r_0} \frac{(m\Omega_+ - \omega)^2 - [\omega - m\varpi(r)]^2}{2(m\Omega_+ - \omega)}\frac{r^2 + a^2}{\Delta}\mathrm{d}r. \tag{4.92}
$$

Factorizing the numerator gives

$$
J_m^{\text{low}} = \frac{m}{2(m\Omega_+ - \omega)}\int_{r_+}^{r_0} (\Omega_+ - \varpi)[m\Omega_+ - \omega + m\varpi(r) - \omega]\frac{r^2 + a^2}{\Delta}\mathrm{d}r. \tag{4.93}
$$

In this range $r \in (r_+, r_0)$, we have

$$0 \leq m\Omega_+ - \omega + m\varpi(r) - \omega \leq 2\left(m\Omega_+ - \omega\right). \tag{4.94}$$

Therefore,

$$J_m^{\text{low}} \leq m \int_{r_+}^{r_0} (\Omega_+ - \varpi) \frac{r^2 + a^2}{\Delta} \mathrm{d}r = \frac{ma}{r_+^2 + a^2} \int_{r_+}^{r_0} \frac{r + r_+}{r - r_-} \mathrm{d}r. \tag{4.95}$$

It can be evaluated, giving

$$J_m^{\text{low}} \leq \frac{ma}{r_+^2 + a^2} \left[r_0 - r_+ + (r_+ + r_-) \ln \left(\frac{r_0 - r_-}{r_+ - r_-} \right) \right]. \tag{4.96}$$

Finally, we obtain

$$T_{\ell, m \in [m_*, 2m_*)} \geq \mathrm{sech}^2 \left[-\frac{1}{2} \ln \left(m/m_* - 1 \right) + \frac{I_{\ell, m \in [m_*, 2m_*)}}{2\omega \left(m/m_* - 1 \right) r_+} + J_m^{\text{low}} \right]. \tag{4.97}$$

4.3.2 Highly superradiant modes ($m \geq 2m_*$)

In this case, we have $(\omega - m\Omega_+)^2 > \omega^2$. We choose

$$h(r) = \begin{cases} \dfrac{ma}{r^2 + a^2} - \omega & \text{if } r_+ < r < r_0 \\ \omega & \text{if } r \geq r_0 \end{cases}, \tag{4.98}$$

where $h(r) = \tilde{h}(r_*)$ and r_0 is the point at which $ma/\left(r^2 + a^2\right) - \omega = \omega$. That is

$$r_0 = a\sqrt{\frac{m}{2\omega a} - 1}. \tag{4.99}$$

The derivative of $\tilde{h}(r_*)$ is

$$\tilde{h}'(r_*) = \frac{\mathrm{d}\tilde{h}(r_*)}{\mathrm{d}r_*} = \frac{\mathrm{d}r}{\mathrm{d}r_*} \frac{\mathrm{d}h(r)}{\mathrm{d}r} = \begin{cases} -\dfrac{\Delta}{r^2 + a^2} \dfrac{2mar}{\left(r^2 + a^2\right)^2} & \text{if } r_+ < r < r_0 \\ 0 & \text{if } r \geq r_0 \end{cases}. \tag{4.100}$$

We see that $\tilde{h}'(r_*) \leq 0$. Then, $\tilde{h}(r_*)$ is positive and monotone. Moreover, $\tilde{h}(r_*) \geq \omega$ occurs everywhere. Therefore,

$$\int_{-\infty}^{\infty} \frac{|\tilde{h}'(r_*)|}{\tilde{h}(r_*)} \mathrm{d}r_* = |\ln h(r)|_{r_+}^{\infty} = \ln \left(\frac{m\Omega_+ - \omega}{\omega} \right) = \ln \left(m/m_* - 1 \right). \tag{4.101}$$

The $V_{\ell m}(r)$ integral is evaluated, yielding

$$\int_{-\infty}^{\infty} \frac{V_{\ell m}(r)}{2\tilde{h}(r_*)} \mathrm{d}r_* \leq \int_{-\infty}^{\infty} \frac{V_{\ell m}(r)}{2\omega} = \frac{I_{\ell m}}{2\omega r_+}, \tag{4.102}$$

where $I_{\ell m}$ is the same quantity as before. Finally, the remaining integral to be performed is

$$J_m^{\text{high}} = \int_{-\infty}^{\infty} \frac{\tilde{h}^2(r_*) - [\omega - m\varpi(r)]^2}{2\tilde{h}(r_*)} \mathrm{d}r_*. \qquad (4.103)$$

Substituting $\tilde{h}(r_*)$, we obtain

$$J_m^{\text{high}} = \int_{r_0}^{\infty} \frac{\omega^2 - [\omega - m\varpi(r)]^2}{2\omega} \frac{r^2 + a^2}{\Delta} \mathrm{d}r. \qquad (4.104)$$

Factorizing the numerator gives

$$J_m^{\text{high}} = \frac{m}{2\omega} \int_{r_0}^{\infty} \varpi(r)[2\omega - m\varpi(r)] \frac{r^2 + a^2}{\Delta} \mathrm{d}r = \frac{ma}{2\omega} \int_{r_0}^{\infty} \frac{2\omega - m\varpi(r)}{\Delta} \mathrm{d}r. \qquad (4.105)$$

In this range $r \geq r_0$, we have

$$0 \leq 2\omega - m\varpi(r) \leq 2\omega. \qquad (4.106)$$

If $m > 2m_*$, then,

$$J_m^{\text{high}} \leq ma \int_{r_0}^{\infty} \frac{1}{\Delta} \mathrm{d}r, \qquad (4.107)$$

which is finite. If $m = 2m_*$, we have

$$r_0 = a\sqrt{\frac{1}{a\Omega_+} - 1} = a\sqrt{\frac{r_+^2 + a^2}{a^2} - 1} = r_+. \qquad (4.108)$$

Therefore,

$$J_m^{\text{high}} = ma \int_{r_+}^{\infty} \left[1 - \frac{\varpi(r)}{\Omega_+} \right] \frac{1}{\Delta} \mathrm{d}r, \qquad (4.109)$$

which is also finite. Finally, we obtain

$$T_{\ell,m \geq 2m_*} \geq \mathrm{sech}^2 \left[\frac{1}{2} \ln (m/m_* - 1) + \frac{I_{\ell,m \geq 2m_*}}{2\omega r_+} + J_m^{\text{high}} \right]. \qquad (4.110)$$

4.3.3 Summary (superradiant modes)

For the superradiant modes, we have

$$T_{\ell,m \in [m_*,2m_*)} \geq \mathrm{sech}^2 \left[-\frac{1}{2} \ln (m/m_* - 1) + \frac{I_{\ell,m \in [m_*,2m_*)}}{2\omega (m/m_* - 1) r_+} + J_m^{\text{low}} \right] \qquad (4.111)$$

and

$$T_{\ell,m \geq 2m_*} \geq \mathrm{sech}^2 \left[\frac{1}{2} \ln (m/m_* - 1) + \frac{I_{\ell,m \geq 2m_*}}{2\omega r_+} + J_m^{\text{high}} \right]. \qquad (4.112)$$

4.4 Discussion

In this chapter, we have calculated the rigorous bounds on the greybody factors for massless scalar field emitted from Kerr-Newman black holes. We have used the methods developed by Boonserm and Visser [8, 9, 10] to derive rigorous bounds on the greybody factors. Although for rotating black holes we lose the assumption of spherical symmetry, which is possessed by non-rotating black holes, we can assume axial symmetry which makes the separation of variables possible. We have also used spheroidal coordinates instead of spherical coordinates that are normally used with non-rotating black holes.

In order to obtain the bounds, we divide the scalar modes into five cases depending on the value of m. Specifically, we have divided these modes into the following; zero-angular-momentum mode ($m = 0$), negative-angular-momentum mode ($m < 0$), and low-lying positive-angular-momentum mode [$m \in (0, m_*)$], which are all referred to as non-superradiant modes ($m < m_*$), and also the low-lying superradiant mode [$m \in [m_*, 2m_*)$] and highly superradiant mode ($m \geq 2m_*$), which are referred to as superradiant modes ($m \geq m_*$). For the zero-angular-momentum mode ($m = 0$), we have chosen $h(r) = \omega$. For the negative-angular-momentum mode ($m < 0$) and the low-lying positive-angular-momentum mode [$m \in (0, m_*)$], we have chosen $h(r) = \omega - m\varpi$. On the other hand, for the low-lying superradiant mode [$m \in [m_*, 2m_*)$], we have chosen

$$
h(r) = \begin{cases} m\Omega_+ - \omega & \text{if } r_+ < r < r_0 \\ \omega - \dfrac{ma}{r^2 + a^2} & \text{if } r \geq r_0 \end{cases} .
\tag{4.113}
$$

For the highly superradiant modes ($m \geq 2m_*$), we have chosen

$$
h(r) = \begin{cases} \dfrac{ma}{r^2 + a^2} - \omega & \text{if } r_+ < r < r_0 \\ \omega & \text{if } r \geq r_0 \end{cases} .
\tag{4.114}
$$

In each of these cases, we choose an appropriate function $h(r)$ in order that the bounds can be calculated. Moreover, for rotating black holes, there is a new phenomenon called super-radiance, a phenomenon where the reflection coefficients are greater than unity, which disappears from non-rotating black holes.

Chapter V

Greybody factors for dirty black holes

In this chapter, we calculate the rigorous bounds on the greybody factors for dirty black holes, ones which are surrounded by matters and energies instead of vacuum. The presence of such matters and energies changes the main features of black holes, such as the variations in the Regge-Wheeler equation and greybody factors. In addition to scalar field (spin 0), we are also interested in vector field (spin 1) and spin 2 field emitted from the black holes. We follow from [58].

5.1   Dirty black holes

Dirty black holes are in an environment of matters and energies [59, 60, 61]. The spacetime for dirty black holes is a generic, static, spherically symmetric spacetime with the metric

$$\mathrm{d}s^2 = -e^{-2\phi(r)}\left[1 - \frac{2Gm(r)}{r}\right]\mathrm{d}t^2 + \left[1 - \frac{2Gm(r)}{r}\right]^{-1}\mathrm{d}r^2 + r^2\mathrm{d}\Omega^2, \qquad (5.1)$$

where $\phi(r)$ is related to the distribution of matter and $m(r)$ is the total mass within the radius r from center of a black hole. There are singularities in this metric at $r = 0$ and $r = r_H$, where

$$r_H = 2Gm(r_H). \qquad (5.2)$$

Like other black holes we have introduced in chapter II, the point $r = 0$ is a true singularity while the surface $r = r_H$ is not; it is just a coordinate singularity and a place where the event horizon is located. We assume asymptotic flatness. Then, $m(\infty)$ is finite and $\phi(\infty) = 0$.

5.2   Classical energy conditions

The Einstein's equations in spacetime give by equation (5.1) are

$$\frac{\mathrm{d}m}{\mathrm{d}r} = 4\pi\rho r^2 \quad \text{and} \quad \frac{\mathrm{d}\phi}{\mathrm{d}r} = -\frac{4\pi(\rho + p_r)r}{1 - 2m(r)/r}, \qquad (5.3)$$

where ρ and p_r are the energy density and radial pressure of matter fields, respectively. Classical energy conditions are coordinate-invariant constraints on the energy-momentum tensor. There are various types of classical energy conditions. For example, the weak and null energy conditions state that

$$\text{WEC} \Rightarrow \rho \geq 0 \Rightarrow m(r_H) \leq m(r) \leq m(\infty) \tag{5.4}$$

$$\text{NEC} \Rightarrow \rho + p_r \geq 0 \Rightarrow \phi(r_H) \geq \phi(r) \geq 0. \tag{5.5}$$

That is, there are specific requirements that the energy density is nonnegative and the pressure is not too large compared to the energy density. Furthermore, they are also useful in obtaining the bounds on the greybody factors.

5.3 Regge-Wheeler equation

5.3.1 Scalar emission

In this section, we look at a massless uncharged scalar field emitted from the dirty black hole. Comparing equation (5.1) with equation (3.1), we find

$$A(r) = e^{-2\phi(r)} \left[1 - \frac{2Gm(r)}{r} \right], \quad B(r) = 1 - \frac{2Gm(r)}{r} \quad \text{and} \quad d = 4. \tag{5.6}$$

From equation (3.23), the Regge-Wheeler equation is

$$\frac{\mathrm{d}^2 \psi_\ell(r)}{\mathrm{d}r_*^2} + \left[\omega^2 - V_\ell(r) \right] \psi_\ell(r) = 0. \tag{5.7}$$

In this case, from equation (3.15), the tortoise coordinate r_* is given by

$$\frac{\mathrm{d}r_*}{\mathrm{d}r} = e^{\phi(r)} \left[1 - \frac{2Gm(r)}{r} \right]^{-1} \tag{5.8}$$

and from equation (3.24), we have the effective potential

$$V_\ell(r) = e^{-2\phi(r)} \left[1 - \frac{2Gm(r)}{r} \right] \frac{\ell(\ell+1)}{r^2} + \frac{1}{r} \frac{\mathrm{d}^2 r}{\mathrm{d}r_*^2}. \tag{5.9}$$

Using the Einstein equations

$$\frac{\mathrm{d}m(r)}{\mathrm{d}r} = \frac{4\pi \rho r^2}{G} \quad \text{and} \quad \frac{\mathrm{d}\phi(r)}{\mathrm{d}r} = -\frac{4\pi(\rho + p_r)r}{1 - 2Gm(r)/r}, \tag{5.10}$$

we obtain

$$\frac{1}{r} \frac{\mathrm{d}^2 r}{\mathrm{d}r_*^2} = e^{-2\phi(r)} \left[1 - \frac{2Gm(r)}{r} \right] \left[\frac{2Gm(r)}{r^3} - 4\pi(\rho - p_r) \right]. \tag{5.11}$$

Therefore,

$$V_\ell(r) = e^{-2\phi(r)} \left[1 - \frac{2Gm(r)}{r} \right] \left[\frac{\ell(\ell+1)}{r^2} + \frac{2Gm(r)}{r^3} - 4\pi(\rho - p_r) \right]. \tag{5.12}$$

5.3.2 Vector emission

In this section, we look at a vector field emitted from the dirty black hole. While the equation of motion of a scalar field on the black hole background is the Klein-Gordon equation, the equation of motion of a vector field is the **Maxwell equation**

$$\frac{1}{\sqrt{-g}}\partial_\mu \left(\sqrt{-g}g^{\mu\nu}g^{\rho\sigma}F_{\nu\sigma}\right) = 0, \tag{5.13}$$

where $F_{\mu\nu} = \partial_\mu A_\nu - \partial_\nu A_\mu$ is the field strength tensor. This equation is equivalent to

$$\nabla_\mu F^{\mu\nu} = 0, \tag{5.14}$$

where ∇_μ is the covariant derivative. The Regge-Wheeler equation is

$$\frac{\mathrm{d}^2\psi_\ell(r)}{\mathrm{d}r_*^2} + \left[\omega^2 - V_\ell(r)\right]\psi_\ell(r) = 0. \tag{5.15}$$

In this case, the tortoise coordinate r_* is given by

$$\frac{\mathrm{d}r_*}{\mathrm{d}r} = e^{\phi(r)}\left[1 - \frac{2Gm(r)}{r}\right]^{-1} \tag{5.16}$$

and we have the effective potential

$$V_\ell(r) = e^{-2\phi(r)}\left[1 - \frac{2Gm(r)}{r}\right]\frac{\ell(\ell+1)}{r^2}. \tag{5.17}$$

5.3.3 Spin 2 emission

In this section, we look at a spin 2 field emitted from the dirty black hole. The Regge-Wheeler equation is

$$\frac{\mathrm{d}^2\psi_\ell(r)}{\mathrm{d}r_*^2} + \left[\omega^2 - V_\ell(r)\right]\psi_\ell(r) = 0. \tag{5.18}$$

In this case, the tortoise coordinate r_* is given by

$$\frac{\mathrm{d}r_*}{\mathrm{d}r} = e^{\phi(r)}\left[1 - \frac{2Gm(r)}{r}\right]^{-1} \tag{5.19}$$

and we have the effective potential [62]

$$V_\ell(r) = e^{-2\phi(r)}\left[1 - \frac{2Gm(r)}{r}\right]\left[\frac{\ell(\ell+1)}{r^2} - \frac{6Gm(r)}{r^3} + 4\pi(\rho - p_r)\right]. \tag{5.20}$$

Using the Einstein equations (5.10), we obtain

$$V_\ell(r) = e^{-2\phi(r)}\left[1 - \frac{2Gm(r)}{r}\right]\left[\frac{\ell(\ell+1)}{r^2} - \frac{4Gm(r)}{r^3}\right] - \frac{1}{r}\frac{\mathrm{d}^2 r}{\mathrm{d}r_*^2}. \tag{5.21}$$

5.3.4 Spins zero, one, and two

We can combine all the effective potentials into a single formula as

$$V_\ell(r) = e^{-2\phi(r)} \left[1 - \frac{2Gm(r)}{r} \right] \left[\frac{\ell(\ell+1)}{r^2} - \frac{2S(S-1)Gm(r)}{r^3} \right] + \frac{1-S}{r} \frac{\mathrm{d}^2 r}{\mathrm{d}r_*^2}, \quad (5.22)$$

where $S \in \{0, 1, 2\}$. Using the Einstein equations (5.10), we obtain

$$V_\ell(r) = e^{-2\phi(r)} \left[1 - \frac{2Gm(r)}{r} \right]$$
$$\times \left[\frac{\ell(\ell+1)}{r^2} + \frac{2(1-S^2)Gm(r)}{r^3} - 4(1-S)\pi(\rho - p_r) \right]. \quad (5.23)$$

5.4 Rigorous bounds on greybody factors

The rigorous bound on the greybody factor for $h(r) = \omega$ is given by

$$T \geq \operatorname{sech}^2 \left[\frac{1}{2\omega} \int_{-\infty}^{\infty} V_\ell(r) \mathrm{d}r_* \right]. \quad (5.24)$$

Using equation (5.8), the effective potential in equation (5.22) becomes

$$V_\ell(r)\mathrm{d}r_* = e^{-\phi(r)} \left[\frac{\ell(\ell+1)}{r^2} - \frac{2S(S-1)Gm(r)}{r^3} \right] \mathrm{d}r$$
$$+ \frac{1-S}{r} \frac{\mathrm{d}}{\mathrm{d}r} \left[e^{-\phi(r)} \left(1 - \frac{2Gm(r)}{r} \right) \right] \mathrm{d}r. \quad (5.25)$$

Using

$$u \frac{\mathrm{d}v}{\mathrm{d}r} = \frac{\mathrm{d}(uv)}{\mathrm{d}r} - v \frac{\mathrm{d}u}{\mathrm{d}r}, \quad (5.26)$$

then,

$$V_\ell(r)\mathrm{d}r_* = e^{-\phi(r)} \left[\frac{\ell(\ell+1)}{r^2} - \frac{2S(S-1)Gm(r)}{r^3} + \frac{1-S}{r^2} \left(1 - \frac{2Gm(r)}{r} \right) \right] \mathrm{d}r$$
$$+ (1-S) \frac{\mathrm{d}}{\mathrm{d}r} \left[\frac{1}{r} e^{-\phi(r)} \left(1 - \frac{2Gm(r)}{r} \right) \right] \mathrm{d}r. \quad (5.27)$$

Therefore,

$$\int_{-\infty}^{\infty} V_\ell(r)\mathrm{d}r_* = \int_{r_H}^{\infty} \frac{e^{-\phi(r)}}{r^2} \left[\ell(\ell+1) + (1-S) - (S-1)^2 \frac{2Gm(r)}{r} \right] \mathrm{d}r, \quad (5.28)$$

where the total derivative term vanishes both at r_H and at spatial infinity. Using the WEC, equation (5.4), we see that the above integral is bounded above by

$$\int_{-\infty}^{\infty} V_\ell(r)\mathrm{d}r_* \leq \int_{r_H}^{\infty} \frac{e^{-\phi(r)}}{r^2} \left[\ell(\ell+1) + (1-S) - (S-1)^2 \frac{r_H}{r} \right] \mathrm{d}r. \quad (5.29)$$

Using the NEC, equation (5.5), we obtain $e^{-\phi(r)} \leq 1$. Thus,

$$\int_{-\infty}^{\infty} V_\ell(r) \mathrm{d}r_* \leq \int_{r_H}^{\infty} \frac{1}{r^2}\left[\ell(\ell+1) + (1-S) - (S-1)^2\frac{r_H}{r}\right]\mathrm{d}r. \tag{5.30}$$

Performing this integral, we obtain

$$\int_{-\infty}^{\infty} V_\ell(r)\mathrm{d}r_* \leq \frac{1}{r_H}\left[\ell(\ell+1) + (1-S) - \frac{(S-1)^2}{2}\right] = \frac{1}{r_H}\left[\ell(\ell+1) + \frac{1-S^2}{2}\right]. \tag{5.31}$$

Therefore, from equation (5.24), we obtain the rigorous bounds on the greybody factors

$$T \geq \mathrm{sech}^2\left[\frac{1}{2\omega r_H}\left\{\ell(\ell+1) + \frac{1-S^2}{2}\right\}\right]. \tag{5.32}$$

5.5   Discussion

In this chapter, we calculated the rigorous bounds on the greybody factors for massless scalar field, massless vector field, and massless spin 2 field emitted from dirty black holes. A dirty black hole is a black hole surrounded by matters and energies rather than vacuum. In the absence of these matters and energies, a dirty black hole reduces to a Schwarzschild black hole. For a scalar field, we started calculating the rigorous bounds on the greybody factors with the Klein-Gordon equation in a curved spacetime, for a vector field, we initiated the calculations of the rigorous bounds on the greybody factors with the Maxwell's equations in a curved spacetime, while for a spin 2 field, we began calculating the rigorous bounds on the greybody factors with axial spin 2 perturbations on a curved spacetime. The summaries are shown in table V.1.

Types of Hawking radiation	Equation of motion
A scalar field	The Klein-Gordon equation in curved spacetime
A vector field	The Maxwell equation in curved spacetime
A spin 2 field	Axial spin 2 perturbations on curved spacetime

Table V.1: Equation of motion of different types of Hawking radiation.

We have used the methods developed by Boonserm and Visser [8, 9, 10] and the classical energy constraints on the spacetime geometry to extract very general and rigorous bounds on the greybody factors. Specifically, we have used the weak energy condition (WEC) and the null energy condition (NEC). We have chosen $h(r) = \omega$ as we had done in chapter III in order to derive the rigorous bounds on the greybody factors.

Chapter VI

Conclusions

We began this dissertation with a review of quantum mechanics in order to provide some basics for the study and comprehension of quantum black holes. Specifically, we have reviewed the Schrödinger equation and some one-dimensional problems with various potentials such as a delta function potential, a rectangular barrier potential, an Eckart potential, and a Hulthen potential. These are the basics necessary for studying Hawking radiation emitted from black holes since equations of motion of Hawking radiation in the black hole backgrounds take the form of the Schrödinger-like equations with various potentials. We have also introduced general aspects of black holes and their classification.

A classical black hole rests on the belief that anything that enters a black hole cannot escape, not even light. As a result, it cannot directly be seen by an observer. A black hole is a singularity surrounded by a surface known as an event horizon which acts as a boundary of the black hole. The singularity of a black hole is the spacetime region with infinite curvature, where all of the laws of physics break down. The event horizon separates the black hole from the universe. In the standard (four-dimensional) general relativity, classical black holes is classified into four types which can be summarized in table VI.1.

	No rotation ($a = 0$)	With rotation ($a \neq 0$)
No charge ($Q = 0$)	Schwarzschild	Kerr
With charge ($Q \neq 0$)	Reissner-Nordström	Kerr-Newman

Table VI.1: Classification of classical black holes in general relativity.

For non-rotating black holes such as Schwarzschild black holes and Reissner-Nordström black holes, their singularities are point singularities, whereas for rotating black holes such as Kerr black holes and Kerr-Newman black holes, their singularities become ring singularities as a result of rotation. The Schwarzschild black holes have only one event horizon while the others have two event horizons (in

the usual case). Moreover, we have also studied the generalization of Schwarzschild black holes to d dimensions, which is called Schwarzschild-Tangherlini black holes and also black holes which are the solutions to the low-energy string theory such as charged dilatonic black holes both in $(2 + 1)$ and in $(3 + 1)$ dimensions.

On the other hand, from a quantum point of view, Stephen Hawking showed, in 1974, that a black hole is in actuality not 'black' but rather can emit radiation, which became known as Hawking radiation [1]. Hawking radiation is a thermal radiation with a Hawking temperature which is inversely proportional to the black hole mass. Emission of Hawking radiation leads to black hole evaporation. Eventually, a black hole will disappear. This Hawking radiation propagates in a curved spacetime represented by the potential of the Schrödinger-like equations. When the Hawking radiation is scattered by the potential, part of it will be reflected back into the black hole and the rest will be transmitted out of the black hole. This phenomenon is analogous to one-dimensional potential problems in quantum mechanics. An observer away from the black hole can only observe the transmitted wave. This transmitted wave can be thought of as a greybody radiation because the incident wave, which is a blackbody radiation, is modified by the curvature of spacetime. Therefore, a greybody factor is defined as a transmission probability.

Moreover, there is a new phenomenon, superradiance, arising in the rotating black holes, which is absent in non-rotating black holes. Superradiance is a phenomenon where the reflection coefficients are greater than unity. This is because the incoming wave can actually extract energy from the system instead of losing energy.

In this dissertation, we have obtained rigorous bounds on the greybody factors for massless scalar field emitted from non-rotating black holes. In particular, we have studied the Reissner-Nordström black holes, Schwarzschild-Tangherlini black holes, charged dilatonic black holes in $(2 + 1)$ dimensions, and charged dilatonic black holes in $(3 + 1)$ dimensions. Moreover, we have obtained rigorous bounds on the greybody factors for massless scalar field emitted from Kerr-Newman black holes, and dirty black holes. We have also calculated rigorous bounds on the greybody factors for massless vector field and massless spin 2 field emitted from the dirty black holes.

We have used the methods developed by Boonserm and Visser [8, 9, 10] to derive rigorous bounds on the greybody factors. For non-rotating black holes, including dirty black holes, we have made an assumption of spherical symmetry to simplify problems. Although Kerr-Newman black holes, which are the rotating

black holes, do not possess spherical symmetry, we have assumed axial symmetry. For dirty black holes, we have also used the classical energy constraints on the spacetime geometry to extract very general and rigorous bounds on the greybody factors.

The advantage of these methods is that we do not have to explicitly solve the Regge-Wheeler equations in case of non-rotating black holes and dirty black holes, and the radial Teukolsky equations in case of Kerr-Newman black holes to obtain the greybody factors. In fact, setting up these methods implicitly solves these Schrödinger-like equations already. Moreover, these methods can work in all frequency regimes while other approximations can only be valid in some limits. Rigorous bounds on greybody factors for various types of black holes are summarized in table VI.2

Black holes	Bounds on greybody factors
Reissner-Nordström	$T \geq \mathrm{sech}^2 \left[\frac{1}{2\omega} \left\{ \frac{\ell(\ell+1)}{r_+} + \frac{GM}{r_+^2} - \frac{2G(Q^2+P^2)}{3r_+^3} \right\} \right]$
Schwarzschild-Tangherlini	$T \geq \mathrm{sech}^2 \left[\frac{4\ell(\ell+d-3)+(d-2)(d-3)}{8\omega r_0} \right]$
(2 + 1) charged dilatonic	Equation (3.69)
(3 + 1) charged dilatonic	$T \geq \mathrm{sech}^2 \left[\frac{1}{2\omega r_-} \left\{ 1 - \frac{r_+ - r_-}{r_-} \ln\left(\frac{r_+}{r_+ - r_-} \right) \right\} \right]$
Kerr-Newman	Equations (4.79), (4.80), (4.111), (4.112)
Dirty	$T \geq \mathrm{sech}^2 \left[\frac{1}{2\omega r_H} \left\{ \ell(\ell+1) + \frac{1-S^2}{2} \right\} \right]$

Table VI.2: The summary of bounds on greybody factors for each black hole.

For non-rotating black holes and dirty black holes, it is straightforward to derive rigorous bounds on the greybody factors. In particular, we have chosen $h(r) = \omega$ for all non-rotating black holes which have been studied in this dissertation and for dirty black holes. For Kerr-Newman black holes, the situations are more complicated when rigorous bounds on the greybody factors become dependent on scalar angular momentum modes. That is, we have to divide the scalar modes into five cases depending on the value of m. Specifically, we have divided these modes into zero-angular-momentum modes ($m = 0$), negative-angular-momentum modes ($m < 0$), and low-lying positive-angular-momentum modes [$m \in (0, m_*)$], which are all referred to as non-superradiant modes ($m < m_*$), as well as low-lying superradiant modes [$m \in [m_*, 2m_*)$] and highly superradiant modes ($m \geq 2m_*$), which are referred to as superradiant modes ($m \geq m_*$). For the zero-angular-momentum modes ($m = 0$), we have chosen $h(r) = \omega$, for the negative-angular-momentum modes ($m < 0$) and low-lying positive-angular-

momentum modes [$m \in (0, m_*)$], we have chosen $h(r) = \omega - m\varpi$, and for the low-lying superradiant modes [$m \in [m_*, 2m_*)$], we have chosen

$$h(r) = \begin{cases} m\Omega_+ - \omega & \text{if } r_+ < r < r_0 \\ \omega - \dfrac{ma}{r^2 + a^2} & \text{if } r \geq r_0 \end{cases} . \tag{6.1}$$

For the highly superradiant modes ($m \geq 2m_*$), we have chosen

$$h(r) = \begin{cases} \dfrac{ma}{r^2 + a^2} - \omega & \text{if } r_+ < r < r_0 \\ \omega & \text{if } r \geq r_0 \end{cases} . \tag{6.2}$$

Choosing the appropriate function $h(r)$ leads to the easiest rigorous bounds. For the outlook, we can choose another form of the function $h(r)$ to obtain better bounds. The generalization of a particle with other spins such as a fermion is also interesting. Moreover, we can apply the methods used in this dissertation to other black holes or even other systems.

REFERENCES

[1] Hawking, S.W. Particle creation by black holes. Commun. Math. Phys. 43 (August 1975): 199-220.

[2] Parikh, M.K. and Wilczek, F. Hawking radiation as tunneling. Phys. Rev. Lett. 85 (December 2000): 5042-5045.

[3] Fleming, C.H. Hawking radiation as tunneling. (May 2005).

[4] Lange, P. Calculation of Hawking radiation as quantum mechanical tunneling. Master's Thesis, Department of Physics and Astronomy, Uppsala University, 2007.

[5] Fernando, S. Greybody factors of charged dilaton black holes in 2 + 1 dimensions. Gen. Relativ. Gravit. 37 (March 2005): 461-481.

[6] Kim, W. and Oh, J.J. Greybody factor and Hawking radiation of charged dilatonic black holes. J. Korean Phys. Soc. 52 (April 2008): 986-991.

[7] Escobedo, J. Greybody factors Hawking radiation in disguise. Master's Thesis, Institute for Theoretical Physics, Institute of Physics, Faculty of Science, University of Amsterdam, 2008.

[8] Visser, M. Some general bounds for 1-D scattering. Phys. Rev. A 59 (January 1999): 427438.

[9] Boonserm, P. and Visser, M. Bounding the Bogoliubov coefficients. Annals Phys. 323 (November 2008): 2779-2798.

[10] Boonserm, P. Rigorous bounds on transmission reflection and Bogoliubov coefficients. Doctoral dissertation, School of Mathematics, Statistics and Operations Research, Faculty of Science, Victoria University of Wellington, 2009.

[11] Boonserm, P. and Visser, M. Bounding the greybody factors for Schwarzschild black holes. Phys. Rev. D 78 (November 2008): 101502.

[12] Boonserm, P. and Visser, M. Quasi-normal frequencies: key analytic results. JHEP 03 (March 2011): 073.

[13] Baym, G. Lectures on quantum mechanics. New York: The Benjamin/Cummings Publishing Company, 1969.

[14] Gasiorowicz, S. Quantum physics. New York: Wiley, 1996.

[15] Landau, L.D. and Lifshitz, E.M. Quantum mechanics: non-relativistic theory. New York: Pergamon Press, 1977.

[16] Schiff, L.I. Quantum mechanics. New York: McGraw-Hill College, 1955.

[17] Messiah, A. Quantum mechanics. Amsterdam: North-Holland, 1958.

[18] Brandsen, B.H. and Joachain, C.J. Quantum mechanics. New York: Prentice Hall, 2000.

[19] Eckart, C. The penetration of a potential barrier by electrons. Phys. Rev. 35 (June 1930): 1303-1309.

[20] Morse, P.M. and Feshbach, H. Methods of theorectical physics. New York: McGraw-Hill, 1953.

[21] Guo, J.Y., Yu, Y., and Jin, S.W. Transmission resonance for a Dirac particle in a one-dimensional Hulthen potential. Eur. J. Phys. 7 (March 2009): 168-174.

[22] Carroll, S.M. An introduction to general relativity: spacetime and geometry. New York: Addison-Wesley, 2004.

[23] Foster, J. and Nightingale, J.D. A short course in general relativity. China: Beijing World Publishing Corporation, 1998.

[24] Kerr, R.P. Gravitational field of a spinning mass as an example of algebraically special metrics. Phys. Rev. Lett. 11 (September 1963): 237-238.

[25] Wiltshire, D.L., Visser, M., and Scott, S.M. The Kerr spacetime: rotating black holes in general relativity. Cambridge, UK: Cambridge University Press, 2009.

[26] http://www.zamandayolculuk.com/cetinbal/singularites.htm.

[27] Newman, E.T. and Janis, A.I. Note on the Kerr spinning particle metric. J. Math. Phys. 6 (June 1965): 915-917.

[28] Newman, E.T., Couch, E., Chinnapared, K., Exton, A., Prakash A., and Torrence R. Metric of a rotating, charged mass. J. Math. Phys. 6 (June 1965): 918-918.

[29] Ngampitipan, T. and Boonserm, P. Bounding the greybody factors for non-rotating black holes. Int. J. Mod. Phys. D 22 (June 2013): 1350058.

[30] Boonserm, P. and Visser, M. Transmission probabilities and the Miller-Good transformation. J. Phys. A: Math. Theor. 42 (January 2009): 045301.

[31] Boonserm, P. and Visser, M. Analytic bounds on transmission probabilities. Annals Phys. 325 (July 2010): 1328-1339.

[32] Boonserm, P. and Visser, M. Reformulating the Schrödinger equation as a Shabat-Zakharov system. J. Math. Phys. 51 (February 2010): 022105.

[33] Ngampitipan, T. and Boonserm, P. Bounding the greybody factors for the Reissner-Nordström black holes. J. Phys. Conf. Ser. 435 (April 2013): 012027.

[34] Tangherlini, F.R. Schwarzschild field in n dimensions and the dimensionality of space problem. Nuovo Cimento 27 (February 1963): 636-651.

[35] Boonserm, P., Ngampitipan, T., and Visser, M. Bounding the greybody factors for scalar field excitations on the Kerr-Newman spacetime. JHEP 03 (March 2014): 113.

[36] Carter, B. Hamilton-Jacobi and Schrödinger separable solutions of Einsteins equations. Commun. Math. Phys. 10 (April 1968): 280-310.

[37] Sasaki, M. and Tagoshi, H. Analytic black hole perturbation approach to gravitational radiation. Living Rev. Rel. 6 (November 2003): 6.

[38] Press, W.H. and Teukolsky, S.A. Perturbations of a rotating black hole. II. Dynamical stability of the Kerr metric. Astrophys. J. 185 (October 1973): 649-674.

[39] Fackerell, E.D. and Crossman, R.G. Spin-weighted angular spheroidal functions. J. Math. Phys. 18 (September 1977): 1849-1854.

[40] Shibata, M., Sasaki, M., Tagoshi, H., and Tanaka, T. Gravitational waves from a particle orbiting around a rotating black hole: post-Newtonian expansion. Phys. Rev. D 51 (February 1995): 1646-1663.

[41] Tagoshi, H., Shibata, M., Tanaka, T., and Sasaki, M. Post-Newtonian expansion of gravitational waves from a particle in circular orbits around a rotating black hole: up to $O(v^8)$ beyond the quadrupole formula. Phys. Rev. D 54 (July 1996): 1439-1459.

[42] Maier, R.S. The 192 solutions of the Heun equation. Math. Comput. 76 (April 2007): 811-843.

[43] Ronveaux, A. Heuns differential equations. Oxford, UK: Clarendon Press, Oxford University Press, 1995.

[44] Sleeman, B.D. and Kuznetzov, V.B. Heun functions. In Olver, F.W.J., Lozier, D.M., Boisvert, R.F., and Clark, C.W. (eds.), NIST handbook of mathematical functions, Cambridge UK: Cambridge University Press, 2010.

[45] Valent, G. Heun functions versus elliptic functions. In Elaydi, S., Cushing, J., Lasser, R., Papageorgiou, V., and Ruffing, A. (eds.), Difference equations, special functions and orthogonal polynomials, Singapore: World Scientific Pub Co Inc, 2007.

[46] Kokkotas, K.D., Konoplya, R.A., and Zhidenko, A. Quasinormal modes, scattering and Hawking radiation of Kerr-Newman black holes in a magnetic field. Phys. Rev. D 83 (January 2011): 024031.

[47] Frolov, V. and Novikov, I.D. Black hole physics: basic concepts and new developments. Dordrecht, Netherlands: Kluwer Academic, 1998.

[48] Raine, D.J. and Thomas, E.G. Black holes: an introduction. London, UK: Imperial College Press, 2005.

[49] Kazazakis, V.D. Quasi-normal modes of scalar fields in Kerr background. Master's Thesis, Institute for Theoretical Physics, Institute of Physics, Faculty of Science, University of Amsterdam, 2012.

[50] Manogue, C.A. The Klein paradox and superradiance. Annals of Physics 181 (February 1988): 261-283.

[51] Starobinskij, A.A. Amplification of waves during reflection from a rotating black hole. Soviet Journal of Experimental and Theoretical Physics 37 (July 1973): 28-32.

[52] Starobinskij, A.A. and Churilov, S.M. Amplification of electromagnetic and gravitational waves scattered by a rotating black hole. Zhurnal Eksperimental noi i Teoreticheskoi Fiziki 65 (July 1973): 3-11.

[53] Zel'Dovich, Y.B. Amplification of cylindrical electromagnetic waves reflected from a rotating body. Soviet Journal of Experimental and Theoretical Physics 35 (December 1972): 1085-1087.

[54] Bekenstein, J.D. and Schiffer, M. The many faces of superradiance. Phys. Rev. D 58 (August 1998): 064014.

[55] Boonserm, P., Ngampitipan, T., and Visser, M. Superradiance and flux conservation. Phys. Rev. D 90 (September 2014): 064013.

[56] Richartz, M., Weinfurtner, S., Penner, A.J., and Unruh, W.G. Generalised superradiant scattering. Phys. Rev. D 80 (December 2009): 124016.

[57] Ngampitipan, T., Boonserm, P., and Visser, M. Rigorous bound on transmission probability for $m = 0$ scalar excitations of Kerr-Newman black holes. In Siam Physics Congress (SPC2014)

[58] Boonserm, P., Ngampitipan, T., and Visser, M. Regge-Wheeler equation, linear stability, and greybody factors for dirty black holes. Phys. Rev. D 88 (August 2013): 041502.

[59] Visser, M. Dirty black holes: Thermodynamics and horizon structure. Phys. Rev. D 46 (September 1992): 2445-2451.

[60] Visser, M. Dirty black holes: Entropy versus area. Phys. Rev. D 48 (July 1993): 583-591.

[61] Visser, M. Dirty black holes: Entropy as a surface term. Phys. Rev. D 48 (December 1993): 5697-5705.

[62] Kojima, Y., Yoshida, S., and Futamase, T. Non-radial pulsation of boson star I: Formulation. Prog. Theor. Phys. 86 (August 1991): 401-410.

VITAE

Mr. Tritos Ngampitipan was born on 29 October 1986. He received his Bachelor's degree in physics with the first class honors from Chulalongkorn University in 2008 and Master's degree in physics from from Chulalongkorn University in 2011. He has studied black holes for his Doctoral's degree. His research interests are bounding greybody factors for various types of black holes.

Publications

1. Boonserm, P., Ngampitipan, T., and Visser, M. Bounding the greybody factors for scalar field excitations on the Kerr-Newman spacetime. <u>JHEP</u> 03 (March 2014): 113.
   [arXiv: 1401.0568 [gr-qc]]

2. Ngampitipan, T. and Boonserm, P. Transmission Probability for Charged Dilatonic Black Holes in Various Dimensions. <u>JPS Conf. Proc.</u> 1 (March 2014): 013100

3. Boonserm, P., Ngampitipan, T., and Visser, M. Regge-Wheeler equation, linear stability, and greybody factors for dirty black holes. <u>Phys. Rev. D</u> 88 (August 2013): 041502
   [arXiv: 1305.1416 [gr-qc]]

4. Ngampitipan, T. and Boonserm, P. Bounding the greybody factors for non-rotating black holes. <u>Int. J. Mod. Phys. D</u> 22 (June 2013): 1350058.
   [arXiv: 1211.4070 [math-ph]]

5. Ngampitipan, T. and Boonserm, P. Bounding the greybody factors for the Reissner-Nordström black holes. <u>J. Phys. Conf. Ser.</u> 435 (April 2013): 012027
   [arXiv: 1301.7527 [math-ph]]

6. Ngampitipan, T. and Wongjun P. Dynamics of three-form dark energy with dark matter couplings <u>JCAP</u> 11 (November 2011): 036
   [arXiv: 1108.0140 [hep-ph]]